

STRUCTURE-FUNCTION STUDIES OF JHD2,
A HISTONE H3K4 DEMETHYLASE

By

Fu Huang

Dissertation

Submitted to the Faculty of the
Graduate School of Vanderbilt University
in partial fulfillment of the requirements

for the degree of

DOCTOR OF PHILOSOPHY

in

Biochemistry

May 2011

Nashville, Tennessee

Approved:

Professor Zu-Wen Sun

Professor Bruce D. Carter

Professor Katherine L. Friedman

Professor Scott W. Hiebert

Professor Conrad Wagner

To my parents

ACKNOWLEDGEMENTS

I owe my deepest gratitude to Dr. Zu-Wen Sun, my generous graduate mentor. Without him, it would not have been possible for me to start my Ph.D. training as early as when I graduated from college. Throughout my graduate study, he has led me into the chromatin field with tremendous knowledge and great patience, guided me through every step in my scientific career, and has been very supportive whenever I need his help. I have learned from him not only the knowledge and skills, but also the most important things about being a Scientist: critical thinking and the drive to seek the truth. Many, many thanks to you, Dr. Sun, for equipping me with everything needed for my future career, for your support, for your consideration, and for your generosity.

I would like to thank my committee members: Dr. Bruce D. Carter, Dr. Katherine L. Friedman, Dr. Scott W. Hiebert and Dr. Conrad Wagner. I was very fortunate to have the privilege of meeting with such a great panel of experts on numerous occasions during my committee meetings. Thank you so much for your willingness to help and to meet with me at my request amidst your busy schedules. I am truly grateful for your patience, your understanding, your support and all the helpful advice that you gave me in my committee meetings.

I am forever indebted to Dr. Bon-chu Chung, the amazing mentor of mine who has never stopped supporting me since I was 19. She gave me the opportunity to learn science in her laboratory as an undergraduate student, and I would not have committed myself to the scientific career without this experience. Her kind guidance, advice and support have made important impact on my career. Thank you with all my heart, Dr. Chung, for your

kindness, timely help and wise advice.

I was fortunate to have great colleagues here in Vanderbilt. I am indebted to Dr. Mahesh B. Chandrasekharan, who has unselfishly taught me so many things vital to my graduate study and my career: how to think, how to write and how to plan for my future. To me, he has been not only a colleague, but also a teacher and a life-long friend. Other than discussing with me about my graduate project and giving me valuable suggestions, he also provides important data shown in Chapters I, III and VI of this dissertation. Thank you, Mahesh, for your generous help and warm friendship. I am grateful for Dr. Srividya Bhaskara's kind help with the cell transfection. Also, I would like to thank Yi-Chun Chen and people in Dr. David Cortez's laboratory for their help with some experiments. Many thanks to Eric Zhang and David Wu for making our laboratory run smoothly.

Many people in the Biochemistry department have made the environment amazingly supportive. I am heartily thankful to Dr. Michael R. Waterman, who gave me the opportunity to join Dr. Sun's laboratory. I owe Marlene Jayne my deep gratitude. She has taken care of virtually everything in the department for me so that I could concentrate on my study. Thanks to Robert Dortch, Brenda Bilbrey and Peggy Fisher for their administrative support. I am grateful for all your help that has made this dissertation possible.

I would like to thank Dr. Ethan Lee for generously providing the α -Myc antibody, and Drs. Scott D. Briggs, Masami Horikoshi, M. Mitchell Smith, Brian D. Strahl and P. Anthony Weil for the yeast strains. I also thank Drs. Ralf Janknecht and Yang Shi for providing the plasmids, Dr. Wei-Hua Wu for the purified recombinant H3, and Vanderbilt University Center for Structural Biology for the bacterial expression vectors. I thank

Vanderbilt-Ingram Cancer Center, The Kleberg Foundation and NIH (RO1CA109355) for funding this study.

I am most indebted to my loving parents, Sheng-Chi Huang and Chia-Fen Chen. It would not have been possible for me to complete this dissertation without their endless love and incredible support. They have been always considerate and have thought for me even more than I have for myself. I am so fortunate to have such wonderful parents! Thank you, Dad and Mom, for everything you have given me.

TABLE OF CONTENTS

| | |
|--|------|
| DEDICATION | ii |
| ACKNOWLEDGMENTS | iii |
| LIST OF TABLES | viii |
| LIST OF FIGURES | ix |
| LIST OF ABBREVIATIONS | xii |
| Chapter | |
| I. INTRODUCTION | 1 |
| Histone H3 Lysine 4 (H3K4) Methylation..... | 5 |
| The Establishment of H3K4 Methylation..... | 9 |
| The Removal of H3K4 Methylation | 14 |
| The H3K4-Specific Demethylase Jhd2..... | 17 |
| Research Aims | 18 |
| II. EXPERIMENTAL PROCEDURES | 21 |
| Yeast Strains..... | 21 |
| DNA Constructs..... | 21 |
| Western Blot Analysis..... | 24 |
| <i>INO1</i> Induction and Repression..... | 28 |
| Chromatin Immunoprecipitation (ChIP)..... | 28 |
| PCR Analysis | 29 |
| Cell Fractionation..... | 30 |
| Protein Synthesis Inhibition..... | 30 |
| Proteasome Inhibition..... | 31 |
| Tertiary Structure Prediction..... | 31 |
| Immobilization of Nucleosomes..... | 31 |
| <i>In vitro</i> Nucleosome-Binding Assay..... | 32 |
| <i>In vitro</i> Pull-Down Assay..... | 33 |
| III. JHD2 FUNCTIONS AS AN H3K4-SPECIFIC DEMETHYLASE DURING TRANSCRIPTIONAL ACTIVATION AND REPRESSION..... | 35 |
| Introduction..... | 35 |
| Results..... | 35 |

| | |
|---|----|
| Discussion..... | 42 |
| IV. THE JMJN-JMJC INTERDOMAIN INTERACTION IN JHD2 IS CRITICAL FOR ITS PROTEIN STABILITY MEDIATED BY THE E3 LIGASE NOT4..... | 47 |
| Introduction..... | 47 |
| Results..... | 48 |
| Discussion..... | 64 |
| V. THE PHD FINGER IN JHD2 IS IMPORTANT FOR ITS CHROMATIN ASSOCIATION BY INTERACTING WITH HISTONE H2A..... | 69 |
| Introduction..... | 69 |
| Results..... | 70 |
| Discussion..... | 86 |
| VI. SUMMARY AND FUTURE DIRECTIONS | 89 |
| Summary | 89 |
| Future Directions | 91 |
| REFERENCES | 99 |

LIST OF TABLES

| Table | Page |
|--|------|
| 1. <i>Saccharomyces cerevisiae</i> strains | 22 |
| 2. Plasmids | 25 |

LIST OF FIGURES

| Figure | Page |
|---|------|
| 1. Structure and histone modifications of the nucleosome core particle | 3 |
| 2. Different methylation states of arginine (A) and lysine (B) | 4 |
| 3. Distribution of three different states of H3K4 methylation in active <i>S. cerevisiae</i> genes | 6 |
| 4. Biological roles of H3K4 methylation..... | 8 |
| 5. Contributions of the individual COMPASS subunits to Set1-mediated H3K4 methylation..... | 11 |
| 6. The components of yeast Set1/COMPASS complex and their homologs in human..... | 12 |
| 7. Mechanisms of the demethylation by histone lysine demethylases..... | 16 |
| 8. Jhd2 is an H3K4-specific demethylase | 37 |
| 9. Jhd2 plays a role in regulating the H3K4me3 levels at the <i>PMAI</i> gene..... | 39 |
| 10. Jhd2 is localized to the <i>HSP104</i> gene..... | 40 |
| 11. Jhd2 functions as a H3K4 demethylase in the subtelomeric regions..... | 41 |
| 12. Jhd2 is critical for the prompt removal of H3K4me3 at <i>INO1</i> upon repression following induction..... | 43 |
| 13. Mutations in the conserved regions of Jhd2 can affect its activity and overall protein levels..... | 49 |
| 14. The JmjN domain in Jhd2 is important for its global protein level and subcellular localization | 52 |

| | |
|---|----|
| 15. The global protein level and subcellular localization of Jhd2 are sensitive to its structural integrity | 54 |
| 16. Western blot analysis of the levels of Jhd2 and jhd2(T359R) in the WCEs and nuclear extracts..... | 55 |
| 17. Loss of the JmjN domain in Jhd2 causes protein instability mediated by the E3 ligase Not4 and the proteasome..... | 57 |
| 18. The N- and C-terminal parts in Jhd2 interact with each other | 59 |
| 19. Residues that might mediate the JmjN-JmjC interaction are critical for the global protein levels and subcellular localization of Jhd2 | 60 |
| 20. Loss of the JmjN-JmjC interdomain interaction in Jhd2 causes protein instability mediated by the proteasome..... | 62 |
| 21. The positive charge at amino acid position 37 in JmjN domain is important for the demethylase function of Jhd2..... | 63 |
| 22. The two zinc fingers in PHD domain are important for the function of Jhd2 as an H3K4 demethylase..... | 71 |
| 23. The Jhd2 PHD finger interacts with mononucleosomes in vitro | 73 |
| 24. ChIP analysis of the levels of WT Jhd2 or PHD finger mutant variants at <i>HSP104</i> | 74 |
| 25. ChIP analysis of the levels of H3K4me3 and Jhd2 occupancy at <i>HSP104</i> in WT and <i>spp1Δ</i> cells | 76 |
| 26. The Jhd2-chromatin association is independent of H3K4 methylation | 78 |
| 27. The Jhd2 PHD finger interacts with H2A in vitro | 80 |
| 28. The $\alpha 1$ helix in H2A is important for the Jhd2 PHD finger-H2A interaction..... | 81 |

| | |
|---|----|
| 29. The amino acids 24-27 and 34-37 in H2A are important for the Jhd2 PHD finger-H2A interaction | 82 |
| 30. The L24 and F26 residues in H2A are important for Jhd2 function | 84 |
| 31. The H2A L26 residue is critical for normal chromatin association of Jhd2 | 85 |
| 32. Model for the regulation of Jhd2 | 90 |
| 33. Jhd2-LexA activates the <i>(lexAop)₈-LacZ</i> reporter | 92 |
| 34. The putative NLSs and NES in Jhd2 | 94 |
| 35. MMS treatment affects the global protein levels and subcellular localization of Jhd2..... | 96 |
| 36. The H2A F26 residue is in close proximity to the H2B K123 residue | 98 |

LIST OF ABBREVIATIONS

| | |
|------------------|--|
| α -KG | α -ketoglutarate |
| ChIP | chromatin immunoprecipitation |
| BHC80 | BRAF-HDAC complex 80 |
| Bre1 | brefeldin A sensitivity 1 |
| Bre2 | brefeldin A sensitivity 2 |
| CHX | cycloheximide |
| COMPASS | complex proteins associated with Set1 |
| CTD | C-terminal domain |
| DMA | dimethyl adipimidate |
| EtBr | ethidium bromide |
| FAD | flavin adenine dinucleotide |
| Fe ²⁺ | ferrous ion |
| GST | glutathione-S-transferase |
| H2Bub1 | H2B lysine K123 mono-ubiquitination |
| HDAC | histone deacetylase |
| ING2 | inhibitor of growth family, member 2 |
| JARID | Jumonji/ARID domain-containing |
| Jhd1 | JmjC domain-containing histone demethylase 1 |
| Jhd2 | JmjC domain-containing histone demethylase 2 |
| JHDM | JmjC domain-containing histone demethylase |
| JmjC | Jumonji C |

| | |
|--------|--|
| JMJD2A | Jumonji domain containing 2A |
| JmjN | Jumonji N |
| LSD1 | lysine-specific demethylase 1 |
| MBP | maltose binding protein |
| me1 | monomethylation |
| me2 | dimethylation |
| me3 | trimethylation |
| MLL | mixed lineage leukemia |
| MMS | methyl methanesulfonate |
| MudPIT | multidimensional protein identification technology |
| NES | nuclear export signal |
| NLS | nuclear localization signal |
| Not4 | negative on TATA 4 |
| ORF | open reading frame |
| Paf1 | RNA polymerase-associated factor 1 |
| Pdr5 | pleiotropic drug resistance 5 |
| PHD | plant homeodomain |
| PolII | RNA polymerase II |
| PTM | post-translational modification |
| qPCR | quantitative real-time PCR |
| Rad6 | radiation sensitive 6 |
| Rpb1 | RNA Polymerase 1 |
| Rpd3 | reduced potassium dependency 3 |

| | |
|--------|---|
| Rph1 | regulator of PHR1 1 |
| SC | synthetic complete medium |
| Sdc1 | Set1c, homologue of Dpy30 from <i>C.elegans</i> 1 |
| SET | Su(var)-E(z)-Trithorax |
| Set1 | SET domain-containing 1 |
| Set3 | SET domain-containing 3 |
| Set3C | Set3 histone deacetylase complex |
| Shg1 | Set1c, hypothetical G 1 |
| SMCX | selected mouse cDNA on the X |
| Spp1 | Set1c, PHD finger protein 1 |
| Swd1 | Set1c, WD40 repeat protein 1 |
| Swd2 | Set1c, WD40 repeat protein 2 |
| Swd3 | Set1c, WD40 repeat protein 3 |
| TEL06R | the right arm of chromosome VI |
| Ubp8 | ubiquitin-specific processing protease 8 |
| Ubp10 | ubiquitin-specific processing protease 10 |
| XLMR | X-linked mental retardation |

CHAPTER I

INTRODUCTION

In eukaryotic cells, DNA is packed into a highly organized nuclear structure called chromatin. The basic unit of chromatin is a nucleosome, which is composed of 146 base pairs of DNA wrapped around the histone octamer containing two copies each of histones H2A, H2B, H3, and H4 (Fig. 1A). The histone octamer has a core tetramer formed by two stably associated H3-H4 dimers, and the H3-H4 tetramer is flanked by two separate H2A-H2B dimers (1-3). The formation of histone octamer is mainly through the interactions between the hydrophobic globular (histone-fold) domains of the four histones. In addition, the histone tail regions protruding from the nucleosome core disc are relatively flexible and rich in positively-charged amino acids (arginines and lysines), many of which are targeted for enzyme-catalyzed chemical modifications (Fig. 1B) (4).

Given their close contact with DNA, histones can regulate the accessibility of underlying genetic information to factors involved in all DNA-templated processes. A role for histones in transcription was first shown when incorporation of histone inhibited the ability of DNA to serve as the template for *in vitro* RNA synthesis (5). Subsequently, the yeast galactose signaling system was used to show that the depletion of histone H4 results in the activation of genes present in the repressive or uninduced condition, providing the first *in vivo* evidence that histones play a general negative role in gene expression (6). To gain access to the underlying DNA, cellular processes

employ five different mechanisms to remodel the chromatin: modifications of DNA (7-10), nucleosome remodeling by ATP-dependent machineries (11), histone exchange mediated by chaperones (12), histone variant incorporation, and extensive post-translational modifications (PTMs) on histones (13). The concept that the PTMs of histones might play an important role in regulating gene expression was initially shown by demonstrating that histones are acetylated *in vivo* and this modification compromised the ability of histones to impede transcription (14). Extensive research over the past 40 years has now revealed that, in addition to acetylation, histones are modified by methylation, phosphorylation, ADP-ribosylation, citrullination, ubiquitination and sumoylation, and these modifications contribute to the overall complexity of epigenetic regulation (Fig.1B) (15).

Among these PTMs, histone methylation has received particular attention, since it can occur in different states based on the number of methyl groups added. Methylation of the guanidino group of arginine occurs in two distinct states, either due to the addition of a single methyl group (monomethylation) or two methyl groups [dimethylation; wherein the methyl groups can be added to a single (asymmetric) or both guanidino (symmetric) groups] (Fig. 2A). On the other hand, methylation on the ϵ -amino group of lysine can be present in three distinct states by the addition of either a single methyl group (monomethylation, me1), or two methyl groups (dimethylation, me2), or three methyl groups (trimethylation, me3) (Fig. 2B). Other than the potential complexity provided by the different chemical states, histone methylation can be involved in the activation or repression of transcription depending on the position of the modified residue and/or the specific protein factors present in different types of cell that recognize the methyl mark

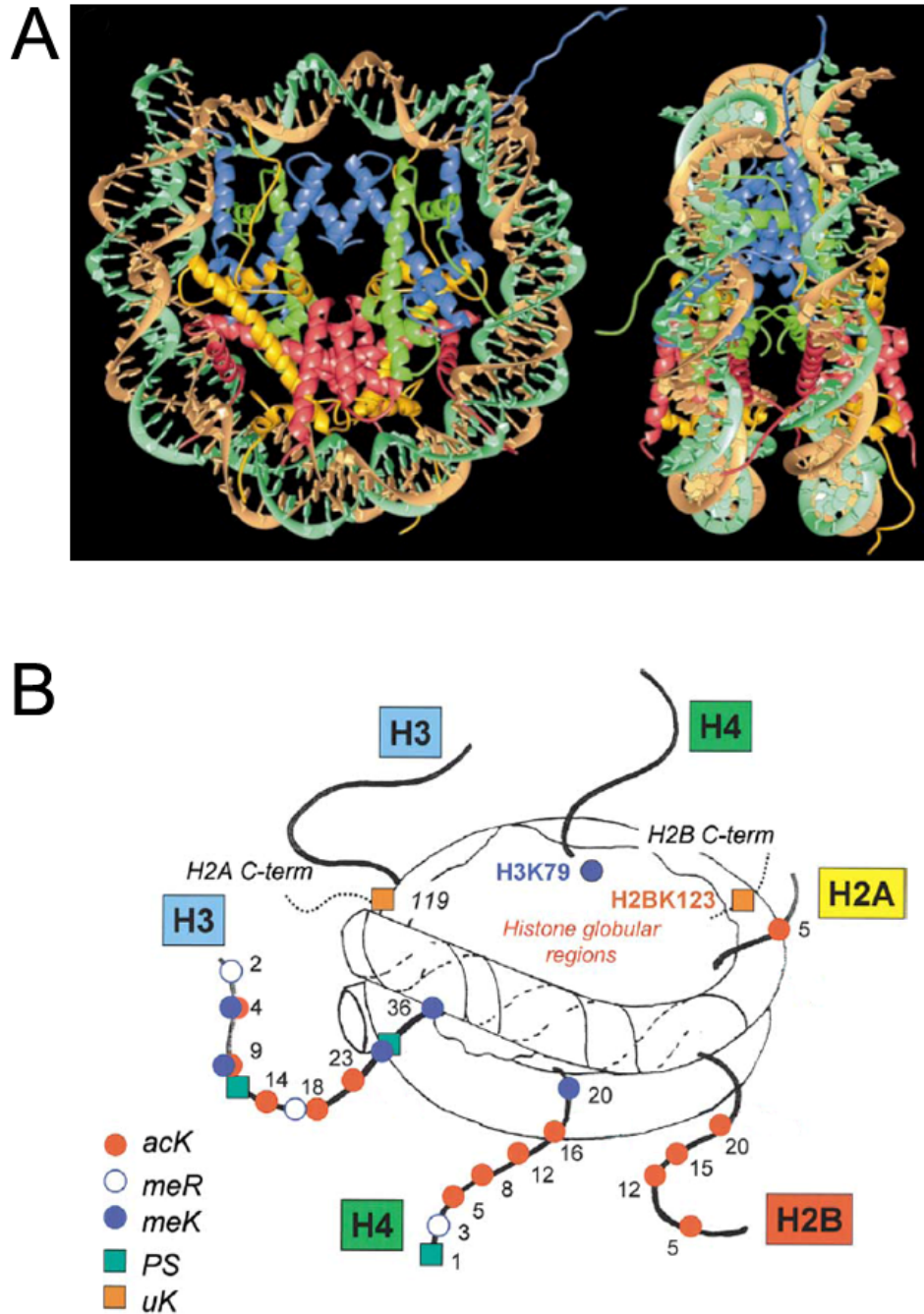


Figure 1. Structure and histone modifications of the nucleosome core particle. A, Crystal structure of the *Xenopus laevis* nucleosome core particle. The 146-bp DNA phosphodiester backbones are shown in brown and turquoise. The histone protein main chains of H2A (yellow), H2B (red), H3 (blue) and H4 (green) are shown. Reproduced from (1) B, Histone modifications on the nucleosome core particle. Sites of post-translational modification are indicated by colored symbols defined in the key; acK, acetyl lysine; meR, methyl arginine; meK, methyl lysine; PS, phosphoryl serine; and uK, ubiquitinated lysine. Adapted from (16).

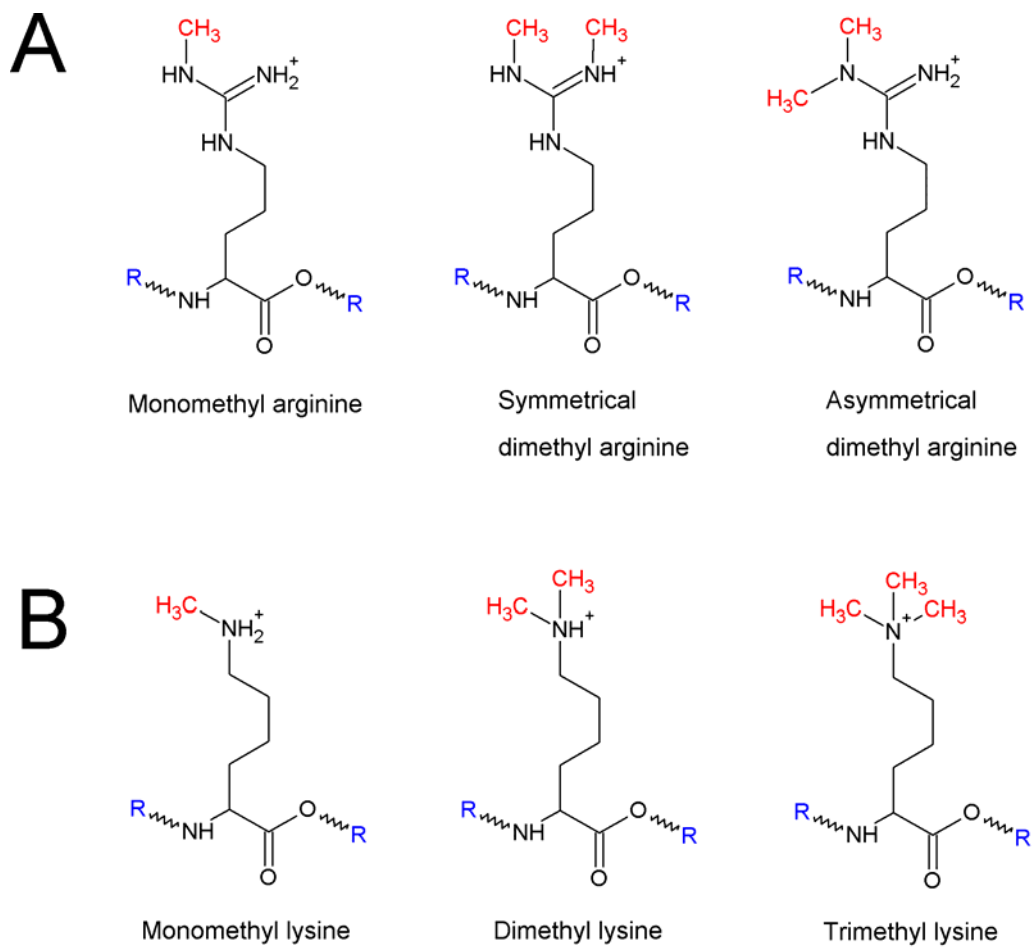


Figure 2. Different methylation states of arginine (A) and lysine (B).

(17-18). Methylation of lysine 4 in histone H3 (H3K4), the main focus of my study, is an intriguing histone modification mark that displays all the different levels of complexity described above.

Histone H3 Lysine 4 (H3K4) Methylation

H3K4 methylation was first found in the trout testes (19). Initial mapping of this histone mark in budding yeast suggested that H3K4 methylation occurs in actively transcribed regions (20). Further analysis of the genome-wide distribution using chromatin immunoprecipitation (ChIP) assays revealed distinct patterns of occupancy for the three different H3K4 methylation states at different genomic loci in yeast, plant and metazoans (21-25). In budding yeast and Arabidopsis, H3K4 monomethylation (H3K4me1) is most abundant at the 3' ends of active genes (Fig. 3), and dimethylation (H3K4me2) spreads throughout the active genes peaking in the middle of the coding regions. However, in vertebrate cells, H3K4me2 is localized in discrete zones near active genes. Unlike the distribution of H3K4me2, H3K4 trimethylation (H3K4me3) is highly associated with the 5' ends of actively transcribed genes in all examined organisms, including yeast, Arabidopsis, fly, chicken, mouse and human (Fig. 3) (21-25), indicating an evolutionarily conserved role of trimethylated H3K4 in transcription initiation/elongation in all eukaryotic cells.

Recent studies have revealed the intriguing complexity of H3K4 methylation regarding its functions and/or localization. In budding yeast, H3K4me1 is mainly associated with moderately transcribed genes (1-50 mRNA/hr), and also occurs at low

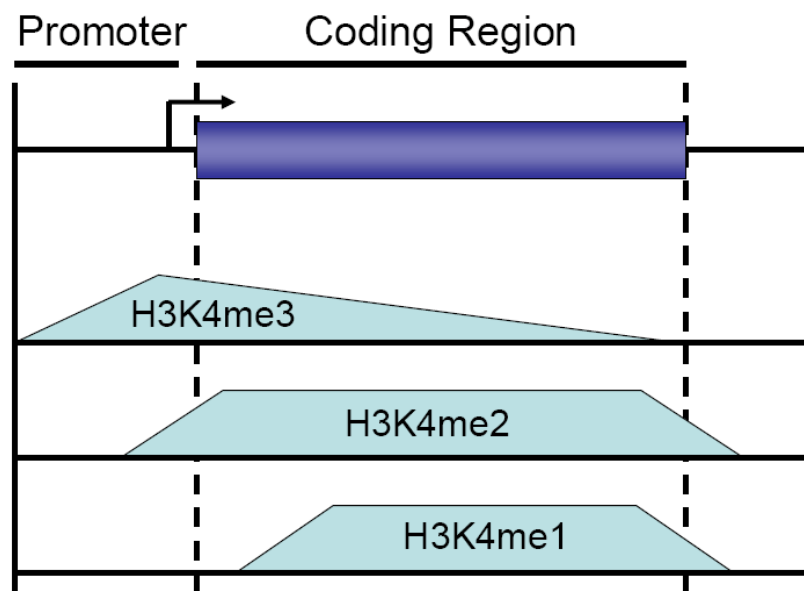


Figure 3. Distribution of three different states of H3K4 methylation in active *S. cerevisiae* genes. Adapted from (26).

levels in inactive genes (<1 mRNA/hr) (27). However, this histone modification is preferentially localized to the repressed genes in *Chlamydomonas* (28), while in mammalian cells, it is considered as an epigenetic mark for enhancers (29-30), suggesting that different species might utilize the monomethylated H3K4 for different tasks. The H3K4me2 mark has been linked to transcriptional regulation, given its general association with active genes. For example, Set3, the defining member of Set3 histone deacetylase complex (Set3C), can recognize this histone mark via its plant homeodomain (PHD) finger. This Set3-H3K4me2 interaction is critical for the association of Set3C with histones and for the co-transcriptional deacetylation of histones at the 5' end of open-reading frames (ORFs) (Fig. 4A) (31). By promoting histone deacetylation to prevent the histone eviction in the coding region, H3K4me2 plays a positive role in the transcription of Set3 target genes (31-32). In contrast, this histone mark is also important for the recruitment of the histone deacetylase Rpd3S complex to the *GALI* gene, contributing to the attenuation of *GALI* in the presence of glucose (33).

The functions of H3K4me3, as compared to those of H3K4me1 and H3K4me2, have been explored in more detail and this modification has been implicated to play a role in diverse cellular processes occurring on chromatin (Fig. 4B). The structure of chromatin can be divided into two states, the loosely-packed euchromatin that is available for active transcription and the densely-packed heterochromatin that is transcriptionally silent. The H3K4me3, as a hallmark of active chromatin, defines the euchromatin- heterochromatin boundary and prevents Sir3 (a silencing protein essential for the formation of heterochromatin state) binding to histone H3 (34-35). In the absence of H3K4me3, the chromatin-bound Sir3 spreads from the heterochromatin into the neighboring euchromatic

regions (34-35). Therefore, H3K4me3 is critical for proper gene silencing in the telomeres and ribosomal DNA locus. Moreover, with the identification of protein domains/modules that recognize trimethylated lysine residues (PHD finger, chromodomain and tudor domain), progress towards uncovering the biological events downstream to H3K4me3 has been expedited. Many factors involved in transcriptional activation, including CHD1, BPTF, Yng1 and ING3-5, can recognize H3K4me3, which correlates well with the proposal that this histone mark has a role in active transcription (36-41). In contrast, H3K4me3 also contributes to gene repression. For instance, ING2 binds H3K4me3 and recruits Sin3/histone deacetylase (HDAC) complex to repress active genes, contributing to the rapid shut-down following DNA damage of genes controlling cell proliferation (39). Other than transcriptional regulation, H3K4me3 can recruit RAG2, the essential subunit in the RAG recombinase complex required for the V(D)J recombination during lymphocyte development (42). RAG2 is recruited onto chromatin by virtue of the interaction between its PHD finger and H3K4me3 (43). Given that all three methylation states on H3K4 have unique roles in transcription and other chromatin-based cellular events, the regulatory mechanisms governing their establishment and removal is an important topic in the chromatin field.

The Establishment of H3K4 Methylation

Set1, the only methyltransferase targeting H3K4 in budding yeast, was first identified in 1997 as a SET [S(u(var)-E(z)-TriThorax)] domain-containing protein that is important for gene silencing at the telomeres (44). Set1 was demonstrated to be capable of methylating

the lysine 4 residue of histone H3 and to be part of a multi-protein complex called COMPASS (Complex Proteins Associated with Set1) (45-47). Other than the catalytic subunit Set1, the Set1/COMPASS complex also contains seven regulatory subunits: Swd1/Cps50/Saf49, Swd2/Cps35/Saf37, Swd3/Cps30/Saf35, Bre2/Cps60, Shg1/Cps15, Sdc1/Cps20/Saf19 and Spp1/Cps40/Saf41 (46-48). Swd1 and Swd3 are required for the complex integrity and all forms of H3K4 methylation (Fig. 5) (35, 49). Lack of Bre2 or Sdc1 results in the complete loss of H3K4me3 with low levels of H3K4me1 and -me2, while Spp1 and Shg1 are only required for high levels of H3K4me3 (Fig. 5) (35, 49). In higher organisms, there are at least ten SET domain-containing methyltransferases targeting the lysine 4 in histone H3, and these enzymes can be divided into two groups based on the evolutionary features of their catalytic SET domains. The six Mixed Lineage Leukemia (MLL)-family members (MLL1-MLL4, SET1A and SET1B) contain SET domains that are related to the SET domain of yeast Set1 and *Drosophila* Trx, and also associate with other regulatory proteins to form complexes similar to the COMPASS complex (Fig. 6) (50-55). The other group of methyltransferases, including ASH1, SET7/9, SMYD3 and PRDM9, contain Trx-unrelated SET domains (56-60). Interestingly, the functions of these multiple enzymes are not redundant, as deletions or truncations in *Mll1*, *Mll2*, and *Mll3* genes resulted in distinguishable phenotypes (61-63). Therefore, it is suggested that the single-cell organism like budding yeast can accomplish the methylation task with one single enzyme, but the higher organisms need multiple H3K4-targeting methyltransferases to cover the regulatory complexity during their development process (64).

The yeast Set1/COMPASS complex is recruited to active genes by the RNA polymerase II (Pol II) elongation machinery (20). Set1 interacts with the Pol II that is

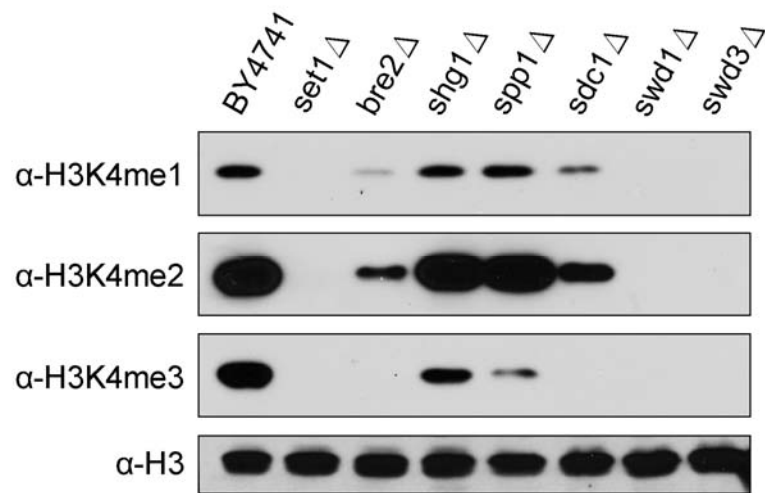


Figure 5. Contributions of the individual COMPASS subunits to Set1-mediated H3K4 methylation. The levels of H3K4 methylation in the indicated mutant cells were examined by Western blotting. From Drs. Zu-Wen Sun and Mahesh B. Chandrasekharan (Unpublished data).

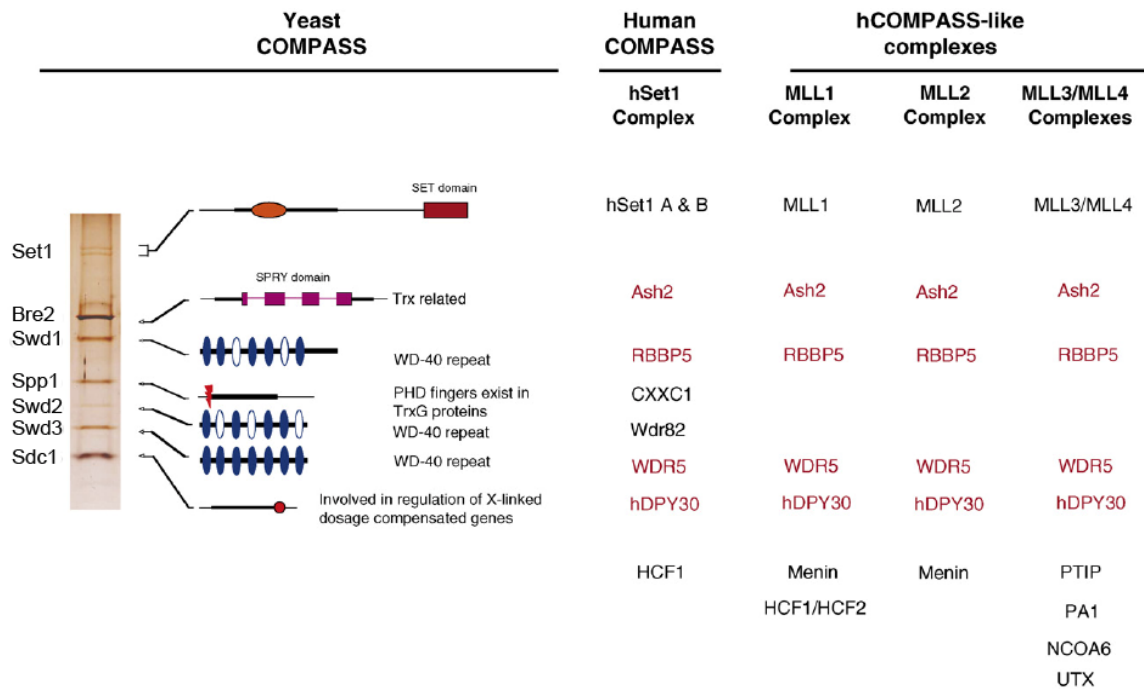


Figure 6. The components of yeast Set1/COMPASS complex and their homologs in human.
Adapted from (65).

phosphorylated at the serine 5 position on its C-terminal domain (CTD) by the kinase Kin28, which mediates the transition between transcriptional initiation and elongation. Moreover, two components in the Pol II-associated Paf1 elongation complex, Rtf1 and Paf1, also interact with Set1 and are important for the recruitment of Set1/COMPASS complex to the actively transcribed ORFs (20, 66). This recruitment mechanism correlates well with the general association of H3K4 methylation with active genes in yeast. Similar mechanisms for the recruitment of MLL proteins also exist in mammals. MLL1 can bind to the Paf1 elongation complex through sequences flanking its CXXC domain, and this interaction is required for MLL1 recruitment to target loci (67-68). In addition, the specific recruitment of MLL1 also depends on the recognition of H3K4me2/me3 by its third PHD finger and the binding of DNA by its CXXC domain (67, 69).

The establishment of H3K4 methylation is also regulated by other histone modifications in *cis* and in *trans*. Asymmetric dimethylation on histone H3 arginine 2 (H3R2) abrogates the ability of Spp1 to recognize H3, preventing Set1/COMPASS complex from trimethylating H3K4 (27). On the other hand, acetylation of histone H3 lysine 14 (H3K14) may promote trimethylation on H3K4, given that mutation at H3K14 or loss of Gcn5, the acetyltransferase targeting H3K14, causes reduction in the H3K4me3 levels (70-71). In addition, the histone H2B lysine K123 mono-ubiquitination (H2Bub1) is required for di- and tri-methylation on H3K4, which is the first *trans*-histone crosstalk pathway to be reported (72-73). The H2Bub1 mark can stabilize the nucleosome, providing a stable working platform/docking site for Set1/COMPASS complex to perform the processive methylation of H3K4 (74). This histone modification is also

suggested to modulate H3K4 methylation through regulating the chromatin association and ubiquitination of Swd2 (75-76). Independent of H2Bub1, arginine 119 (R119) and threonine 122 (T122) in the C-terminal helix of H2B are important for Spp1 binding to chromatin and H3K4 methylation (77). Therefore, a current model proposed for the *trans*-histone crosstalk between H2B ubiquitination and H3K4 methylation is that the H2Bub1 stabilizes the docking site for Set1/COMPASS complex present on the C-terminal helix of H2B, and thereby, contributes to the establishment of H3K4me2 and -me3 marks (78).

The Removal of H3K4 Methylation

Histone lysine methylation had been considered to be an irreversible modification for the following reasons. First, compared to deacetylation (that involves a simple amide bond hydrolysis), removal of a methylation is chemically more difficult, since it requires breaking a more stable C-N covalent bond. Second, pulse-chase experiments demonstrated that the half-lives of the histone and the methyl marks on it were approximately equal, suggesting that the only way to reverse the methylated state of a histone is through passive or active histone exchange (79-80). However, the discovery in 2004 of the first histone demethylase, Lysine-Specific Demethylase 1 (LSD1), has converted the conventional concept to a new model that histone methylation is a dynamic and truly reversible epigenetic mark (81). LSD1 targets H3K4me1 and -me2, and contains an amine oxidase domain that catalyzes the oxidation of the methyl group coupled to the reduction of a cofactor flavin adenine dinucleotide (FAD). The oxidized

methyl group is then released as formaldehyde, leaving the lysine 4 residue of histone H3 in the unmodified state (Fig. 7A) (81). Although LSD1 possesses demethylase activity toward mono- and di-methylated H3K4, it cannot remove the H3K4me3 mark, owing to the requirement of an iminium cation intermediate during the demethylation process (Fig. 7A). Furthermore, unlike many other organisms including fission yeast, budding yeast does not have a homolog of LSD1. Therefore, the demethylation of trimethyl H3K4, and all forms of H3K4 methylation in budding yeast, may be conducted through an alternative mechanism.

Following the discovery of LSD1, JHDM1, the founding member of the JmjC domain-containing Histone Demethylase (JHDM) family was identified in 2006 (82), and other demethylases in the same family were immediately reported independently by different groups (83-85). All of the JHDM family members contain a catalytic JmjC domain that requires ferrous ion (Fe^{2+}) and α -ketoglutarate (α -KG) as cofactors for its demethylase activity. The demethylation mechanism by JHDMs is through the oxygenation of the methyl group coupled to the conversion of α -KG to succinate and carbon dioxide. The resulting carbinolamine intermediate is chemically unstable and undergoes a spontaneous C-N bond cleavage, leaving the methylated lysine in the unmodified state and releasing formaldehyde as a byproduct (Fig. 7B) (82). Other than the JmjC domain, some JHDMs also have a JmjN domain, which is present N-terminal to their JmjC domain. Evidence based on the comparisons of the substrate preferences of JmjC and JmjN/JmjC enzymes supports a possibility that JHDMs with both JmjN and JmjC domains prefer di- or trimethylated substrates, while enzymes that only contain a JmjC domain show demethylase activity toward mono- or dimethylated lysine residues

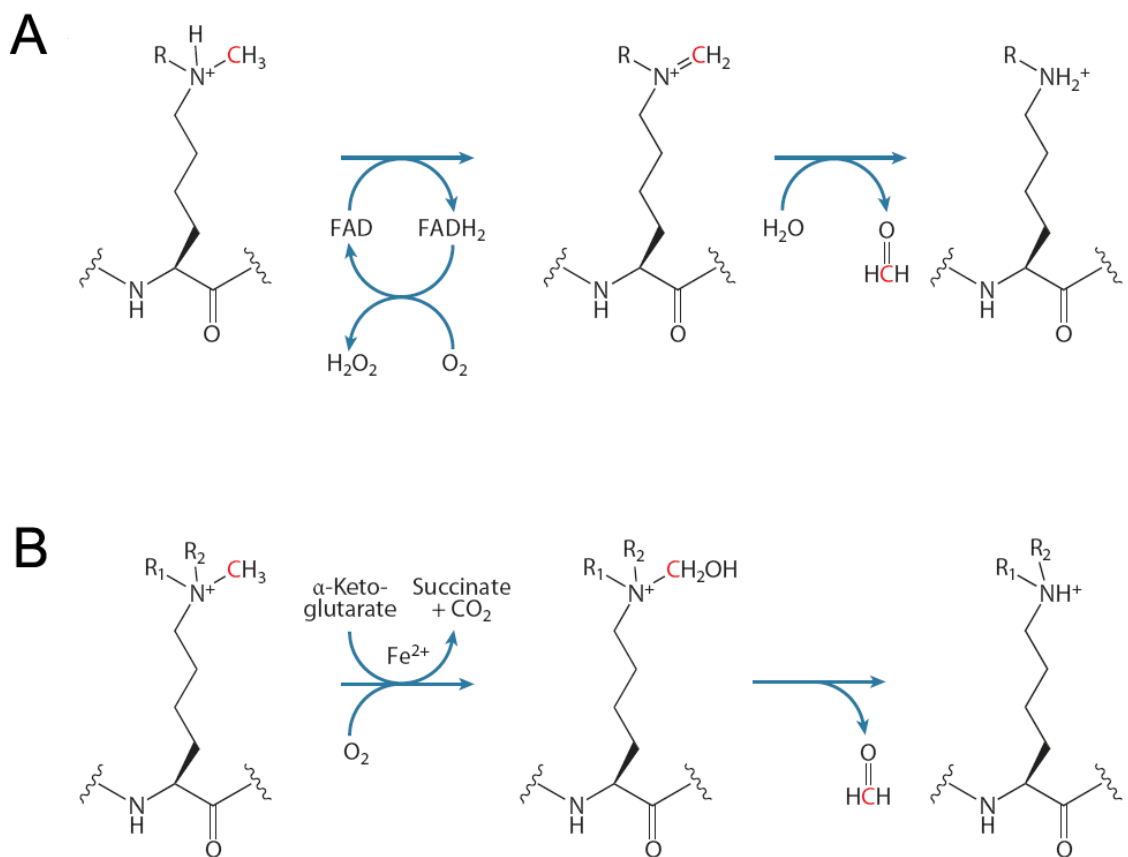


Figure 7. Mechanisms of the demethylation by histone lysine demethylases. A, The FAD-dependent amine oxidase mechanism of lysine demethylation by LSD1. B, The Fe^{2+} and α -ketoglutarate-dependent dioxygenase mechanism of lysine demethylation by the JmjC domain-containing demethylases. From (86).

(87). Therefore, the enzyme responsible for the removal of H3K4me3 mark could be a JmjN/JmjC-containing protein. Indeed, in 2007, several groups independently identified new demethylases with both a JmjN and JmjC domains, JARID1A-1D, Lid and Jhd2, that are capable of erasing the H3K4me3 mark in mammals, fly and budding yeast, respectively (88-94). Among these enzymes, JARID1A and 1B are involved in cell cycle regulation and linked to tumor progression in mammals, and mutations in JARID1C are associated with human X-linked mental retardation, indicating that demethylation on H3K4 at the right time and in the right place is critical for proper development and differentiation in humans (95-98). Therefore, the homolog of JARID1 family proteins in budding yeast, Jhd2, could be a good model for providing important information about human diseases.

The H3K4-Specific Demethylase Jhd2

As mentioned above, the yeast Jhd2 was discovered as a H3K4-specific demethylase in 2007 (88-90). In the *in vitro* demethylase activity assay, Jhd2 is capable of removing all forms of H3K4 methylation (88, 99). However, this enzyme displayed *in vivo* demethylase activity only towards di- and trimethyl H3K4, since cellular levels of H3K4me2 and -me3, but not H3K4me1, were affected following overexpression of Jhd2 or following deletion of Jhd2 from the cells (88-90, 99-100). The ChIP assay further revealed that in the absence of Jhd2, the H3K4 methylation levels at the inducible *GALI* and *SUC2* genes were altered during both the gene activation and attenuation steps (99). In addition, consistent with the fact that the H3K4me3 mark is important for proper gene

silencing, overexpression of Jhd2 causes a partial relief of telomeric silencing, and the loss of this demethylase also delays the establishment of silencing at the mating loci (88, 101). To date, Jhd2 has not been found to be present as a component of any protein complex; instead, size-exclusion chromatography indicated that Jhd2 exists as a monomeric protein in cells (88). Supporting this observation, a recent study showed that Jhd2 is regulated at the protein levels by the proteasomal degradation following the E3 ligase Not4-mediated polyubiquitination (100). Despite these advances in the understanding of Jhd2 functions, many fundamental questions pertaining to its substrate specificity and selectivity, domain contributions, chromatin association and its overall regulation remained unanswered.

Research Aims

A unifying theme in this work is the characterization of the function and regulation of Jhd2 as the yeast H3K4-specific demethylase. Jhd2 has a role in regulating the levels of H3K4 methylation in the inducible *GAL1* gene during both the activation and repression steps (99). However, whether Jhd2 also functions as a H3K4-demethylase at other types of loci on chromatin was unknown. Furthermore, probably owing to its low chromatin-bound levels of Jhd2, detection of its locus-specific occupancy by ChIP assay was thought to be difficult. Therefore, the direct evidence of the localization of Jhd2 to where it functions was lacking. In Chapter III, the chromatin occupancy of Jhd2 at different genomic loci detected by a modified ChIP assay that lowers the non-specific background signal will be described. In addition, the discoveries that H3K4me3 plays

important roles in transcriptional regulation and Jhd2 can modulate the levels of this histone mark in the inducible *GAL1* gene are extended in this study (64, 99). The real-time changes in the Jhd2 and H3K4me3 occupancies in another inducible gene, *INO1*, following a repression-induction-repression treatment course as discussed in Chapter III has provided further important information about the dynamics in transcriptional regulation. The results support the role of Jhd2 as a demethylase that removes the H3K4 methylation mark and is involved in both transcriptional repression and activation. This result also reveals the prompt removal of H3K4me3 at *INO1* gene in response to repressive conditions. Moreover, the differences between the real-time changes in H3K4me3 levels in the WT and in the *jhd2Δ* cells suggest that the H3K4 methylation can be removed through both active demethylation and passive histone replacement.

As Jhd2 is a newly identified enzyme, very little is known about the mechanisms that regulate the demethylation of H3K4 by this protein. Therefore, Chapter IV and V will discuss the structural insights into the regulation of Jhd2. Similar to other histone demethylases that target trimethylated substrates, Jhd2 contains both a JmjN and JmjC domain. However, in contrast to the well-characterized catalytic JmjC domain, the roles of JmjN domain in regulating the functions of histone demethylases have remained unclear. Previous reports have implied that the JmjN domain is involved in substrate selectivity and the maintenance of protein levels (87, 102). In addition, the JmjN domain in another histone demethylase, JMJD2A, interacts with the JmjC domain based on its crystal structure (102). Sequence alignment revealed that the residues mediating the JmjN-JmjC interaction in JMJD2A are conserved in Jhd2 and other JmjN/JmjC

demethylases. Therefore, the hypothesis that this inter-domain interaction in Jhd2 is involved in the regulation of its demethylase function and protein levels was proposed. Evidence supporting this hypothesis and revealing a role of the JmjN domain in the E3 ligase Not4-mediated proteasomal degradation of Jhd2 will be presented in Chapter IV.

In addition to the JmjN and the catalytic JmjC domains, Jhd2 also contains another conserved motif, namely, the PHD finger. Since PHD fingers present in other proteins have been demonstrated to bind trimethylated or unmodified lysine residues in histones (91, 103-104), it is conceivable that the PHD finger in Jhd2 may mediate its chromatin association by recognizing histones. Chapter V will discuss the roles of PHD finger in mediating the Jhd2-chromatin interaction. Data obtained from ChIP assays that demonstrate the importance of the PHD finger for the Jhd2 occupancy on chromatin will be described. Further, the binding sites on histones for the Jhd2 PHD finger and their roles in modulating the demethylase function of Jhd2 *in vivo* will also be described in Chapter V. These structural and functional insights into the Jhd2-catalyzed demethylation of H3K4 are beneficial to the understanding of transcriptional regulation and human diseases.

CHAPTER II

EXPERIMENTAL PROCEDURES

Yeast Strains

Deletion mutants lacking Jhd2, Set1, Swd1, Sdc1 or Spp1 in YMH171 strain were created using PCR products containing the disrupted gene locus and the inserted KanMX4 selection module amplified from the genomic DNA template isolated from the respective BY4742-based yeast deletion strains (Open Biosystems). Jhd2 was genomically tagged with 9 copies of Myc at its C-terminus in YMH171 following PCR amplification using pYM6 as the template (105). MSY421, a histone H3/H4 shuffle strain (73), was used to mobilize the H3 N-terminal deletion mutant [H3(1-28 Δ)]. The *Flag-H2B* and *Flag-H2B/set1 Δ* strains were derived from YZS276 (73). Detailed genotypes of the yeast strains described in this study are listed in Table 1.

DNA Constructs

All the plasmids used in this study are listed in Table 2. For overexpressing the jumonji-domain containing proteins, PCR products containing the entire ORFs for *RPH1*, *GIS1*, *ECM5*, *JHD1* or *JHD2*, and 500 bp of DNA upstream and downstream of each ORF were mobilized into a high copy vector, YEplac112 (106). The C-terminal LexA epitope-tagged Jhd2 was created by PCR amplifying the ORF of *JHD2* and mobilizing it between the *ADHI* promoter and a fragment of the LexA DNA binding domain in pFBL23 (107). An XhoI-KpnI fragment containing the sequence encoding 9 copies of

Table 1. *Saccharomyces cerevisiae* strains

| Strain | Genotype | Source |
|----------|--|-----------------|
| YMH171 | <i>Mat α ura3-52 leu2-3,112 his3 trp1Δ</i> | (108) |
| YZS499 | <i>jhd2Δ::KanMX4</i> ; derived from YMH171 | This study |
| YZS500 | <i>JHD2-9Myc::klTRP1</i> ; derived from YMH171 | This study |
| YZS512 | <i>swd1Δ::KanMX4</i> ; derived from YMH171 | This study |
| YZS513 | <i>sdc1Δ::KanMX4</i> ; derived from YMH171 | This study |
| YZS514 | <i>spp1Δ::KanMX4</i> ; derived from YMH171 | This study |
| YZS515 | <i>set1Δ::KanMX4</i> ; derived from YMH171 | This study |
| MSY421 | <i>Mat α hht1-hhf1Δ hht2-hhf2Δ leu2-3,112 ura3-52 trp1-289 his3-Δ1</i> pMS329 (<i>HHT1-HHF1, URA3, CEN</i>) | (73) |
| YZS209 | pZS136 (<i>HHT2-HHF2, TRP1, CEN</i>); derived from MSY421 | This study |
| YZS211 | pMS358 [<i>hht1-2(1-28Δ)-HHF1, LEU2, CEN</i>]; derived from MYS421 | This study |
| YZS276 | <i>Mat a hta1-htb1Δ::LEU2 hta2-htb2Δ leu2-2,-112 ura3-1 trp1-1 his3-11,-15</i> <i>ade2-1 can1-100 ssd1 HTA1-Flag-HTB1 (CEN, HIS3)</i> | (73) |
| YZS522 | <i>set1Δ::KanMX4</i> ; derived from YZS276 | This study |
| BY4742 | <i>Mat α his3Δ1 leu2Δ0 lys2Δ0 ura3Δ0</i> | Open Biosystems |
| D147 | <i>not4Δ::KanMX4</i> ; derived from BY4742 | Open Biosystems |
| VU156 | <i>pdr5Δ::KanMX4</i> ; derived from BY4742 | Open Biosystems |
| HTA1WT | <i>Mat α hta1-htb1Δ hta2-htb2Δ lys2-128δ his3Δ200 ura3-52</i> pRS313 (<i>HTA1-HTB1, HIS3, CEN</i>) | (109) |
| HTA1L24A | pRS313 [<i>hta1-(L24A)-HTB1, HIS3, CEN</i>]; derived from HTA1WT | (109) |
| HTA1T25A | pRS313 [<i>hta1-(T25A)-HTB1, HIS3, CEN</i>]; derived from HTA1WT | (109) |
| HTA1F26A | pRS313 [<i>hta1-(F26A)-HTB1, HIS3, CEN</i>]; derived from HTA1WT | (109) |
| HTA1P27A | pRS313 [<i>hta1-(P27A)-HTB1, HIS3, CEN</i>]; derived from HTA1WT | (109) |
| HTA1R36A | pRS313 [<i>hta1-(R36A)-HTB1, HIS3, CEN</i>]; derived from HTA1WT | (109) |
| HTA1R37A | pRS313 [<i>hta1-(R37A)-HTB1, HIS3, CEN</i>]; derived from HTA1WT | (109) |
| L40 | <i>Mat a his3Δ200 trp1-901 leu2-3,112 ade2 lys2-801am URA3::(lexAop)₈-lacZ</i> <i>LYS2::(lexAop)₄-HIS3</i> | (110) |

Myc epitope (9Myc) and the *CYCI* terminator was obtained following PCR amplification and mobilized into pRS314. Subsequently, a 500 bp PCR product containing the *JHD2* promoter was mobilized upstream of the region coding for 9Myc as a SacI-SpeI fragment. The entire *JHD2* promoter-9Myc-*CYCI* terminator module was mobilized as a SacI-KpnI fragment into pRS316. The ORF of *JHD2* was then PCR amplified and mobilized between the *JHD2* promoter and the 9Myc-*CYCI*-terminator sequence in pRS314 or pRS316 as a SpeI-XhoI fragment. Point and truncation mutants of Jhd2 were made by PCR-based site-directed mutagenesis using pRS314-*JHD2*-9Myc or pRS316-*JHD2*-9Myc as the template. For overexpression of *JHD2* or its mutant derivatives, a fragment containing the WT or mutant ORF, the promoter and the *CYCI* terminator region was excised from the pRS314-based construct and mobilized into the high copy vector, pRS426. To obtain purified, recombinant Jhd2 PHD finger or its variants, a sequence encoding either the WT PHD finger or its mutant derivatives was amplified by PCR and mobilized into a bacterial expression vector, pBG101 (provided by the Vanderbilt Structural Biology Core). The plasmids, pCS3⁺-6Myc and pCS3⁺-*SMCX*-6Myc, were kindly provided by Ralf Janknecht (*III*), and the pCS3⁺-*smcx(S451R)*-6Myc construct was made by PCR-based site-directed mutagenesis. The *MBP-JHD2(1-237)* construct was obtained by PCR amplifying and mobilizing the first 711 bp of DNA in the ORF of *JHD2* as an NdeI-NcoI fragment into the vector pLM302 (provided by the Vanderbilt Structural Biology Core). Similarly, the last 1329 bp of DNA in the ORF of *JHD2* was PCR amplified and mobilized as a BamHI-EcoRI fragment into the vector pGEX-2T (GE Healthcare) for expressing the recombinant GST-tagged amino acids 277-729 of Jhd2 in bacteria. *HTAI* containing truncations was PCR amplified and mobilized as an

NdeI-BamHI fragment to replace the wild-type sequence in H2A-pET11a (kindly provided by Brad Cairns) (112). All the constructs created using PCR amplification were verified by DNA sequencing.

Western Blot Analysis

To determine changes in Jhd2 levels, whole cell extracts (WCEs) were prepared as described (74) and analyzed by Western blotting using antibodies raised against Myc epitope (9E10, gift from Ethan Lee) and Pgk1 (22C5, Molecular Probes) at 1:1000 and 1:5000 dilution, respectively. Crude nuclear extracts were used to examine the levels of H3K4 methylation following the cell fractionation procedure described previously (74). The following antibodies were purchased from Millipore and used in Western blotting to detect H3K4 methylation (dilutions are indicated in parentheses): α -H3K4me1 (1:1000), α -H3K4me2 (1:10000) and α -H3K4me3 (1:2500). The histone H3 loading was monitored using α -H3 (1:7500, Active Motif). For mammalian WCEs, HeLa cells were transfected with pCS3⁺-6Myc, pCS3⁺-SMCX-6Myc or pCS3⁺-smcx(S451R)-6Myc using Lipofectamine method. Following a two-day incubation at 37°C, cells were washed prior to and after harvesting with ice-cold 1X phosphate-buffered saline (PBS; Sigma), and boiled in 1X Laemmli sample buffer (Bio-Rad) for 10 min. After centrifugation (16100 × g for 5 min), equal volumes of WCEs were subjected to Western blot analysis using α -Myc (1:1000) and α - β -actin (1:10000, Sigma) antibodies.

Table 2. Plasmids

| Plasmid | Inserted Gene | Promoter | Vector | Source |
|-----------|------------------------------|--------------|-----------|------------|
| pYM6 | <i>9Myc & kTRP1</i> | None | pWZV87 | (105) |
| YEplac112 | None | None | YEplac112 | (106) |
| pFH1 | <i>RPH1</i> | <i>RPH1p</i> | YEplac112 | This Study |
| pFH2 | <i>GIS1</i> | <i>GIS1p</i> | YEplac112 | This Study |
| pFH3 | <i>ECM5</i> | <i>ECM5p</i> | YEplac112 | This Study |
| pFH4 | <i>JHD1</i> | <i>JHD1p</i> | YEplac112 | This Study |
| pFH5 | <i>JHD2</i> | <i>JHD2p</i> | YEplac112 | This Study |
| pFH6 | <i>jhd2 H427A</i> | <i>JHD2p</i> | YEplac112 | This Study |
| pFH7 | <i>jhd2 Y346A</i> | <i>JHD2p</i> | YEplac112 | This Study |
| pFH8 | <i>jhd2 H261A</i> | <i>JHD2p</i> | YEplac112 | This Study |
| pFH9 | <i>jhd2 T359R</i> | <i>JHD2p</i> | YEplac112 | This Study |
| p424GPD | None | <i>GPDp</i> | p424GPD | (113) |
| pFH10 | <i>JHD2</i> | <i>GPDp</i> | p424GPD | This Study |
| pFH11 | <i>jhd2 H427A</i> | <i>GPDp</i> | p424GPD | This Study |
| pFH12 | <i>jhd2 Y346A</i> | <i>GPDp</i> | p424GPD | This Study |
| pFH13 | <i>jhd2 H261A</i> | <i>GPDp</i> | p424GPD | This Study |
| pFH14 | <i>jhd2 T359R</i> | <i>GPDp</i> | p424GPD | This Study |
| pFBL23 | <i>LexA</i> | <i>ADH1p</i> | pN1102 | (107) |
| pFH15 | <i>JHD2-LexA</i> | <i>ADH1p</i> | pN1102 | This Study |
| pFH16 | <i>9Myc</i> | <i>JHD2p</i> | pRS314 | This Study |
| pFH17 | <i>JHD2-9Myc</i> | <i>JHD2p</i> | pRS314 | This Study |
| pFH18 | <i>jhd2 H427A-9Myc</i> | <i>JHD2p</i> | pRS314 | This Study |
| pFH19 | <i>jhd2 Y346A-9Myc</i> | <i>JHD2p</i> | pRS314 | This Study |
| pFH20 | <i>jhd2 H261A-9Myc</i> | <i>JHD2p</i> | pRS314 | This Study |
| pFH21 | <i>jhd2 T359R-9Myc</i> | <i>JHD2p</i> | pRS314 | This Study |
| pFH22 | <i>jhd2 jmjNΔ-9Myc</i> | <i>JHD2p</i> | pRS314 | This Study |
| pFH23 | <i>jhd2 NPΔ-9Myc</i> | <i>JHD2p</i> | pRS314 | This Study |
| pFH24 | <i>jhd2 P/CΔ-9Myc</i> | <i>JHD2p</i> | pRS314 | This Study |
| pFH25 | <i>jhd2 jmjCΔ-9Myc</i> | <i>JHD2p</i> | pRS314 | This Study |
| pFH26 | <i>jhd2 CA-9Myc</i> | <i>JHD2p</i> | pRS314 | This Study |
| pFH27 | <i>jhd2 K37E-9Myc</i> | <i>JHD2p</i> | pRS314 | This Study |
| pFH28 | <i>jhd2 E507K-9Myc</i> | <i>JHD2p</i> | pRS314 | This Study |
| pFH29 | <i>jhd2 K37E, E507K-9Myc</i> | <i>JHD2p</i> | pRS314 | This Study |
| pFH30 | <i>jhd2 G34R-9Myc</i> | <i>JHD2p</i> | pRS314 | This Study |
| pFH31 | <i>jhd2 C1,2A-9Myc</i> | <i>JHD2p</i> | pRS314 | This Study |
| pFH32 | <i>jhd2 C7,8A-9Myc</i> | <i>JHD2p</i> | pRS314 | This Study |

Table 2. Plasmids (continued)

| Plasmid | Inserted Gene | Promoter | Vector | Source |
|-------------------------|---------------------------------|--------------|-------------------------|---------------|
| pCS3 ⁺ -6Myc | <i>6Myc</i> | CMV | pCS3 ⁺ -6Myc | (111) |
| pFH33 | <i>6Myc-smcx S451R</i> | CMV | pCS3 ⁺ -6Myc | This Study |
| pRS426 | None | None | pRS426 | (114) |
| pFH34 | <i>JHD2-9Myc</i> | <i>JHD2p</i> | pRS426 | This Study |
| pFH35 | <i>jhd2 jmjNA-9Myc</i> | <i>JHD2p</i> | pRS426 | This Study |
| pFH36 | <i>jhd2 NPΔ-9Myc</i> | <i>JHD2p</i> | pRS426 | This Study |
| pFH37 | <i>jhd2 CΔ-9Myc</i> | <i>JHD2p</i> | pRS426 | This Study |
| pFH38 | <i>jhd2 K37E-9Myc</i> | <i>JHD2p</i> | pRS426 | This Study |
| pFH39 | <i>jhd2 E507K-9Myc</i> | <i>JHD2p</i> | pRS426 | This Study |
| pFH40 | <i>jhd2 K37E, E507K-9Myc</i> | <i>JHD2p</i> | pRS426 | This Study |
| pFH41 | <i>jhd2 G34R-9Myc</i> | <i>JHD2p</i> | pRS426 | This Study |
| pFH42 | <i>jhd2 K37R-9Myc</i> | <i>JHD2p</i> | pRS426 | This Study |
| pFH43 | <i>jhd2 K37A-9Myc</i> | <i>JHD2p</i> | pRS426 | This Study |
| pFH44 | <i>jhd2 K37Q-9Myc</i> | <i>JHD2p</i> | pRS426 | This Study |
| pFH45 | <i>jhd2 C1,2A-9Myc</i> | <i>JHD2p</i> | pRS426 | This Study |
| pFH46 | <i>jhd2 C7,8A-9Myc</i> | <i>JHD2p</i> | pRS426 | This Study |
| pFH47 | <i>9Myc</i> | <i>JHD2p</i> | pRS316 | This Study |
| pFH48 | <i>JHD2-9Myc</i> | <i>JHD2p</i> | pRS316 | This Study |
| pFH49 | <i>jhd2 H427A-9Myc</i> | <i>JHD2p</i> | pRS316 | This Study |
| pFH50 | <i>jhd2 jmjNA-9Myc</i> | <i>JHD2p</i> | pRS316 | This Study |
| pFH51 | <i>jhd2 K37E-9Myc</i> | <i>JHD2p</i> | pRS316 | This Study |
| pFH52 | <i>jhd2 E507K-9Myc</i> | <i>JHD2p</i> | pRS316 | This Study |
| pFH53 | <i>jhd2 K37E, E507K-9Myc</i> | <i>JHD2p</i> | pRS316 | This Study |
| pBG101 | <i>6His-GST</i> | <i>T7lac</i> | pBG101 | VUCSB* |
| pFH54 | <i>6His-GST-JHD2(PHD)</i> | <i>T7lac</i> | pBG101 | This Study |
| pFH55 | <i>6His-GST-jhd2(PHD C1,2A)</i> | <i>T7lac</i> | pBG101 | This Study |
| pFH56 | <i>6His-GST-jhd2(PHD C7,8A)</i> | <i>T7lac</i> | pBG101 | This Study |
| pBHC80-PHD | <i>GST-BHC80(PHD)</i> | <i>T7lac</i> | pGEX-4T-1 | (103) |
| pING2-PHD | <i>GST-ING2(PHD)</i> | <i>T7lac</i> | pGEX-4T-1 | (103) |
| pLM302 | <i>HIS-MBP</i> | <i>T7lac</i> | pLM302 | VUCSB* |
| pFH57 | <i>JHD2(1-237)-MBP</i> | <i>T7lac</i> | pLM302 | This Study |
| pGEX-2T | <i>GST</i> | <i>T7lac</i> | pGEX-2T | GE Healthcare |
| pFH58 | <i>GST-JHD2(277-729)</i> | <i>T7lac</i> | pGEX-2T | This Study |
| H2A-pET11a | <i>HTA1</i> | <i>T7lac</i> | pET-11a | (112) |
| pFH59 | <i>hta1(2-38)Δ</i> | <i>T7lac</i> | pET-11a | This Study |
| pFH60 | <i>hta1(25-38)Δ</i> | <i>T7lac</i> | pET-11a | This Study |

Table 2. Plasmids (continued)

| Plasmid | Inserted Gene | Promoter | Vector | Source |
|---------|-----------------------|--------------|---------|------------|
| pFH61 | <i>hta1(80-98)Δ</i> | <i>T7lac</i> | pET-11a | This Study |
| pFH62 | <i>hta1(98-132)Δ</i> | <i>T7lac</i> | pET-11a | This Study |
| pFH63 | <i>hta1(121-132)Δ</i> | <i>T7lac</i> | pET-11a | This Study |
| pFH64 | <i>hta1(LTFP)Δ</i> | <i>T7lac</i> | pET-11a | This Study |
| pFH65 | <i>hta1(LLRR)Δ</i> | <i>T7lac</i> | pET-11a | This Study |

*Vanderbilt University Center for Structural Biology

INO1 Induction and Repression

WT and *jhd2Δ* strains were grown in yeast minimal synthetic complete medium without inositol (SC-Ino; BIO101) supplemented with 200 μM inositol and 2 mM choline (*INO1*-repression medium) at 30°C overnight (115). The overnight cultures were re-inoculated into the *INO1*-repression medium at 2×10^6 cells/ml and grown at 30°C to log phase. Cells (4×10^8) were subjected to formaldehyde cross-linking for ChIP assay (*INO1* repressed state). The remaining cells were harvested, washed once with SC-Ino medium, inoculated at 4×10^6 cells/ml into a fresh SC-Ino medium and grown at 30°C for 2 hr to activate *INO1* expression. Again, cells (4×10^8) were set aside and subjected to formaldehyde cross-linking (*INO1* induced state). To assess temporal changes in histone modification or Jhd2 occupancy following *INO1* repression, cells grown in inducing medium were re-inoculated into *INO1*-repression medium at the following initial cell densities and grown at 30°C for the various time periods (indicated within parentheses) to obtain $\sim 4 \times 10^8$ cells: 7×10^6 cells/ml (20 min), 6×10^6 cells/ml (1 hr), 4×10^6 cells/ml (2 hr), and 2×10^6 cells/ml (4 hr). Cultures grown to different incubation time following *INO1* re-repression were then subjected to formaldehyde cross-linking for ChIP assay (*INO1*-re-repression time course).

Chromatin Immunoprecipitation (ChIP)

Double cross-linking using dimethyl adipimidate (DMA; Sigma) and formaldehyde were done essentially as described previously (116) with minor modifications: Following incubation in 10 mM DMA, cells were washed and resuspended in 1X PBS containing 1% formaldehyde, and incubated at room temperature for 45 min with gentle agitation.

The cross-linking was stopped by adding 130 mM glycine and incubation for 10 min at room temperature. Cells were then washed twice with 1X PBS and harvested to prepare soluble chromatin for immunoprecipitating H3, H3K4me3, Jhd2-LexA, and Jhd2-9Myc using α -H3, α -H3K4me3, α -LexA (Active Motif) and α -Myc, respectively. ChIP assay was performed as described in (117) with modifications in the wash steps. After immunoprecipitation, the chromatin-bound agarose beads were washed twice with 1 ml of FA140 buffer (50 mM HEPES pH 7.6, 140 mM NaCl, 1 mM EDTA, 1% Triton-X-100, 0.1% Na Deoxycholate, 1 mM PMSF, 1 μ g/ml Pepstatin A, 1 μ g/ml Aprotinin and 1 μ g/ml Leupeptin), twice with 1 ml of FA500 buffer (FA140 buffer with 500 mM NaCl), and then once with 1 ml of LiCl/NP40 buffer (10 mM Tris.HCl pH 8.0, 250 mM LiCl, 1 mM EDTA, 0.5% NP-40, 0.5% Na Deoxycholate, 1 mM PMSF, 1 μ g/ml Pepstatin A, 1 μ g/ml Aprotinin and 1 μ g/ml Leupeptin) followed by elution and purification of bound DNA.

PCR Analysis

The data analysis of quantitative real-time PCR (qPCR) following ChIP was performed as described by Chandrasekharan et al. (74) with modifications. Briefly, occupancy of H3K4me3 was calculated using the $2^{-\Delta\Delta CT}$ method (Bio-Rad Real-Time PCR applications guide). The occupancy of H3K4me3 in *set1 Δ* strain was used as a control to determine non-specific immunoprecipitation and any value obtained for this strain was subtracted from the H3K4me3 occupancy values obtained from all other strains. Soluble chromatin from yeast strains transformed with plasmid vectors were used as negative controls (“no tag”) for ChIP of Jhd2-9Myc and Jhd2-LexA. The $2^{-\Delta CT}$ value

obtained for the negative control was subtracted from $2^{-\Delta CT}$ values obtained for test samples containing epitope-tagged WT or mutant Jhd2. DNA primers used in this study are available upon request.

Cell Fractionation

Spheroplast preparation and nuclei isolation were performed as previously described (74). WCEs were prepared by bead-beating spheroplasts in SUME buffer (1% SDS, 8 M Urea, 10 mM MOPS pH 6.8 and 10 mM EDTA, 1 mM PMSF, 1 μ g/ml Pepstatin A, 1 μ g/ml Aprotinin and 1 μ g/ml Leupeptin) followed by centrifugation ($16100 \times g$ for 20 min). Nuclear extracts were obtained by lysing isolated nuclei in SUME buffer followed by sonication and centrifugation ($16100 \times g$ for 15 min). For chromatin fractions, isolated nuclei were resuspended in a hypotonic solution (3 mM EDTA, 0.2 mM EGTA, 1 mM DTT, 1 mM PMSF, 1 μ g/ml Pepstatin A, 1 μ g/ml Aprotinin and 1 μ g/ml Leupeptin) and incubated on ice for 30 min. After centrifugation ($1700 \times g$ for 5 min), the chromatin pellet was washed with the hypotonic solution, and then re-suspended in SUME buffer. Following brief sonication, soluble chromatin was obtained by centrifugation at $16100 \times g$ for 15 min. Protein concentration of the clarified lysate was measured using Bio-Rad D₆ Protein Assay Kit following the manufacturer's instructions, and equal amount of total protein was subjected to Western blotting using α -Myc, α -Pgk1 or α -H3 antibodies.

Protein Synthesis Inhibition

Cycloheximide treatment of yeast was done as described previously (118) with minor modifications. Briefly, a 25 ml culture was grown to log phase, and cycloheximide

was added to a final concentration of 35 $\mu\text{g/ml}$ to inhibit the translation machinery. 3.5×10^7 cells were collected at 0, 20, 40 and 60 min after cycloheximide treatment and boiled in 100 μl 1X Laemmli sample buffer (Bio-Rad) for 10 min. Following centrifugation ($16100 \times g$ for 5 min), equal volume of lysates were subjected to Western blot analysis using α -Myc or α -Pgk1 antibodies.

Proteasome Inhibition

A mid-log phase yeast culture (25 ml) was treated either with DMSO or 0.1 mM MG132 (the proteasome inhibitor) for 30 min. The effect of proteasomal inhibition on Jhd2 or its mutant derivatives was examined in a *pdr5 Δ* strain to allow efficient uptake of MG132 (100). Whole cell extracts were prepared and subjected to Western blotting as described above.

Tertiary Structure Prediction

The sequence of PHD domain in Jhd2 was submitted to SWISS-MODEL (<http://swissmodel.expasy.org/>) for structure prediction. The software uses a homology-based search and predicts the structure utilizing solved structure(s) as a reference. The template used for the structure prediction is the solution structure of the PHD finger in SMCY/JARID1D (PDB # 2E6R).

Immobilization of Nucleosomes

Nuclei from *Flag-H2B* or *Flag-H2B/set1 Δ* strains were isolated as previously described (26), and the DNA content was determined by measuring the OD₂₆₀ of an

aliquot of nuclei diluted in 1N NaOH. Nuclei (equivalent to 660 μg DNA) were resuspended in 200 μl EBTX buffer (50 mM HEPES pH 7.6, 0.1 M KCl, 2.5 mM MgCl_2 , 0.25% Triton-X-100, 1 mM PMSF, 5 mM NEM, 1 $\mu\text{g}/\text{ml}$ Pepstatin A, 1 $\mu\text{g}/\text{ml}$ Aprotinin and 1 $\mu\text{g}/\text{ml}$ Leupeptin). MNase digestion was performed twice by adding 5 μl 0.1 M CaCl_2 and 500 units MNase (Worthington) to the nuclei suspension followed by incubation at room temperature for 10 min, and then 4.5 μl 0.1 M EGTA pH 8.0 was added to stop the digestion. After centrifugation ($9300 \times g$ for 10 min), supernatants from the two digestions were combined. The nucleosome-enriched supernatant was diluted by adding an equal volume of EBTX buffer containing 10% glycerol, and subjected to α -Flag affinity chromatography (M2, Sigma). After extensive washes with EBTX with 5% glycerol, the immobilized nucleosomes were stored at 4°C until further use in the *in vitro* nucleosome-binding assay. DNA was isolated from an aliquot of the immobilized nucleosomes by phenol-chloroform extraction and ethanol precipitation and resolved in a 2% agarose gel to examine the size of the nucleosomes bound to α -Flag-conjugated agarose beads.

In vitro Nucleosome-Binding Assay

Recombinant glutathione-S-transferase (GST)-tagged WT and mutant PHD finger (amino acid 209-320) of Jhd2 were purified from *Escherichia coli* using glutathione-Sepharose 4B beads following the manufacturer instructions (GE Healthcare). GST-tagged PHD finger (2 μg) was incubated with 5 μl nucleosome-containing beads in 200 μl binding buffer (50 mM Tris.HCl pH 8.0, 150 mM NaCl, 1.5 mM MgCl_2 , 0.2% Triton-X-100, 5% glycerol, 1 mM PMSF, 1 $\mu\text{g}/\text{ml}$ Pepstatin A, 1 $\mu\text{g}/\text{ml}$ Aprotinin and 1

μg/ml Leupeptin) for 2 hr at 4°C. After three washes with the binding buffer, the beads were boiled in 1X Laemmli sample buffer (Bio-Rad) for 10 min. Following centrifugation (16100 × g for 5 min), the supernatant was subjected to Western blot analysis using α-GST (1:20000, GE Healthcare) and α-Flag (M2, 1:5000, Sigma) antibodies.

In vitro Pull-Down Assay

E.coli cells expressing recombinant maltose binding protein (MBP)-tagged N-terminal part of Jhd2 [Jhd2(1-237)-MBP], GST-tagged C-terminal part of Jhd2 [GST-Jhd2(277-729)], or histone H2A mutants were lysed in lysis buffer (20 mM Tris.HCl pH 7.5, 150 mM NaCl, 5% glycerol, 0.01% NP-40, 1 mM DTT, 1 mM PMSF, 1 μg/ml Pepstatin A, 1 μg/ml Aprotinin and 1 μg/ml Leupeptin) by sonication. Following centrifugation (16100 × g for 15 min), the supernatant (lysate) was collected. To examine the interaction between the N-terminal and C-terminal parts of Jhd2, the lysate containing Jhd2(1-237)-MBP (200 μg total protein) was incubated with the lysate containing GST-Jhd2(277-729) (200 μg total protein) in 200 μl lysis buffer for 1 hr at 4°C. For *in vitro* binding of PHD fingers to the H2A mutants, purified GST-tagged PHD finger (5 μg) was incubated with the *E.coli* lysates containing H2A mutants (60 μg total protein) in 200 μl lysis buffer for 1 hr at 4°C. Incubation was continued for another 1 hr at 4°C after 10 μl amylose-conjugated agarose beads (New England Biolabs) or glutathione-Sepharose 4B beads (GE Healthcare) were added to pull down Jhd2(1-237)-MBP or GST-tagged PHD finger, respectively. Following 4 washes with wash buffer (lysis buffer containing 0.1% NP-40), the beads were boiled in 1X Laemmli sample buffer (Bio-Rad) for 10 min.

Following centrifugation ($16100 \times g$ for 5 min), the supernatant was subjected to Western blotting using α -GST (1:20000, GE Healthcare) or α -H2A (1:5000, Active Motif) antibody.

CHAPTER III

JHD2 FUNCTIONS AS A H3K4-SPECIFIC DEMETHYLASE DURING TRANSCRIPTIONAL ACTIVATION AND REPRESSION

Introduction

Since the discovery of histone methylation in 1975, the enzyme that removes this histone mark was the “holy grail” of the chromatin field (19). Following the identification of the first histone demethylase, LSD1 (81), several JmjC domain-containing proteins were immediately reported to also possess the enzymatic activity of demethylating histones in human (82, 84-85, 119-120). Given the absence of a homolog of LSD1 in budding yeast, the attention for the candidates of yeast histone demethylases have been focused on proteins containing the conserved JmjC domain. In 2006, Dr. Mahesh B. Chandrasekharan, the postdoctoral fellow in our laboratory, indentified a yeast JmjC-containing protein called Jhd2 as the H3K4-specific demethylase (Fig. 8A). Subsequently, I started to characterize the function of Jhd2 as a histone demethylase. In this chapter, data obtained from *in vivo* demethylase activity assay and ChIP assay are described to demonstrate the role of Jhd2 at different genomic loci *in vivo*.

Results

Jhd2 is an H3K4 Methylation-Specific Demethylase

The JmjC domain-containing histone demethylases are evolutionarily highly

conserved across many genera (119). There are five JmjC domain-containing proteins (Rph1, Gis1, Ecm5, Jhd1 and Jhd2) in budding yeast. Overexpression of *JHD2* through a high copy, 2 μ -based plasmid led to a decrease in H3K4me3 and a modest increase in H3K4me1 levels (Fig. 8A, lane 6), and deletion of *JHD2* resulted in a slight increase in H3K4me3 levels (Fig. 8B). In addition, overexpression of *JHD2* in the *sdc1 Δ* strain, which contained no detectable H3K4me3 and lower levels of H3K4me1 and -me2 (Fig. 5), reduced the levels of H3K4me1 and -me2 (Fig. 8C). Moreover, none of the JmjC domain-containing proteins exhibited any apparent demethylation of K79-methylated H3 under the same condition (Fig. 8D). Thus, Jhd2 is an H3K4 methylation-specific demethylase that can remove mono-, di- and tri-methylated H3K4 marks in yeast.

Jhd2 Localizes to and Functions at a Constitutively Expressed Gene

Given the genome-wide distribution of H3K4 methylation (21, 26) and since H3K4me3 is closely associated with gene transcription (17, 121), I tested whether Jhd2 plays a role in controlling this H3 modification during transcription. Towards this end, chromatin immunoprecipitation (ChIP) assays were undertaken to assess the occurrence and changes, if any, in Jhd2 occupancy and in H3K4me3 levels at the highly expressed *PMAI* gene. As compared to the WT, deletion of *JHD2* (*jhd2 Δ*) or overexpression of *JHD2-LexA* led to a two-fold increase or decrease in H3K4me3 at the promoter and ORF regions of *PMAI*, respectively (Fig. 9A). This result suggests that Jhd2 might be present on constitutively and highly expressed genes to maintain their normal H3K4 methylation levels. Indeed, ChIP data showed that Jhd2-LexA is present on the promoter and ORF regions of the *PMAI* gene (Fig. 9B). Interestingly, the distribution pattern of Jhd2-LexA

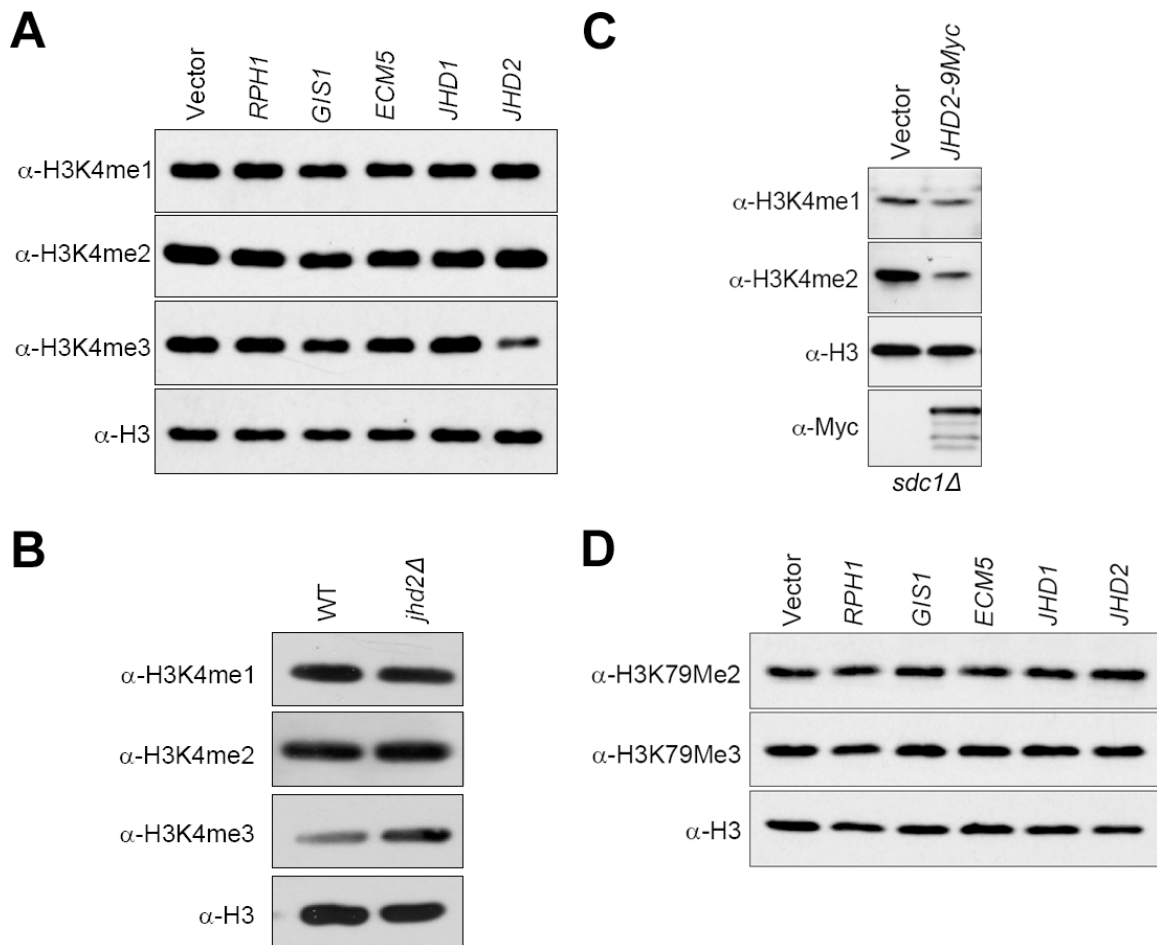


Figure 8. Jhd2 is a H3K4-specific demethylase. (A) Western blot analysis of H3K4 methylation levels in crude nuclear extracts obtained from yeast strains which overexpress the indicated JmjC-domain-containing proteins. (B) Western blot analysis of H3K4 methylation levels in crude nuclear extracts obtained from WT and *jhd2* Δ strains. (C) Western blot analysis of H3K4 methylation levels in crude nuclear extracts obtained from the *sdc1* Δ strain with overexpressed *JHD2-9Myc*. (D) Western blot analysis of H3K79 methylation levels in crude nuclear extracts obtained from yeast strains overexpressing the indicated JmjC-domain-containing proteins.

across the *PMAI* gene is similar to that seen for H3K4me3 (compare Figs. 9A and 9B). Similar results were obtained from ChIP assays of *HSP104* (Fig. 10A and 10B), which is expressed at very low levels under normal conditions (122). Given that H3K4me3 is the substrate for Jhd2, the data suggest that Jhd2 might be actively recruited during gene transcription to dynamically regulate the H3K4 methylation levels.

Jhd2 Localizes to and Functions at Subtelomeric Regions

Since proper levels of H3K4me3 are important for gene silencing at telomeres (34-35), I hypothesized that Jhd2 may also function as a H3K4 demethylase in the subtelomeric regions. Therefore, a ChIP assay was performed to examine the H3K4me3 levels and Jhd2 occupancies in the regions close to the telomere at the right end of chromosome VI in the presence or absence of overexpressed *JHD2*. Indeed, overexpression of *JHD2-LexA* led to a decrease in H3K4me3 at both the proximal region of *YFR055W* ORF (5' ORF) and the ORF-free regions (Fig. 11A). Interestingly, the levels of Jhd2-LexA at the ORF-free regions were higher as compared to the actively transcribed *YFR055W* (Fig. 11B), while the H3K4me3 levels at the proximal region of *YFR055W* were ~10 fold greater than the ORF-free regions (Fig. 11A). Consistent with the previous report that overexpression of *JHD2* led to a slight defect in telomeric silencing (88), my data suggest that the high levels of Jhd2 may play a role in maintaining the low H3K4me3 levels in the ORF-free regions near telomeres.

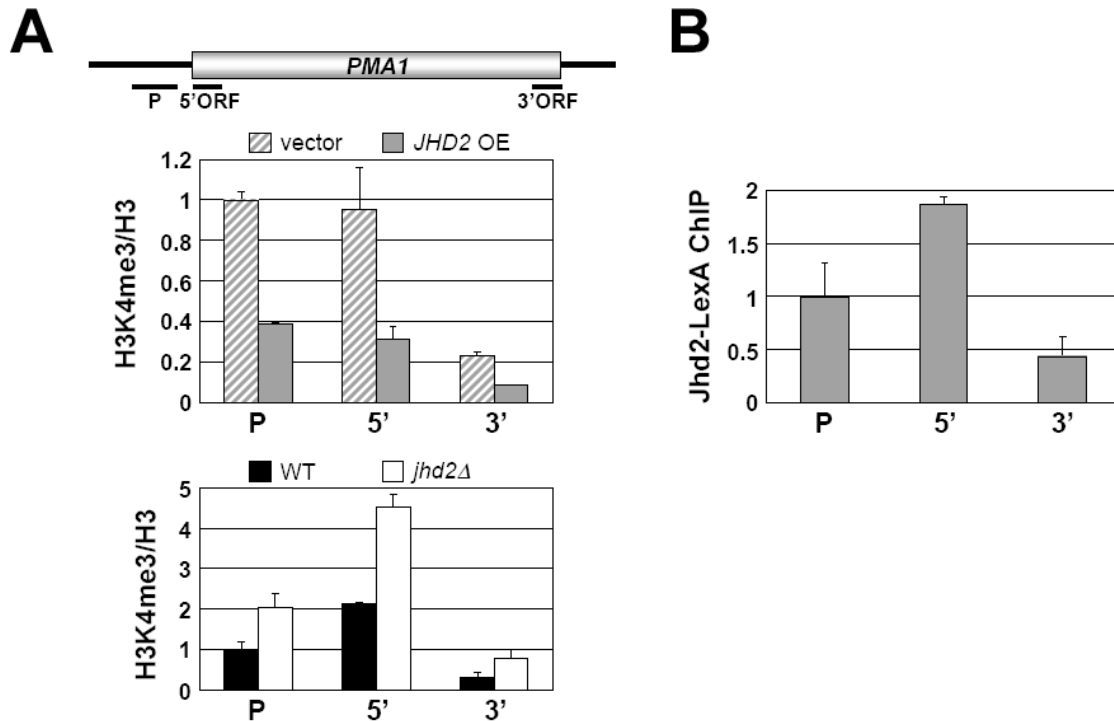


Figure 9. Jhd2 plays a role in regulating the H3K4me3 levels at the *PMA1* gene. (A) Changes in H3K4me3 levels at the *PMA1* locus were analyzed by ChIP assay. Graph depicts the data obtained from wild-type control (WT) and a strain lacking Jhd2 (*jhd2Δ*) in the top panel, and from yeast strains overexpressing *JHD2* (*JHD2* OE) from a high copy plasmid or containing the plasmid vector alone in the bottom panel. The H3K4me3 ChIP signals were first normalized to total histone H3 ChIP signals (H3K4me3/H3) and then the H3K4me3/H3 values at either the promoter, 5' or 3' ORF regions in the controls and test samples were normalized to the H3K4me3/H3 value obtained for the promoter region in WT (top panel) or vector control (bottom panel), which was set as 1. Error bars denote standard error of the mean from two independent experiments. (B) Levels of Jhd2-LexA at *PMA1* were analyzed by ChIP using α -LexA. LexA IP/input values obtained from no-tag control (background) were subtracted from those obtained from yeast cells with overexpressed *JHD2-LexA*, and the resulting differences were defined as Jhd2-LexA occupancy. The Jhd2-LexA occupancies at 5' and 3' ORF regions were normalized to the promoter region, which was arbitrarily set as 1. Error bars denote standard error of the mean from two independent experiments.

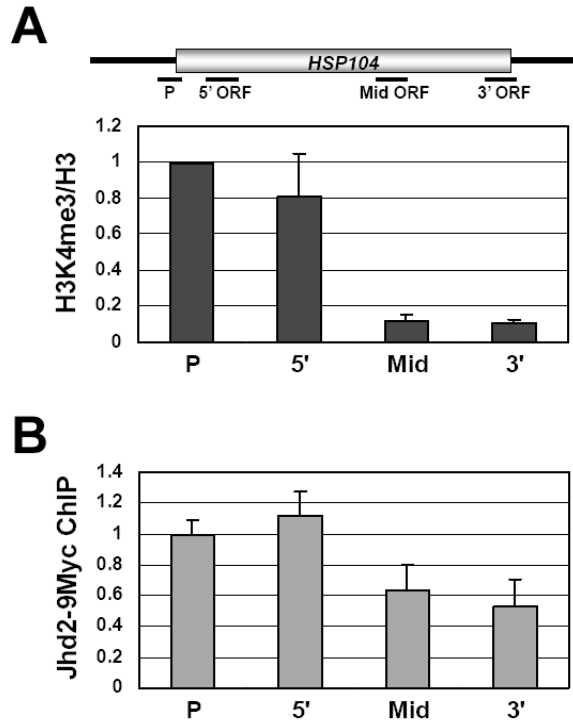


Figure 10. Jhd2 is localized to the *HSP104* gene. (A) ChIP analysis of H3K4me3 levels at the *HSP104* locus in cells expressing N-terminally 9Myc-tagged *JHD2*. The H3K4me3 ChIP signals were first normalized to total histone H3 ChIP signals (H3K4me3/H3) and then the H3K4me3/H3 values at either the promoter, 5', mid or 3' ORF regions in the controls and test samples were normalized to the H3K4me3/H3 value obtained for the promoter region in WT (top panel) or vector control (bottom panel), which was set as 1. Error bars denote standard error of the mean from three independent experiments. (B) Levels of Jhd2-9Myc at *HSP104* were analyzed by ChIP using α -Myc. Myc IP/input values obtained from no-tag control (background) were subtracted from those obtained from yeast cells expressing *JHD2-9Myc*, and the resulting differences were defined as Jhd2-9Myc occupancy. The Jhd2-9Myc occupancies at 5', mid and 3' ORF regions were normalized to the promoter region, which was arbitrarily set as 1. Error bars denote standard error of the mean from three independent experiments.

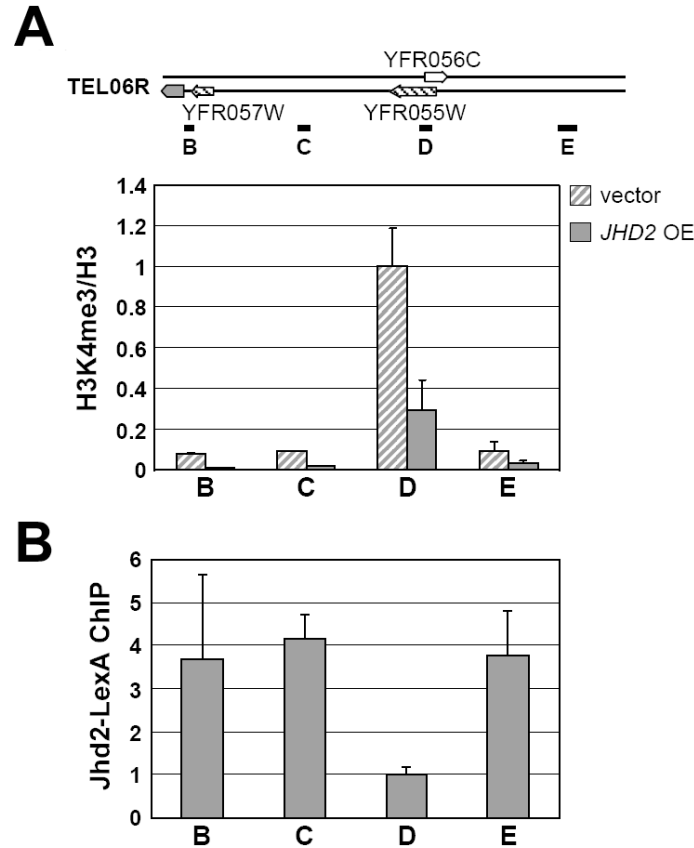


Figure 11. Jhd2 functions as a H3K4 demethylase in the subtelomeric regions. (A) Levels of H3K4me3 at four loci (*black lines*, labeled B-E) in the subtelomeric region close to the right arm of chromosome VI (*TEL06R*) were analyzed by ChIP assay. Graph depicts data obtained from the vector alone control or overexpressing *JHD2-LexA* (*JHD2 OE*). The H3K4me3 levels at different loci are shown as fold change relative to the value obtained for vector alone control at the D locus, which is present within an ORF. Error bars denote standard error of the mean from two independent experiments. **(B)** Levels of Jhd2-LexA at *TEL06R* was analyzed by ChIP using α -LexA. LexA IP/input values obtained from no-tag control were subtracted from those obtained from strains overexpressing *JHD2-LexA*, and the resulting differences were defined as Jhd2-LexA occupancy. Occupancies of Jhd2-LexA at different loci were normalized to the D region. Error bars denote standard error of the mean from two independent experiments.

Jhd2 Localizes to and Functions at the Inducible INO1 Gene during both Activation and Repression Steps

Next, to test whether Jhd2 also has a role in the regulation of H3K4 methylation in an inducible gene, the kinetics of H3K4me3 levels on the *INO1* gene in WT and *jhd2Δ* cells during the activated and repressed states were measured by ChIP assay. Additionally, the Jhd2 occupancy at the 5' ORF region of *INO1* was also measured under the same conditions. Transcription of *INO1*, encoding inositol 1-phosphate synthase, is activated or repressed by the absence or presence of inositol-choline in the media, respectively (123). As shown in Figure 12A, WT and *jhd2Δ* cells display similar levels of H3K4me3 in the *INO1* 5' ORF region during both the initial repressed state and following induction. Upon re-repression, the levels of H3K4me3 decrease rapidly in WT cells. However, in the absence of *JHD2*, the reduction of H3K4me3 levels is delayed and it persists for 2 hr following re-repression as compared to the WT, where it persists for less than 1 hr. Importantly, ChIP data confirm that the Jhd2 occupancy decreases at the 5' ORF of *INO1* upon induction, but increases immediately upon re-repression (Fig. 12B). Also, the global levels of Jhd2 are not affected by the treatments inducing or repressing *INO1* (Fig. 12C). Taken together, these results show that Jhd2 is required for the rapid removal of the H3K4me3 mark upon transcriptional repression of *INO1*.

Discussion

In vivo H3K4 Demethylase Activity of Jhd2

Upon overexpression, human JARID1A and JARID1B H3K4 demethylases have the ability to target all three states of H3K4 methylation (92, 124-125). While Jhd2 displayed

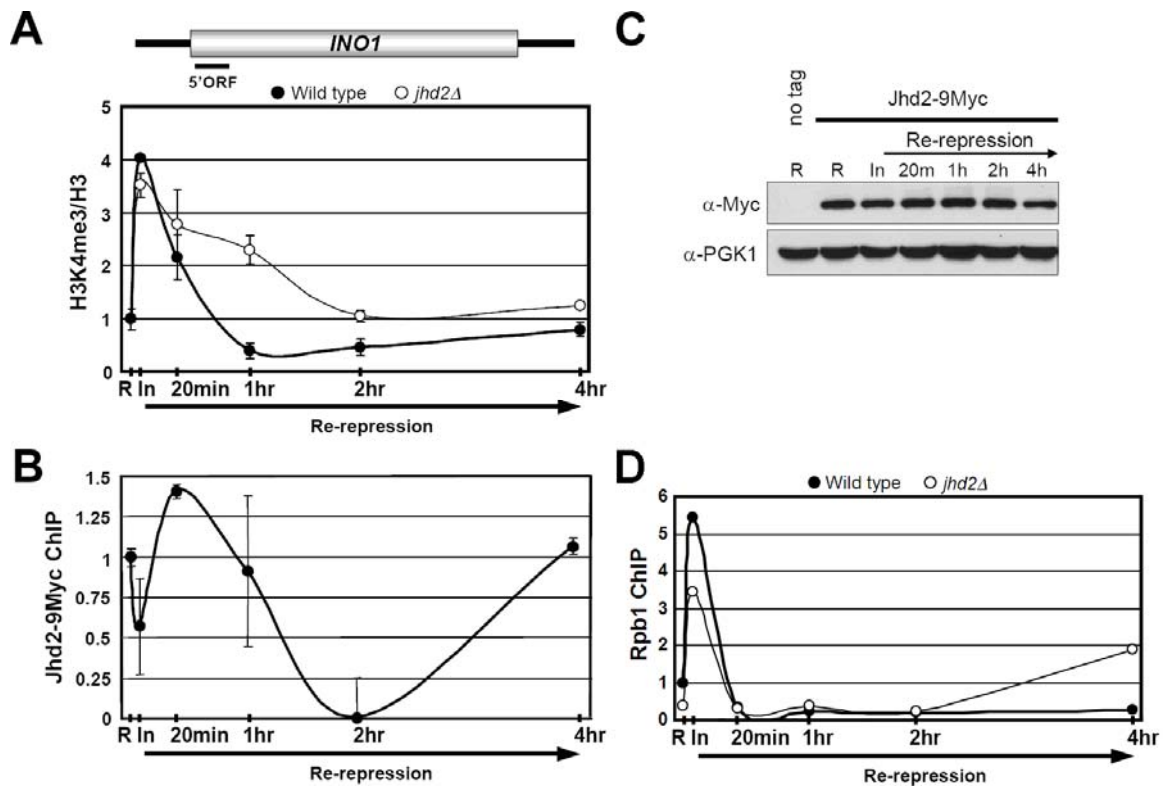


Figure 12. Jhd2 is critical for the prompt removal of H3K4me3 at *INO1* upon repression following induction. (A) Temporal changes in H3K4me3 following the re-repression of *INO1* measured by ChIP assay. WT and *jhd2Δ* strains were grown in the inositol-choline containing medium for 4 hr to repress *INO1* expression (R), then grown in the inositol-free medium for 2 hr to induce *INO1* expression (In), and then *INO1* was repressed again by growing cells in the inositol-choline containing medium for the indicated time periods (Re-repression). Cells at different time points were subjected to ChIP analysis using α -H3K4me3 and α -H3 antibodies. Levels of H3K4me3/H3 at the 5' ORF of *INO1* in WT or the *jhd2Δ* mutant at different time points are shown as fold changes relative to H3K4me3/H3 value obtained at the repressed state for the WT, which was set as 1. Error bars denote standard error of the mean from two independent experiments. (B) Temporal changes in Jhd2-9Myc occupancy following the re-repression of *INO1* measured by ChIP assay performed essentially as described for (A). Chromatin-bound Jhd2-9Myc was immunoprecipitated using α -Myc. Myc IP/input values obtained from the no-tag control (background) were subtracted from those obtained for yeast expressing *JHD2-9Myc*, and the resulting difference was defined as Jhd2-9Myc occupancy. The Jhd2-9Myc occupancies at the 5' ORF of *INO1* at different time points are shown as fold changes relative to the Jhd2-9Myc occupancy obtained at the initial repressed state (R), which was set as 1. Error bars denote standard error of the mean obtained from two independent experiments. (C) The soluble chromatin-containing lysates that were subjected to the ChIP assay in (B) were boiled in 1X Laemmli sample buffer to reverse the protein-protein and protein-DNA crosslinks. After brief spin, the lysates were subjected to Western blot analysis of Jhd2-9Myc levels using α -Myc. Pgk1 was used as the loading control. (D) Temporal changes in Rpb1 occupancy following the re-repression of *INO1* measured by ChIP assay performed essentially as described for (A). Chromatin-bound Rpb1 was immunoprecipitated using α -Rpb1. The Rpb1 IP/input value was defined as Rpb1 occupancy. The Rpb1 occupancies at the 5' ORF of *INO1* at different time points are shown as fold changes relative to the Rpb1 occupancy obtained at the initial repressed state (R) for the WT, which was set as 1.

activity towards all forms of K4-methylated H3 *in vitro* (99), overexpression of Jhd2 resulted in a significant reduction in only H3K4me3 (Fig. 8A) (88, 90). However, when the Set1 H3K4 methyltransferase was targeted for rapid degradation, both H3K4me3 and H3K4me2 were quickly abolished in a Jhd2-dependent manner (89). These findings indicate that Jhd2 can target both H3K4me3 and H3K4me2 *in vivo* and raise the question as to whether it has any intrinsic activity towards H3K4me1 in yeast cells. One possibility is that the *in vivo* activity of Jhd2 towards H3K4me1 in the wild type is masked by the conversion of H3K4me2 into H3K4me1. Indeed, my results show that overexpression of Jhd2 in *sdc1Δ*, which lacks H3K4me3, resulted in a reduction of both H3K4me2 and H3K4me1 (Fig. 8C, lanes 2). Therefore, results obtained in this chapter provide evidence that Jhd2 can demethylate H3K4me1 *in vivo* and, like its human homologs (JARID1A and JARID1B), it targets all forms of K4-methylated H3 for demethylation *in vivo*.

Function of Jhd2 in Transcriptionally Active and Inactive Chromatin Regions

Several studies have identified Jhd2 as an H3K4 specific demethylase in yeast (88-90, 99). However, evidence for its occupancy and distribution on chromatin has been lacking. Our ChIP analyses demonstrated for the first time that Jhd2 binds to the promoter and coding regions of genes with either high (*PMA1*) or low (*HSP104*) expression (Figs. 9B and 10B). Moreover, deletion or overexpression of *JHD2* resulted in a two-fold increase or decrease in H3K4me3 levels at the promoter and ORF regions of *PMA1*, respectively (Fig. 9A). Thus, these results suggest that Jhd2 might be actively recruited during gene transcription to dynamically regulate H3K4 methylation levels.

Besides active genes, I also showed that Jhd2 functions during the activated state, the repressed (un-induced) state and the attenuation phase following repression of the inducible *INO1* gene. Similar to its association with the constitutively expressed genes, Jhd2 also associates with the 5' ORF region of *INO1* during transcriptional induction (Fig. 12B). However, the levels of Jhd2 at the induced state are 2-fold less as compared to the initial repressed state (Fig. 12B). While this decrease in Jhd2 levels might account for the 4-fold increase in the H3K4me3 levels following induction, H3K4me3 levels were not increased in the activated state of *INO1* in the absence of Jhd2 (Fig. 12A). Therefore, these data suggest that even though Jhd2 is present at *INO1* during the activated state, it might play only a minor role in regulating the H3K4me3 levels, and the robust increase in H3K4me3 levels during *INO1* induction is a result of the dominant Set1/COMPASS mediated methylation. I found that during re-repression, the levels of H3K4me3 at the 5' ORF of *INO1* were decreased rapidly in the WT, but not in *jhd2Δ* (Fig. 12A). Furthermore, my ChIP data also revealed that Jhd2 dissociates from the *INO1* 5' ORF region upon induction and quickly re-associates with this region upon re-repression (Fig. 12B). Thus, Jhd2 might play a role in the rapid repression of these induced genes by actively removing this H3 modification mark upon re-repression. To the best of my knowledge, this is the first demonstration that shows the dynamics of histone demethylation and chromatin occupancy of a JmjC-containing protein during activation and repression of an inducible gene.

Similar to *INO1*, H3K4me3 levels are increased during the *GALI* gene re-repression in the absence of Jhd2 (99). However, it is not known whether H3K4 demethylation by Jhd2 is sufficient to reestablish the repressed state of *GALI*. ChIP analysis did not detect

any prolonged occupancy of Rpb1 (the largest subunit of RNA polymerase II) on *INO1* in *jhd2Δ* upon reestablishment of its repression (Fig. 12D), suggesting the involvement of other mechanism(s) in the re-repression of *INO1* and perhaps *GALI*. Indeed, deletion of both *JHD2* and *JHD1*, an H3K36 specific demethylase, led to a higher *GALI* RNA levels during induction than those in the WT or single deletion mutants (99). These findings suggest that Jhd2 and Jhd1 (i.e., H3K4 and H3K36 demethylation) might play a redundant role in the re-repression of activated genes in yeast. Altogether, results in this chapter demonstrate that Jhd2 can dynamically associate with chromatin to modulate H3K4 methylation levels on both active (*PMA1* and *HSP104*) and repressed (*INO1*) genes in yeast. These observations are in contrast to the JARID1 family of H3K4 demethylases from various species, which exert their effects only on repressed genes (87).

Jhd2 is important for maintaining normal telomeric silencing (88). In addition, demethylation of H3K4 has been proposed to be a rate-limiting step in the formation of silent chromatin at the mating type loci, as loss of *JHD2* delayed the establishment of silencing in these regions (101). However, there is no evidence that Jhd2 localizes to these regions to exert its effect on the formation of silent chromatin. My CHIP data showed that when overexpressed, Jhd2 localized and reduced H3K4me3 levels across the telomeric regions of the right arm of chromosome VI (TEL06R) (Fig. 11). In keeping with the fact that H3K4 is hypomethylated at telomeres and silent mating type loci (126), these results suggest that Jhd2 plays an active role in maintaining low levels of H3K4 methylation required for the formation of silent chromatin in these transcriptionally inactive regions.

CHAPTER IV

THE JMjN-JMjC INTERACTION IN Jhd2 IS CRITICAL FOR ITS PROTEIN STABILITY MEDIATED BY THE E3 LIGASE NOT4

Introduction

Jhd2 contains three evolutionally conserved domains: JmjN, PHD, and JmjC (Fig. 13A). As in other JmjC-containing histone demethylases, the JmjC domain in Jhd2 possesses the enzymatic activity that catalyzes the demethylation reaction (82, 88, 99, 120). However, the roles of JmjN domain and PHD finger in regulating the demethylase function of Jhd2 are unknown. Interestingly, a JmjN domain is never found as a stand-alone motif (127). Moreover, many JmjC-containing histone demethylases contain both the JmjN and JmjC domains (119, 127-128), suggesting a structural/functional linkage between these two domains that contributes to the regulation of demethylase function. Indeed, crystal structures have shown that the JmjN domain interacts with the JmjC domain in JMJD2A (an H3K9/K36 demethylase) and Rph1 (an H3K36 demethylase) (102, 129). In addition, the JmjN domain is required for the demethylase function of JMJD2 family members (84, 130). Therefore, the JmjN domain in Jhd2 may also play a role in mediating the demethylation of H3K4, and it is important to understand the mechanism that regulates the function of Jhd2 through its JmjN domain. In this chapter, I will describe experimental evidence demonstrating that the interaction between the JmjN and JmjC domains in Jhd2 mediates the protein's structural integrity and is critical for its protein stability. I will also present data showing that the E3 ligase

Not4 plays a role in monitoring the JmjN-JmjC inter-domain interaction in Jhd2 and targets the structurally defective Jhd2 protein for degradation through the proteasome pathway.

Results

The Cofactor-binding Residues and the PHD Finger are Important for Jhd2 Activity

The JmjC domain-containing enzymes require iron (Fe^{2+}) and α -ketoglutarate (α -KG) as cofactors for their activities (82). All the highly conserved cofactor-binding residues, except Y346 (one of the α -KG binding residues), reside in the JmjC catalytic domain of Jhd2 (Fig. 13A). Besides the JmjC domain, Jhd2 also contains a JmjN and a PHD finger (Fig. 13A). To investigate the importance of these different domains for Jhd2 function, I created point mutations in the conserved residues that bind α -KG (Y346A) or Fe^{2+} (H427A), or reside in the PHD finger (H261A). As compared to the WT, overexpression of these *jhd2* mutant alleles showed that while *jhd2(H261A)* and *jhd2(Y346A)* caused only a modest decrease in H3K4me3 levels, *jhd2(H427A)* had no apparent reduction (Fig. 13B). Thus, binding to cofactors and maintaining an intact PHD finger are important for the function of Jhd2 *in vivo*.

T359R, a Substitution Mutation Corresponding to a Human SMCX Mutation Linked to Mental Retardation, Affects both the Demethylase Function and Global Protein Level of Jhd2

Mutations in SMCX/JARID1C, a human homolog of Jhd2, have been associated with X-linked mental retardation (XLMR) (96, 131-132). Patients carrying one of the well-

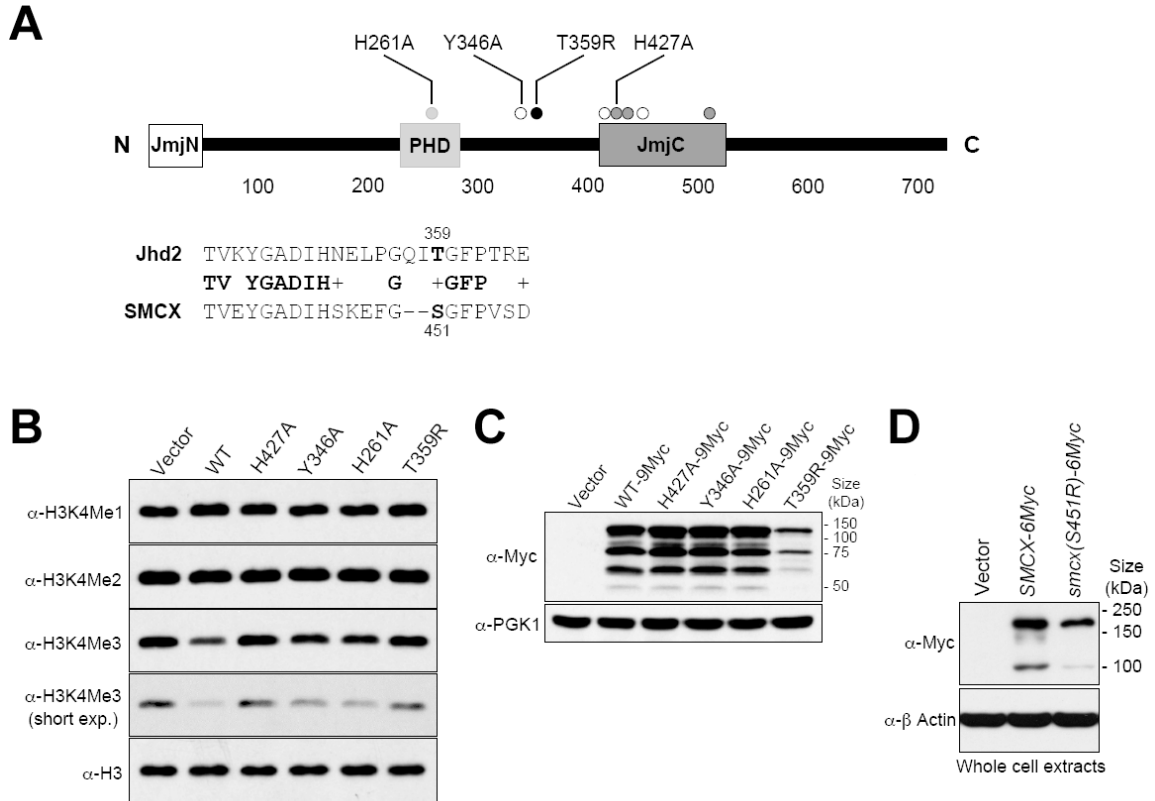


Figure 13. Mutations in the conserved regions of Jhd2 can affect its activity and overall protein levels. (A) Schematic representation and domain locations of Jhd2. The three conserved domains, JmjN, PHD finger and JmjC, are shown. *Dark gray circles*, residues that bind to the cofactor ferrous ion (Fe^{2+}); *white circles*, residues binding to the cofactor α -ketoglutarate (α -KG); *light gray* and *black circles*, a conserved residue (H261) in the PHD finger and a conserved residue (T359) corresponding to a human mental retardation-linked mutation site, respectively. Alignment of the Jhd2 sequence flanking the T359 residue to the SMCX sequence flanking one of the sites mutated in X-linked mental retardation (S451) is also shown. (B) Western blot analysis of H3K4 methylation levels in crude nuclear extracts from cells overexpressing the WT *JHD2* or its mutants. (C) Western blot analysis of the levels of Jhd2-9Myc or its mutant derivatives in the whole cell extracts (WCEs). The level of Pgk1 serves as a control for total protein loading. (D) Whole cell extracts were prepared from HeLa cells expressing 6Myc-tagged *SMCX* or the mutant (*smcx-S451R*), and protein levels were examined using α -Myc. The level of β -actin serves as a control for total protein loading.

characterized XLMR mutations in SMCX (S451R) developed mental retardation and also showed mild deformities in the tongue and fingers (131). However, the molecular consequence(s) of this mutation was not known. The S451 residue resides in a region that is highly conserved from yeast to human (Fig. 13A, bottom panel) (119). To investigate the effect of S451R on SMCX function *in vivo*, I generated a corresponding mutation T359R in Jhd2. Unlike the overexpression of the WT *JHD2*, overexpression of *jhd2(T359R)* did not reduce H3K4me3 levels (Fig. 13B, lane 6), suggesting that this mutation might abrogate the enzymatic activity and create a null allele of Jhd2. Interestingly, the T359R mutation also resulted in a severe reduction in the steady-state protein levels as compared to the WT *JHD2* and other *jhd2* alleles (*H427A*, *H261A* or *Y346A*) (Fig. 13C). This result suggests that the T359 residue might be important for regulating the protein stability of Jhd2. Next, I examined whether the residue S451 in SMCX is important for maintaining protein stability in human cells. To this end, *SMCX-6Myc* and *smcx(S451R)-6Myc* were ectopically expressed in HeLa cells. Western analyses revealed that similar to Jhd2(T359R), the total protein levels of *smcx(S451R)-6Myc* were lower than those of the WT *SMCX-6Myc* (Fig. 13D), suggesting a conserved role for residues T359 and S451 in maintaining the protein stabilities of Jhd2 and SMCX, respectively. Importantly, this decrease in protein levels of *smcx(S451R)* likely accounts for the observed defects in patients harboring this mutation (131).

The Structural Integrity of Jhd2 is Important for its Protein Stability

Although the JmjN domain is highly conserved, it does not exist in all the JmjC

domain-containing histone demethylases (*119*). For example, JmjN domain is absent in the H3K36 demethylases, such as human JHDM1 (JHDM1A and JHDM1B) and yeast Jhd1. To determine the contribution of this domain to Jhd2 function, I created a deletion derivative lacking the JmjN domain [Jhd2(JmjN Δ)] and examined the effect of this truncation on the ability of Jhd2 to remove H3K4 methylation (Fig. 14A). Unlike the WT, overexpression of *jhd2(JmjN Δ)* did not reduce H3K4 methylation (Fig. 14B), indicating that the JmjN domain is essential for Jhd2 function. Intriguingly, protein levels of the overexpressed *jhd2(JmjN Δ)* appeared reduced compared to the WT (Fig. 14B). Indeed, a drastic reduction in steady-state levels of Jhd2(JmjN Δ) is evident when the proteins are expressed from the endogenous *JHD2* promoter using a low copy (*CEN*-based) plasmid (Fig. 14C). This result suggests that the structural integrity of Jhd2 is important for maintaining its whole-cell protein levels. In contrast, levels of Jhd2(JmjN Δ) in the nuclear extracts were higher than the WT (Fig. 14C). Given the increase in nuclear Jhd2(JmjN Δ) levels, it is conceivable that the lack of H3K4 demethylation in this mutant (Fig. 14B) is due to the truncation and not due to reduced global protein levels (Fig. 14C, top panel). Taken together, these novel findings put forth a possibility that the overall protein stability and nuclear localization of Jhd2 might be regulated by its protein structure.

Previous studies have revealed the presence of two SMCX splice variants in human cells and both proteins catalyze *in vivo* H3K4 demethylation. Whereas, the longer form of SMCX is predominantly a nuclear protein (*91, 97, 133*), its shorter splice variant (lacking the C-terminal 120 amino acids) is present at very low levels in the nucleus (*111*). Taken together, these studies and my findings suggest that controlling the nuclear localization of SMCX and Jhd2 might be a mode to regulate their H3K4 demethylation on chromatin.

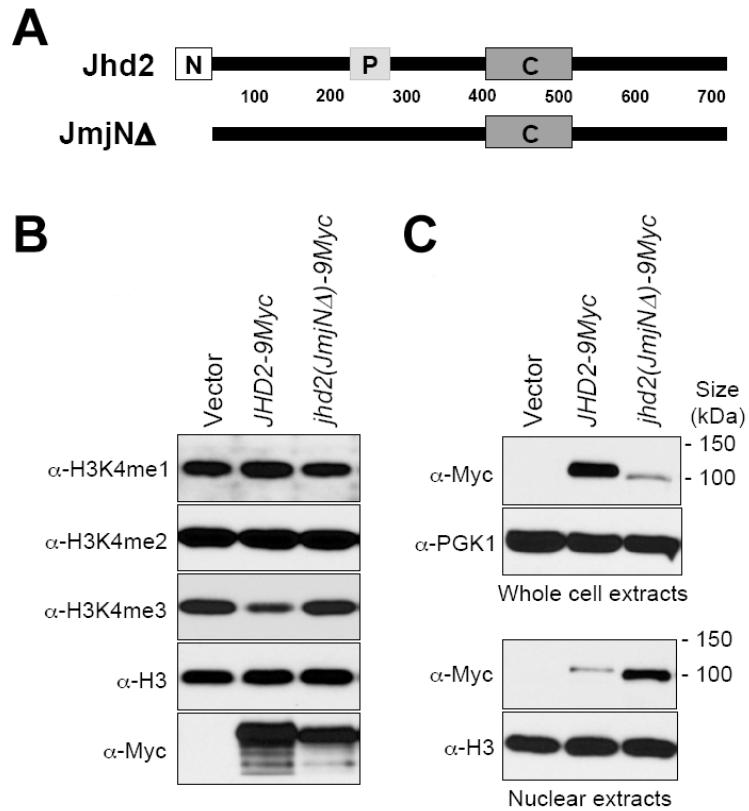


Figure 14. The JmjN domain in Jhd2 is important for its global protein level and subcellular localization. (A) Schematic representation of the Jhd2 and its truncation mutant. The JmjN, PHD and JmjC domains are represented as shown in Figure 13A. (B) Crude nuclear extracts were prepared from *jhd2Δ* strain containing vector alone or overexpressing the WT or mutant *JHD2*. The levels of H3K4 methylation were examined by Western blotting. (C) The levels of Jhd2 and Jhd2(JmjNΔ) in the WCEs (top panel) and nuclear extracts (bottom panel) were examined by Western blotting. Pgk1 and H3 were used as loading controls in the WCEs and nuclear extracts, respectively.

Therefore, I examined the levels of Jhd2 and its mutant derivatives in addition to Jhd2(JmjN Δ) within the nucleus (Fig. 15A). As expected, all deletions of Jhd2 abolished its function as a demethylase (Figs. 14 B and 15B). Moreover, except for the C-terminal deletion mutant [Jhd2(C Δ)], all the mutants showed decreased steady-state protein levels and increased nuclear protein levels similar to Jhd2(JmjN Δ) (Fig. 15C). These results show that any change in the structural integrity of the region encompassing JmjN and JmjC domains of Jhd2 that abrogates its enzymatic function will lead to a decrease in its global protein levels, but increase its nuclear protein levels.

Next, I tested whether these changes in Jhd2 levels in the whole-cell and nuclear extracts are due to the loss of its enzymatic activity. To this end, the whole-cell and nuclear levels of the catalytically-dead allele, Jhd2(H427A), were examined (Fig. 13B). As shown in Figure 17C, both the global and nuclear levels of Jhd2(H427A) are similar to the WT. Thus, the loss of enzymatic activity alone does not alter protein levels of Jhd2 and strongly implicates the protein structural perturbations induced by the deletions as the primary cause for the observed changes in its global and nuclear protein levels. Given that the human XLMR mutation-mimetic change in Jhd2, T359R, also showed a drastic reduction in steady state protein levels (Figs. 13C and 16) and loss of demethylase function (Fig. 13B) similar to that seen for the deletion mutants (Figs. 14 and 15), I assessed the protein levels of this point mutant in the nucleus. Indeed, similar to the deletion derivatives, the nuclear protein levels of Jhd2(T359R) are increased as compared to the WT (Fig. 16), suggesting that this point mutation alone is sufficient to perturb the structural integrity of Jhd2 and alter its global and nuclear protein levels. Collectively, these findings suggest that the protein stability of Jhd2 might be regulated by its structure and not by its enzymatic activity.

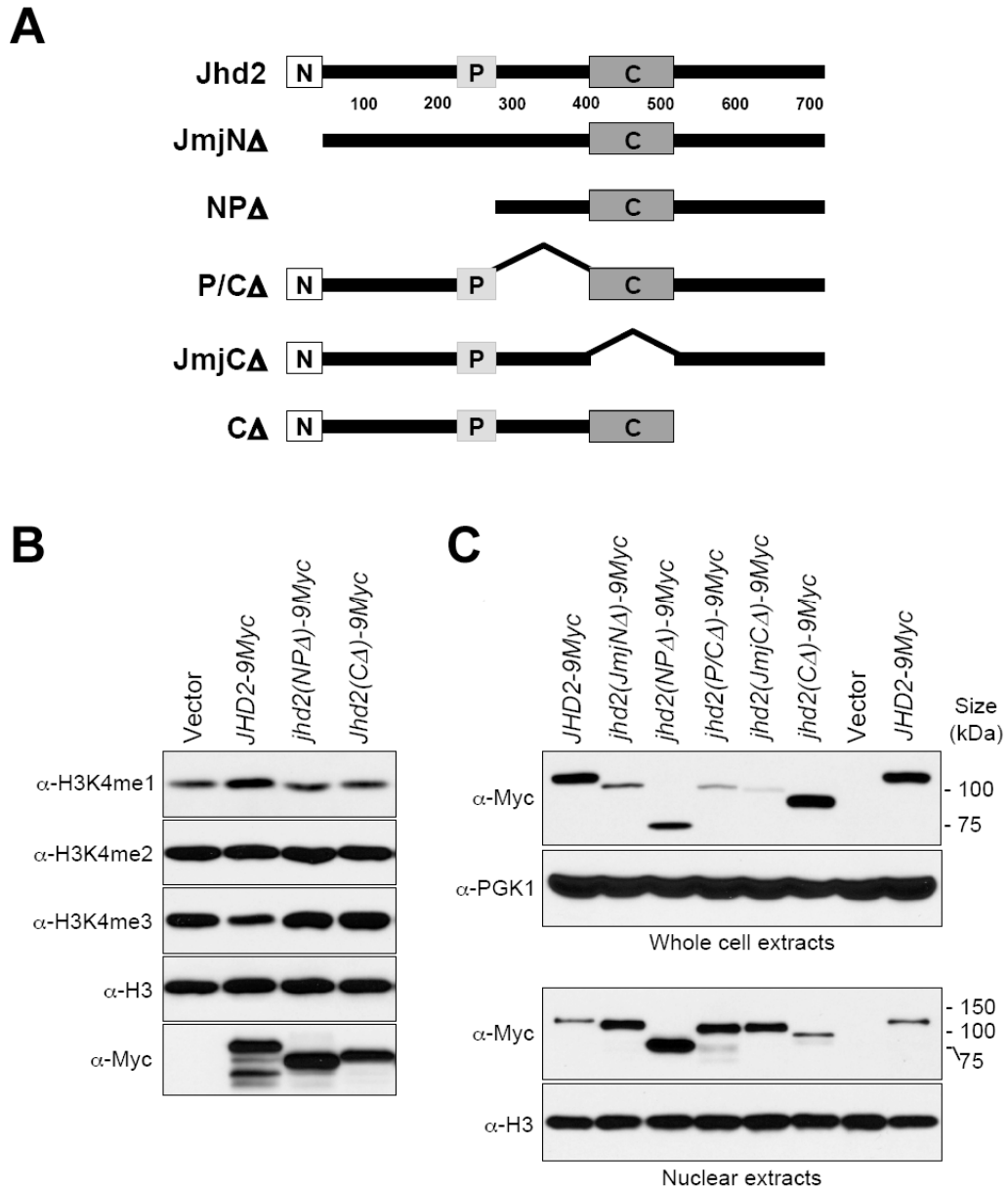


Figure 15. The global protein level and subcellular localization of Jhd2 are sensitive to its structural integrity. (A) Schematic representation of the Jhd2 and its truncation mutants. The JmjN, PHD and JmjC domains are represented as shown in Figure 13A. (B) Crude nuclear extracts were prepared from *jhd2Δ* strain containing vector alone or overexpressing the WT or mutant *JHD2*. The levels of H3K4 methylation were examined by Western blotting. (C) Western blot analysis of the levels of WT Jhd2 and its truncation mutants in the WCEs (top panel) and nuclear extracts (bottom panel).

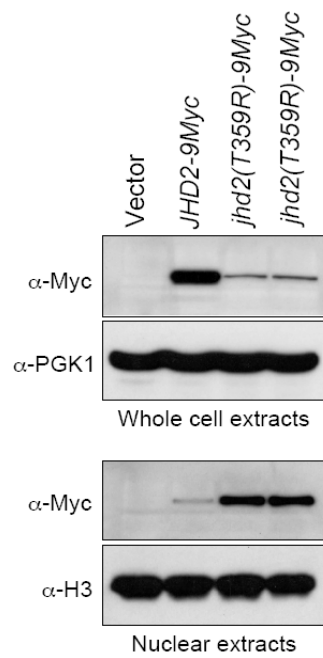


Figure 16. Western blot analysis of the levels of Jhd2 and Jhd2(T359R) in the WCEs and nuclear extracts.

To test whether the protein stability of Jhd2 is compromised by mutations, I examined the global levels of WT Jhd2 and its mutants following inhibition of protein synthesis using cycloheximide. As shown in Figure 17A, deletion of JmjN domain causes rapid degradation of Jhd2. Compared to WT Jhd2 levels, Jhd2(JmjN Δ) is barely detectable at 20 min after cycloheximide treatment and it is completely absent at 40 min following the translational arrest. Recently, the E3 ligase Not4-mediated polyubiquitination followed by proteasomal degradation was shown to modulate the steady-state levels of Jhd2 (100). Therefore, I tested whether the compromised protein stability of Jhd2(JmjN Δ) is due to a high protein turnover mediated by the proteasome. Supporting this possibility, proteasomal inhibition using MG132 resulted in increased steady state levels of Jhd2(JmjN Δ) (Fig. 17B). I further tested whether Not4 is involved in this proteasome-mediated degradation of Jhd2(JmjN Δ). Indeed, the steady state levels of Jhd2(JmjN Δ) are restored nearly to WT levels in the *not4 Δ* strain (Fig. 17C), and this mutant protein is highly stabilized in cells lacking Not4 (Fig. 17D). These findings suggest a protein structure-monitoring role for Not4 in maintaining Jhd2 levels. Additionally, the nuclear protein levels of Jhd2(JmjN Δ) were increased in *not4 Δ* as compared to both WT Jhd2 and Jhd2(H427A) (Fig. 17C). Taken together, these findings reveal that the structural integrity of Jhd2 is a crucial determinant for maintaining its protein stability mediated by Not4.

The Interaction between JmjN and JmjC Domains is Important for Jhd2 Function

Crystal structure of the catalytic-core domain of human JMJD2A, an H3K9me3- and H3K36me3-specific demethylase, has revealed a physical interaction between the two

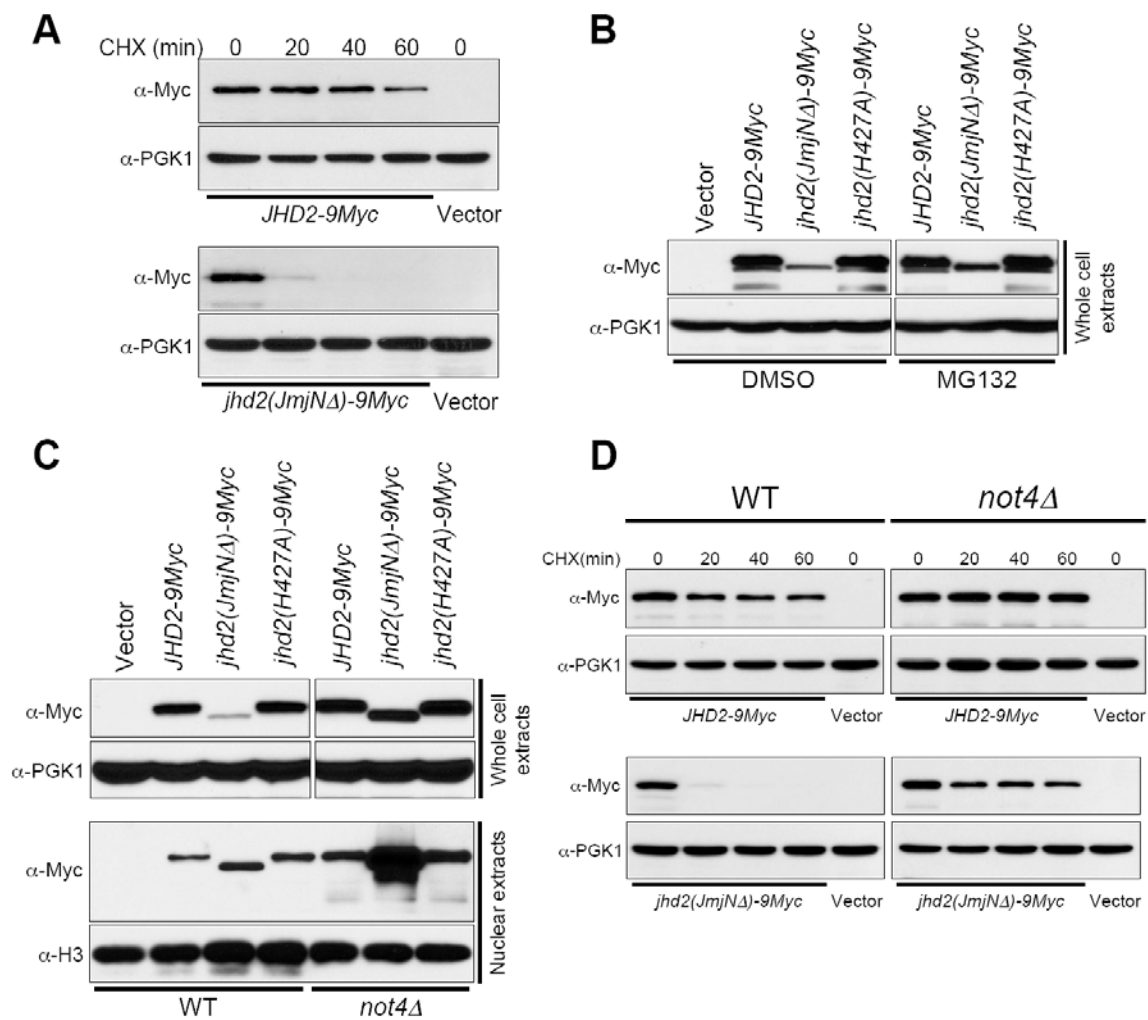


Figure 17. Loss of the JmjN domain in Jhd2 causes protein instability mediated by the E3 ligase Not4 and the proteasome. (A) Cells containing WT Jhd2 or Jhd2(JmjNΔ) mutant were treated with 35 μg/ml cycloheximide (CHX) for the indicated periods of time to terminate protein synthesis. Equal amount of WCEs were subjected to Western blotting using α-Myc and α-Pgk1 antibodies. (B) Western blot analysis of the levels of WT Jhd2 and its mutants in WCEs obtained from cells treated with DMSO (vehicle) or with MG132. (C) The levels of WT Jhd2 and its mutants in WCEs and nuclear extracts obtained from control (WT) or *not4Δ* strains were detected using α-Myc. (D) Western blot analysis of the levels of WT Jhd2 and Jhd2(JmjNΔ) mutant in WCEs obtained from control (WT) or *not4Δ* strains treated with cycloheximide (CHX) for the indicated time.

antiparallel β strands in its JmjN and JmjC domains (Fig. 18A) (102). The residues constituting each β strand of the JmjN and JmjC domains are highly conserved among the demethylases containing both these domains (119), implicating an important role for the inter-domain interactions in regulating demethylation. Indeed, it has been proposed that this JmjN-JmjC interaction might cause a conformational change in the JMJD2A catalytic-core to activate its enzymatic function (102). Although differing in their substrate specificity, the strong sequence similarity between the two β strands in JmjN and JmjC of JMJD2A and Jhd2 (Fig. 19A) suggests that an inter-domain interaction might also occur in Jhd2 to regulate its function. To test this possibility *in vitro*, I performed MBP pull-down assay using Jhd2(1-237)-MBP (encompassing JmjN) and GST-Jhd2(277-729) (encompassing JmjC) (Fig. 18B). Indeed, the JmjN-containing N-terminal part of Jhd2 interacted with its JmjC-containing C-terminal part *in vitro* (Fig. 18C). Next, to test my hypothesis that the JmjN-JmjC interaction in Jhd2 is important for its function *in vivo*, I mutated the conserved residues in the β strands in JmjN and JmjC domains of Jhd2 (Fig. 19A) and assessed their effects on its enzymatic function. Unlike the WT, overexpression of *jhd2(G34R)*, *jhd2(K37E)* and *jhd2(E507K)* did not reduce H3K4me3 levels (Fig. 19B), indicating that these conserved residues are important for Jhd2 function. Moreover, similar to *jhd2(T359R)* null mutant, the global protein levels are reduced and nuclear protein levels are increased in these *jhd2* mutants (Fig. 19C), suggesting that these mutations might also perturb the structural integrity and elicit the proteasome-mediated protein degradation response (100). Indeed, the protein stabilities of Jhd2(K37E) and Jhd2(E507K) are severely compromised (Fig. 20A), and MG132- mediated proteasomal inhibition resulted in increased steady state levels of these two Jhd2 mutants (Fig. 20B).

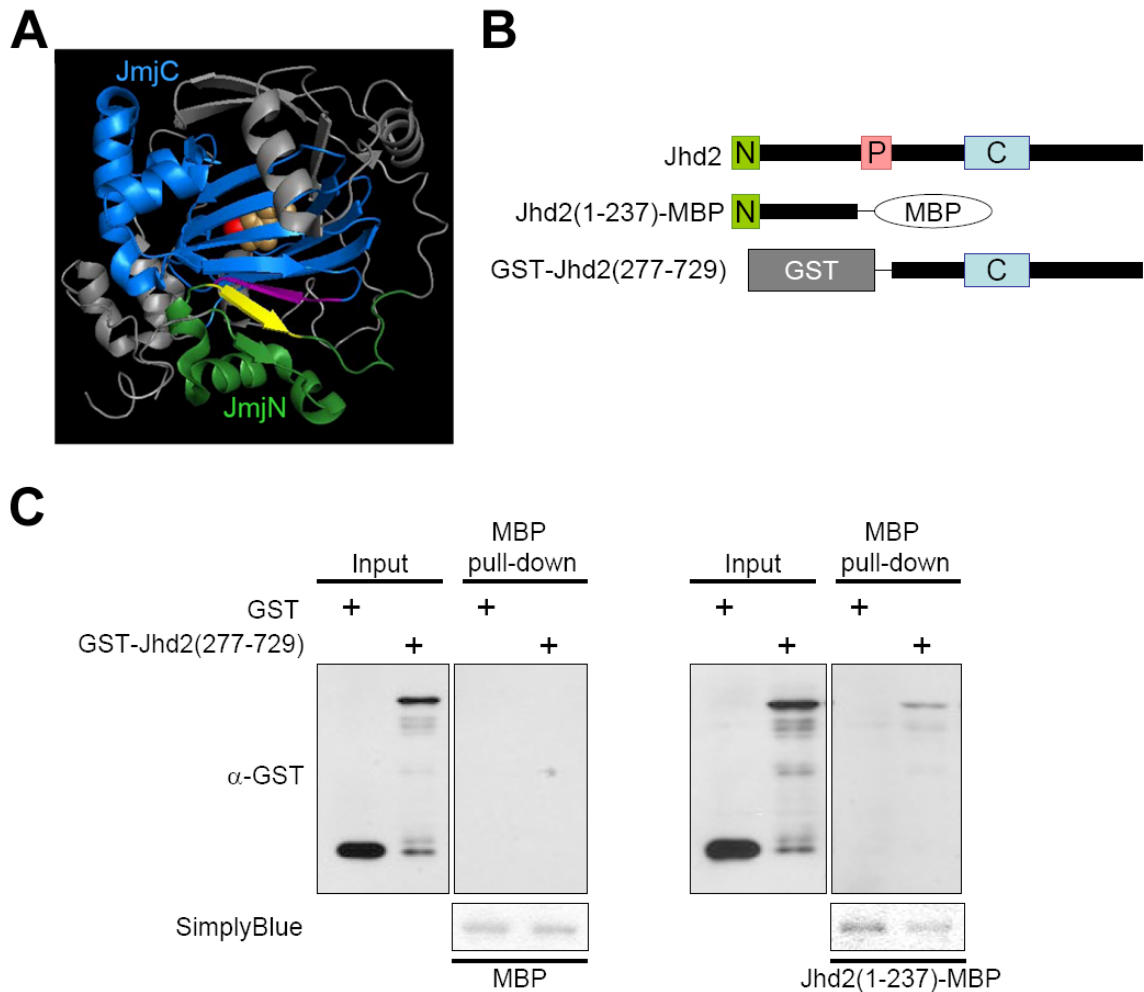


Figure 18. The N- and C-terminal parts in Jhd2 interact with each other. (A) The crystal structure of JMJD2A (PDB # 2GP5). The JmjN (green) and JmjC (blue) domains interact with each other through one β -strand in JmjN domain (yellow) and another one in JmjC domain (purple). The two cofactors, ferrous ion (red) and α -ketoglutarate (brown), are represented by the space-filling model. (B) Schematic representation of Jhd2(1-237)-MBP and GST-Jhd2(277-729). The JmjN (N; green), PHD (P; pink) and JmjC (C; blue) domains are shown. (C) *In vitro* MBP pull-down assay. The MBP- or Jhd2(1-237)-MBP-containing *E.coli* lysates (200 μ g total protein) were incubated with GST- or GST-Jhd2(277-729)-containing *E.coli* lysates (200 μ g total protein) and were pull-downed by the amylose-conjugated beads. After extensive washing, the MBP/Jhd2(1-237)-MBP-bound GST/GST-Jhd2(277-729) were eluted in sample buffer. *E.coli* lysates containing GST or GST-Jhd2(277-729) (1%, Input) and eluates (40%) were subjected to Western blot analysis using α -GST. An aliquot of the eluate (10%) was also used as a control to show the equal loading of MBP or Jhd2(1-237)-MBP, as detected using SimplyBlue stain.

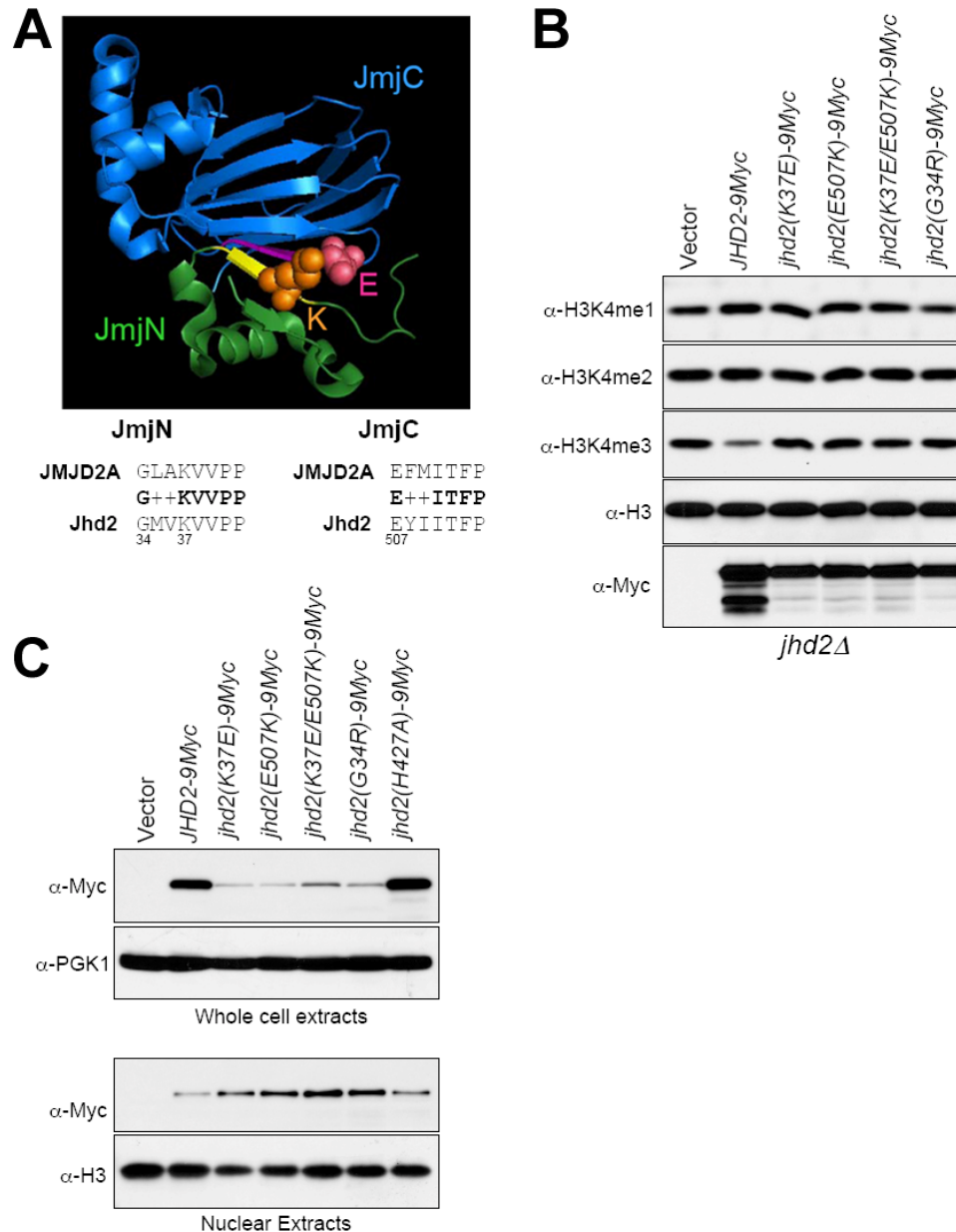


Figure 19. Residues that might mediate the JmjN-JmjC interaction are critical for the global protein levels and subcellular localization of Jhd2. (A) Top panel: the crystal structure of JmjN and JmjC domains of JMJD2A are represented as shown in Figure 18A. The two residues, lysine in JmjN domain (orange) and glutamate in JmjC domain (pink), involved in ionic interaction are represented by the space-filling model. Bottom panel: the protein sequence alignment of residues involved in the JmjN-JmjC interaction of JMJD2A and Jhd2. + denotes similar residues. (B) Western blot analysis of H3K4 methylation levels in the crude nuclear extracts prepared from *jhd2Δ* containing high copy plasmid alone or overexpressing WT *JHD2* or its mutants. (C) WCEs (top panel) and nuclear extracts (bottom panel) were obtained from *jhd2Δ* strain containing low copy plasmids containing WT *JHD2* or mutant variants and subjected to Western blotting using α -Myc, α -Pgk1, and α -H3 antibodies.

The close proximity between K37 in JmjN domain and E507 in JmjC domain suggests a charge-based interaction might occur between these two residues (Fig. 19A). Therefore, I created a charge-switching double mutation (K37E, E507K) and tested whether it can restore Jhd2 function as compared to the single site mutations (K37E or E507K). Overexpression of *jhd2(K37E/E507K)* did not reduce H3K4 methylation (Fig. 19B), indicating a disruption of the enzyme function due to the introduced mutations. However, its whole-cell protein levels were modestly increased as compared to *jhd2(K37E)* or *jhd2(E507K)* (Figs. 19C and 20B). This result suggests that a charge-based interaction might occur between K37 and E507. However, the charged-side chains in K37E and E507K might not be present in a correct orientation for efficient inter-domain interaction, leading to the loss of enzyme function. Alternatively, maintaining a positively charged residue at amino acid position 37 in JmjN domain and/or a negative one at position 507 in JmjC domain might be important for the structural integrity and for inter-domain interactions. Supporting this possibility, only the overexpression of a mutant *jhd2* containing the charge-conserved substitution mutation (K37R), but not *jhd2(K37A)* and *jhd2(K37Q)*, retained demethylation function and reduced H3K4me3 levels similar to overexpression of the WT (Fig. 21A).

To assess how mutations of the K37 residue in Jhd2 affect its *in vivo* demethylase function toward H3K4me2 and -me1, I overexpressed the WT *JHD2* and its mutant alleles (K37R, K37A and K37Q) in a yeast strain lacking H3K4me3 due to the deletion of *SDC1*, a Set1-COMPASS subunit (*134*). Overexpression of the WT *JHD2* (Fig. 21B, lane 2) and *jhd2(K37R)*, but not *jhd2(K37A)* (Fig. 21B, lanes 3-4), reduced H3K4me2 and H3K4me1 in *sdc1Δ* as compared to the control (vector alone). Therefore, the K37

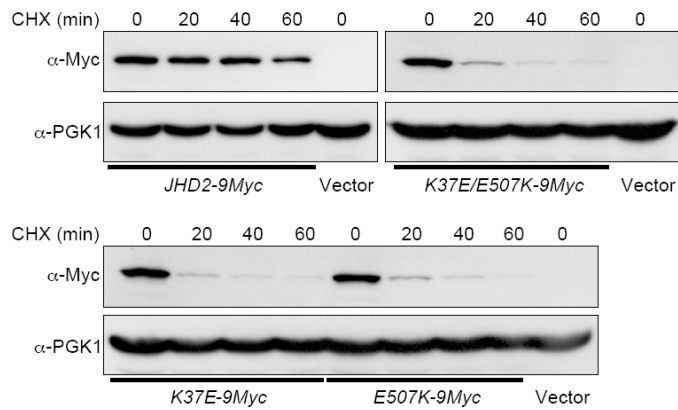
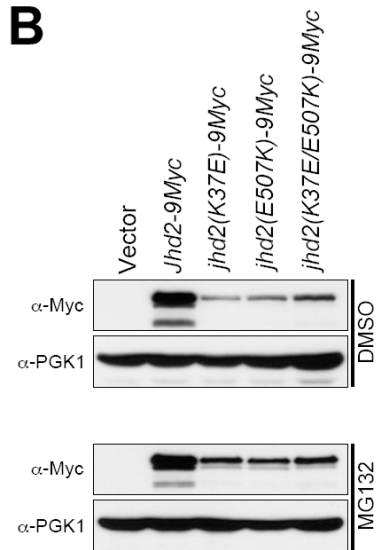
A**B**

Figure 20. Loss of the JmjN-JmjC inter-domain interaction in Jhd2 causes protein instability mediated by the proteasome. (A) Western blot analysis of the levels of WT Jhd2 and its mutants in WCEs obtained from cells treated with cycloheximide (CHX) for the indicated periods of time. **(B)** Western blot analysis of the levels of WT Jhd2 and its mutants in WCEs obtained from cells treated with DMSO (vehicle) or with MG132.

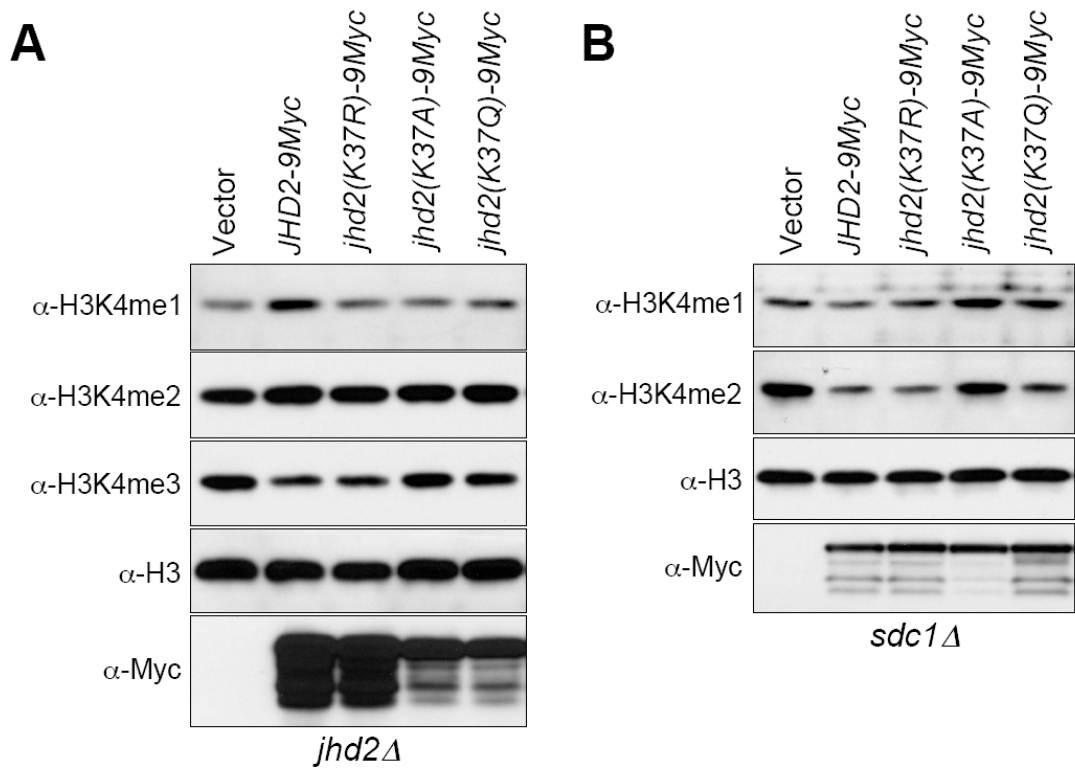


Figure 21. The positive charge at amino acid position 37 in JmjN domain is important for the demethylase function of Jhd2. (A, B) Western blot analysis of H3K4 methylation levels in the crude nuclear extracts prepared from *jhd2Δ* (A) or *sdc1Δ* (B) cells overexpressing WT *JHD2* or its mutant derivatives.

residue in Jhd2 is also critical for the demethylation of H3K4me1 and -me2 catalyzed by Jhd2. Interestingly, overexpression of the acetylation-mimetic *jhd2(K37Q)* allele, which cannot demethylate H3K4me3 (Fig. 21A, lane 5), reduced only H3K4me2 levels (Fig. 21B, lane 5). Given that the K→Q substitution in *jhd2(K37Q)* is an acetylation-mimetic mutation, I hypothesized that the JmjN-JmjC interaction is modulated by acetylation of K37 within the JmjN domain. To test this hypothesis, an N-terminally Flag-tagged Jhd2 was purified and subjected to mass spectrometry to determine whether the K37 residue in Jhd2 was acetylated. The Flag-Jhd2 and Flag-Jhd2(K37R) mutant were also purified and subjected to Western blot analysis using an α -acetylated-lysine antibody to examine the K37 acetylation. Neither of the two methods provided evidence showing that Jhd2 is acetylated at the K37 residue (data not shown). However, the possibility that the K37 acetylation in Jhd2 only occurs upon some specific cellular conditions cannot be ruled out. Nevertheless, my results suggest that the inter-domain interaction between JmjN and JmjC domains through their two β strands might play a role in modulating the demethylation function of Jhd2 towards different methylation states of H3K4.

Discussion

The Role of JmjN Domain in Mediating Jhd2 Demethylase Function

Crystal structure of the catalytic-core domain of human JMJD2A (an H3K9me3- and H3K36me3-specific demethylase) has shown extensive contacts between the two antiparallel β strands in its JmjN and JmjC domains (Figs. 18A and 19A) (102). Given the strong sequence similarity between the β strands in JmjN and JmjC of JMJD2A and

Jhd2 (Fig. 19A), my results suggest that this JmjN-JmjC interaction might also occur in Jhd2 and importantly, this inter-domain interaction is required for Jhd2 activity *in vivo* (Figs. 19B and 21A). Comparison of the substrate preferences of all known JmjC-containing histone demethylases have revealed that enzymes with only a JmjC domain prefer mono- and di-methylated substrates, whereas those containing both JmjN and JmjC domains (JmjN/JmjC) demethylate either di- and tri-methylated lysines or all forms of substrates (87). Therefore, the difference in substrate specificity, especially tri-methylated lysines targeted by the JmjN/JmjC-containing demethylases, is likely to be imparted by the JmjN domain through its interaction with JmjC. Indeed, I found that different amino acid substitutions at the conserved K37 in the JmjN domain exerted differential effects on Jhd2 function. While the charge-conserved mutation [*jhd2(K37R)*] maintained normal Jhd2 activity *in vivo*, *jhd2(K37A)* totally abolished demethylation (Figs. 21A-B). In contrast, *jhd2(K37Q)* demethylated only H3K4me₂, but not H3K4me₃ and H3K4me₁ (Figs. 21A-B). These results suggest that the inter-domain interaction between the two β strands of JmjN and JmjC might play a role in modulating the substrate specificity of Jhd2.

Regulation of Not4-mediated Protein Degradation of Jhd2

The results from this study showed that except for the C-terminal deletion mutant [Jhd2(C Δ)], all the Jhd2 truncation mutants showed decreased steady-state protein levels (Fig. 15C). In contrast, it has been shown that deletion of the PHD finger alone had no apparent effect on Jhd2 protein levels (100). These findings suggest that any change in the structural integrity of the region encompassing JmjN and JmjC, but not the PHD

finger, domains of Jhd2 can lead to a decrease in its global protein levels. In keeping with this hypothesis, I found that point mutations in the conserved antiparallel β strands involved in JmjN-JmjC inter-domain interaction (Fig. 19C), but not those in the conserved C4HC3 zinc-binding motif of the PHD finger (Fig. 22B), also caused a decrease in Jhd2 protein levels. Collectively, these results indicate that any perturbation of the proper inter-domain interaction between the JmjN and JmjC domains can adversely affect the steady state levels of Jhd2.

The mechanism by which Not4 recognizes and targets Jhd2 for degradation is not fully understood. Importantly, I showed that the Jhd2(JmjN Δ) protein is stabilized and its global levels were restored nearly to the WT levels in the *not4 Δ* strain (Figs. 17C-D), suggesting a protein structure monitoring role for Not4 in controlling Jhd2 levels. However, the Jhd2(JmjN Δ) mutant is apparently less stable than the WT Jhd2 even in the absence of Not4 (Fig. 17D), indicating that other parallel pathway(s) may also play a role in the structural quality control of Jhd2. Collectively, based on my findings, I propose that Not4 might modulate the protein levels of Jhd2 by monitoring its structural integrity, especially the proper interaction between the JmjN and JmjC domains.

Jhd2 localizes to both cytoplasm and nucleus (135). The differential subcellular localization of the two SMCX (human homolog of Jhd2) splice variants suggests that controlling the nuclear localization of SMCX and Jhd2 might be a way to regulate their H3K4 demethylation on chromatin (91, 97, 111, 133). Intriguingly, while the deletion and point mutations of Jhd2 resulted in a decrease in steady state levels, their levels in the nucleus were all higher than the WT Jhd2 (Figs. 15C, 16 and 19C). Furthermore, in the *not4 Δ* mutant, the global Jhd2(JmjN Δ) levels were increased and are equivalent to the

WT, but its nuclear levels were dramatically increased and exceed the WT levels (Fig. 17C). These results reveal a link between the structural integrity and subcellular localization of Jhd2. The observation in this study is reminiscent to that seen for the yeast transcription factor Msn2, which upon activation by certain stress conditions (glucose exhaustion, chronic stress or low protein kinase A activity) accumulates in the nucleus (136) and an increase in its protein degradation under these conditions also results in a reduction in its overall whole-cell protein levels. Therefore, I propose that through an unknown mechanism(s) (*e.g.*, increased nuclear import or decreased nuclear export), the Jhd2 mutants accumulate in the nucleus. Subsequently, due to the improper JmjN-JmjC inter-domain interaction, the altered-forms Jhd2 are then targeted for rapid degradation by Not4 leading to lower whole-cell protein levels than the WT Jhd2.

Finally, like Jhd2(P/C Δ) (Fig. 15C), Jhd2(T359R) also displayed lower steady state, but higher nuclear, levels than Jhd2 (Figs. 13C and 16). These results indicate that residues, including T359, located between the PHD finger and JmjC domain are important for the structural integrity of Jhd2. Interestingly, the global levels of human smcx(S451R), a mutation corresponding to Jhd2(T359R), were lower than the WT SMCX/JARID1C (Fig. 13D), suggesting a conserved role for residues T359 and S451 in maintaining the protein stabilities of Jhd2 and SMCX, respectively. Since human Not4 can also polyubiquitinate SMCX *in vitro* (100), my findings suggest the presence of a conserved pathway involving Not4 that modulates the protein stability of both yeast Jhd2 and human SMCX. In addition, deletion of the JmjN domain from JMJD2A also resulted in a reduction in its global protein levels (102, 137). The intriguing similarity in the phenotypes of Jhd2 and JMJD2A mutants due to a loss of JmjN domain further implies

that the protein stability of JARID and JMJD2 family members may be regulated by a conserved mechanism.

CHAPTER V

THE PHD FINGER IN JHD2 IS IMPORTANT FOR ITS CHROMATIN ASSOCIATION BY INTERACTING WITH HISTONE H2A

Introduction

How the chromatin association of Jhd2 is regulated is an important question for further understanding its function in transcriptional regulation. Intriguingly, Jhd2 contains a plant homeodomain (PHD) finger between the JmjN and JmjC domains (Fig. 13A). The PHD finger was first identified in an Arabidopsis protein, HTA3.1 (138), and this conserved domain is present in many proteins involved in modulating chromatin structure and dynamics. In 2006, the PHD fingers in ING2 and BPTF were demonstrated to recognize trimethylated H3K4 and mediate the chromatin association of these two proteins (37, 39, 41). Subsequently, other PHD fingers were also reported to bind either trimethylated H3K4, unmodified H3K4, trimethylated H3K9, or acetylated H3/H4 (43, 91, 103, 139). These findings suggest that the PHD finger in Jhd2 may play a role in mediating its chromatin association and therefore, contribute to the removal of the H3K4 methylation mark. In this chapter, I will show the experimental results demonstrating that the demethylase function and normal chromatin association of Jhd2 is indeed dependent on its PHD finger. Evidence supporting the possibility that the N-terminal region in H2A is critical for the chromatin-Jhd2 PHD finger interaction will also be described. In summary, the findings uncovered in this chapter provide important insights into the regulation of H3K4 demethylation by Jhd2.

Results

The PHD Finger is Required for the Demethylation Activity and Chromatin Association of Jhd2

The PHD finger between JmjN and JmjC domains of the JARID1 family of H3K4 demethylases contains a conserved C4HC3 zinc-binding motif (Fig. 13A) (119). Based on the solution structure of the PHD finger in human SMCY (JARID1D, an H3K4 demethylase; PDB # 2E6R), the three cysteine residues (C1, C2 and C6) together with the histidine residue (H5) present in Jhd2 PHD finger can be predicted to form the first zinc-finger, while the remaining cysteine residues (C3, C4, C7 and C8) form the second one (Fig. 22A). To determine the role for these two zinc-coordinating sites in Jhd2 function, I disrupted the PHD finger by creating two double mutants, *jhd2(C1, 2A)* and *jhd2(C7, 8A)*. Whereas, overexpression of *jhd2(C1, 2A)* resulted in a reduction of H3K4me₃, overexpression of *jhd2(C7, 8A)* had no apparent effect (Fig 22B). Moreover, only the overexpression of *jhd2(C1, 2A)* in *sdc1A* caused a reduction in H3K4me₂, but not *jhd2(C7, 8A)* (Fig. 22C). Collectively, these results show that disruption of the second zinc-binding site within the PHD finger abrogates the demethylase function and therefore, it is more critical for Jhd2 activity towards H3K4me₂ and H3K4me₃ than the first one.

Many, if not all, PHD-containing proteins associate with chromatin through the direct interaction between their PHD finger and the histones (140-141). Therefore, it is conceivable that the loss of demethylation in the PHD finger mutants may be due to a poor association of Jhd2 with chromatin. To test this possibility, *in vitro* nucleosome binding assays were performed. To obtain mononucleosomes, nuclei isolated from the WT yeast strain containing Flag-H2B were digested extensively with micrococcal nuclease

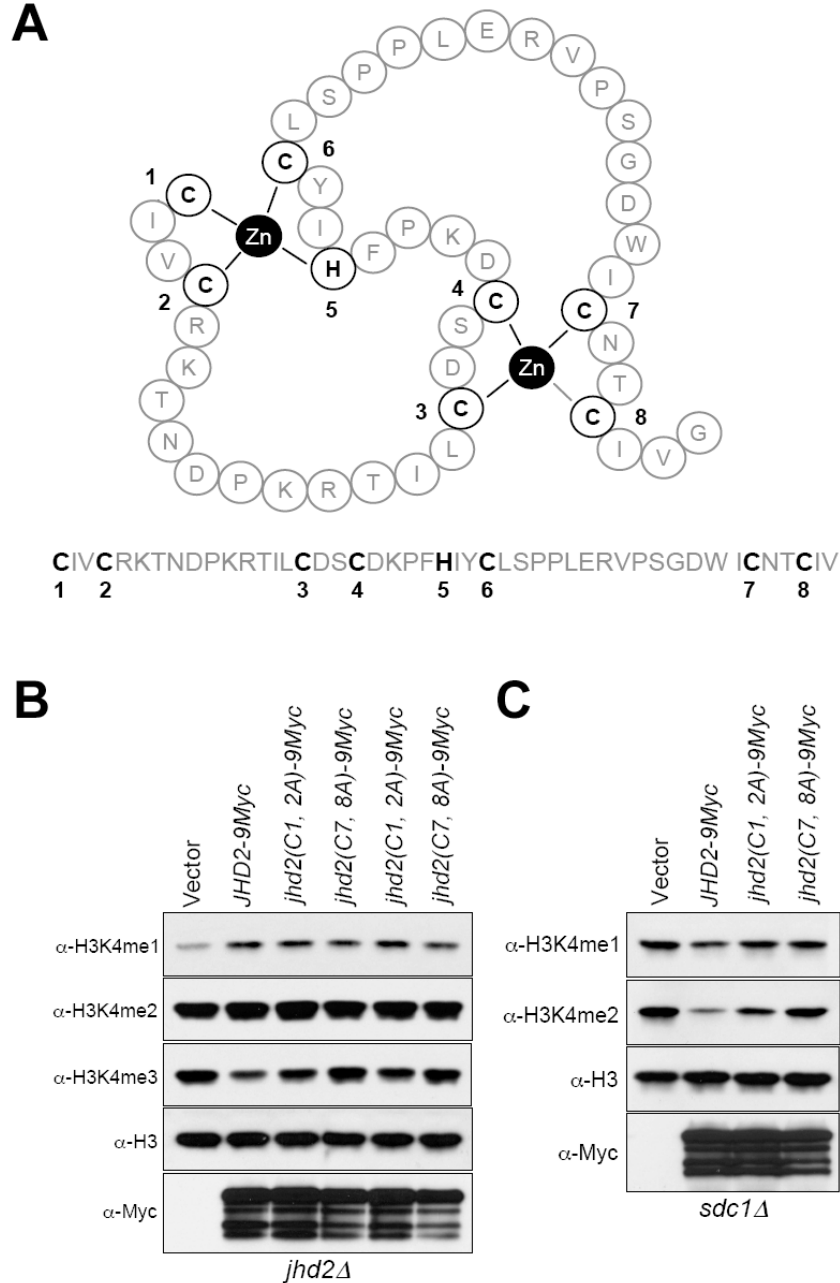


Figure 22. The two zinc fingers in PHD domain are important for the function of Jhd2 as an H3K4 demethylase. (A) A speculative structure for the PHD finger of Jhd2 as predicted by SWISS-MODEL, a knowledge-based protein-modeling algorithm (<http://swissmodel.expasy.org/>). The two zinc-coordinating sites each composed of four residues (cysteine or histidine) are shown. (B, C) Western blot analysis of H3K4 methylation levels in the crude nuclear extracts prepared from *jhd2Δ* (B) or *sdc1Δ* (C) strains overexpressing WT *JHD2* or PHD finger mutant variants.

(MNase) followed by immunoprecipitation using α -Flag agarose beads. Agarose gel electrophoresis of DNA isolated from the immobilized nucleosomes is ~150 bp in length, confirming the presence of mainly mononucleosomes (Fig. 23A). Subsequently, equal amounts of immobilized mononucleosomes were used to pull-down the purified, recombinant GST-tagged PHD finger of Jhd2 (GST-PHD) or its mutants [GST-PHD(C1, 2A) and GST-PHD(C7, 8A)]. As shown in Figure 23B, GST-PHD, but not GST alone, was able to interact with the immobilized nucleosome. However, compared to GST-PHD, both the PHD finger mutants [GST-PHD(C1, 2A) or GST-PHD(C7, 8A)] showed reduced binding to the nucleosome (Fig. 23B, lanes 7-8). This reduced chromatin binding of the PHD finger mutants agrees well with their debilitated demethylase activities as compared to the WT (Figs. 22B-C). However, GST-PHD(C7, 8A) showed better nucleosome binding than GST-PHD(C1, 2A) (Fig. 23B, lanes 7-8), even though only the *jhd2(C7, 8A)* PHD finger mutation abrogated the *in vivo* demethylation activity of Jhd2 (Figs. 22B-C). Therefore, to further confirm whether the PHD finger in Jhd2 is important for its *in vivo* chromatin association, ChIP assays were performed to assess the occupancy of C-terminally 9Myc epitope-tagged Jhd2 and its PHD finger mutants [*jhd2(C1, 2A)* and *jhd2(C7, 8A)*] on the *HSP104* gene. Consistent with their effects on Jhd2 demethylation function, the occupancy of Jhd2(C7, 8A) was more profoundly reduced on the promoter and ORF regions of *HSP104* than Jhd2(C1, 2A) as compared to the WT (Fig. 24). Collectively, my findings showed that the structural integrity of the PHD finger, especially the second zinc-coordinating site, is important for the association of Jhd2 with chromatin in addition to its contributions to the H3K4 demethylase function.

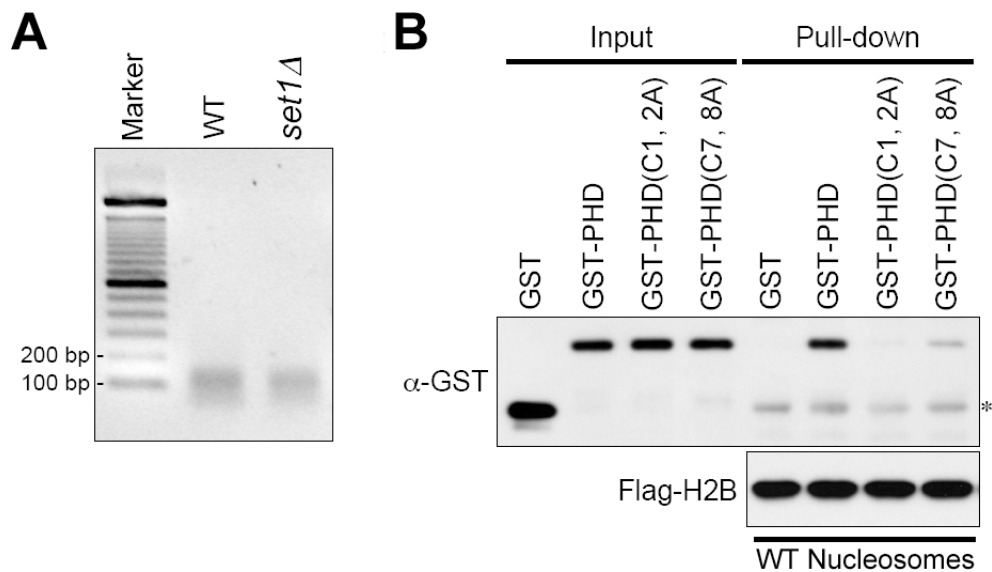


Figure 23. The Jhd2 PHD finger interacts with mononucleosomes *in vitro*. (A) Nuclei isolated from WT or *set1Δ* strains containing Flag-H2B were digested using MNase to solubilize chromatin. The released soluble chromatin was immobilized onto α -Flag (M2)-conjugated agarose beads. The DNA fragments isolated from immobilized chromatin resolved in 2% agarose gel show the presence of predominantly mononucleosomes (~146 bp). *Marker*, 100 bp DNA ladder. (B) *In vitro* mononucleosome binding assay. The immobilized mononucleosomes obtained from the WT were incubated with recombinant GST-tagged WT or mutant PHD fingers of Jhd2 (2 μ g). After extensive washing, the mononucleosome-bound recombinant proteins were eluted in sample buffer. Recombinant proteins (40 ng, Input) and eluates (40%) were subjected to Western blot analysis using α -GST. An aliquot of the eluate (10%) was also used as a control to show the equal loading of immobilized mononucleosomes, as detected using α -Flag. *Asterisk*, denotes the light chain of mouse IgG.

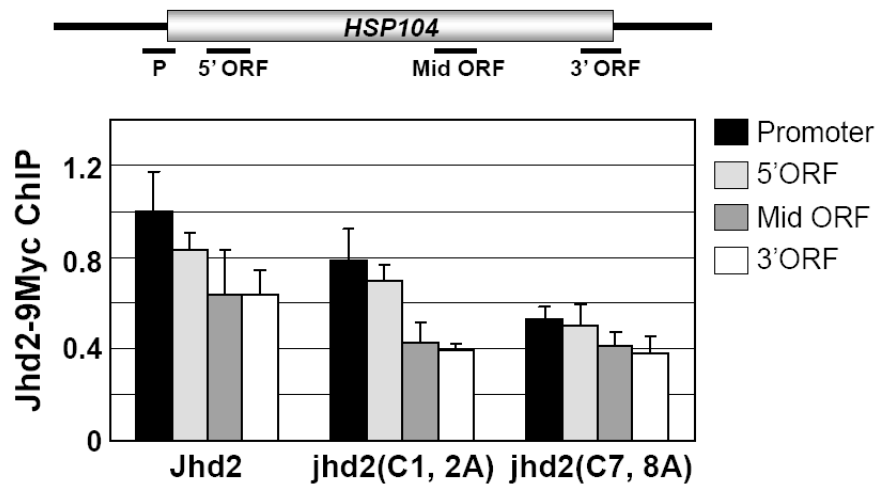


Figure 24. ChIP analysis of the levels of WT Jhd2 or PHD finger mutant variants at *HSP104*. The levels of Jhd2 or its mutant variants at the promoter (P), 5', middle (M) and 3' ORF regions were normalized to the level of WT Jhd2 at the promoter region, which was set as 1. Error bars denote standard error of the mean from three independent experiments.

Chromatin Association of Jhd2 is Independent of H3K4 Methylation and the H3 N-terminal Tail Region

Recently, PHD fingers have emerged as a class of specialized modules that bind to the trimethylated-lysine residues on histones, such as H3K4, -K9 or -K36 (140, 142). Since H3K4me3 is the substrate of Jhd2, it is conceivable that the PHD finger in Jhd2 may mediate its chromatin association by recognizing trimethyl H3K4. To test this possibility, ChIP assays were performed to determine the Jhd2 occupancy on the *HSP104* gene in an *spp1Δ* strain that has reduced levels of H3K4me3 (Fig. 25). Surprisingly, no change in Jhd2 occupancy was evident in *spp1Δ* when compared to the WT, suggesting that the association of Jhd2 with chromatin is independent of H3K4me3.

To further confirm that H3K4me3 is not a prerequisite for the chromatin binding of Jhd2, chromatin fractionation analysis was performed to assess the global levels of Jhd2 on chromatin in the WT or mutants lacking subunits of the Set1-COMPASS complex. To this end, nuclei isolated from the WT and mutants were gently lysed using a hypotonic solution to obtain chromatin as described (5-6). To detect the chromatin-bound Jhd2-9Myc expressed from its endogenous promoter, equal amounts of chromatin from each strain were subjected to Western analyses using α -Myc. Initially, the levels of Jhd2-9Myc on chromatin were assessed in *spp1Δ* and *sdc1Δ* mutants, wherein H3K4me3 levels were either reduced or completely abolished, respectively. As shown in Figure 26A, the chromatin-bound Jhd2-9Myc levels in *spp1Δ* and *sdc1Δ* were similar to those from the WT. This result confirmed that the chromatin-association of Jhd2 is independent of H3K4me3. Additionally, compared to the WT, no change in chromatin-bound Jhd2-9Myc levels was seen in *set1Δ* and *swd1Δ* mutants that completely lack H3K4 methylation (Fig. 26A). This finding suggests that the chromatin binding of Jhd2 is independent of not only

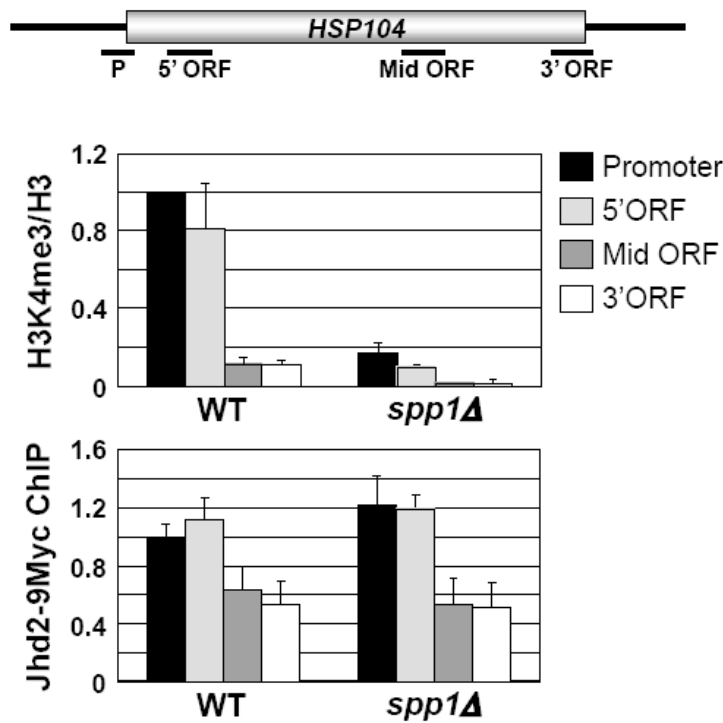


Figure 25. ChIP analysis of the levels of H3K4me3 and Jhd2 occupancy at *HSP104* in WT and *spp1Δ* cells. Top panel, levels of H3K4me3 at the promoter (P), 5', middle (M) and 3' ORF regions in *HSP104* were analyzed by ChIP assay. Graph depicts data obtained from the WT or *spp1Δ* cells. Bottom panel, levels of Jhd2-9Myc at *HSP104* was analyzed by ChIP using α -Myc. Myc IP/input values obtained from no-tag control were subtracted from those obtained from strains expressing *JHD2-9Myc*, and the resulting differences were defined as Jhd2-9Myc occupancy. Fold changes in H3K4me3 levels or Jhd2-9Myc occupancy at various regions of *HSP104* are shown relative to their respective levels at the promoter region in WT, which was set as 1. Error bars denote standard error of the mean from three independent experiments.

H3K4me3, but also all forms of H3K4 methylation.

To determine whether the chromatin-association of Jhd2 mediated by its PHD finger is indeed independent of H3K4 methylation, *in vitro* nucleosome binding assays were performed as described above (Figs. 23A-B). To this end, I used mononucleosomes isolated from the *set1Δ* strain that lacks H3K4 methylation (Fig. 23A) and assessed the ability of Jhd2 PHD finger or its mutant derivatives to bind to the immobilized nucleosomes. As shown in Figure 26B, GST-PHD and its mutant derivatives bind mononucleosomes from *set1Δ* strain similar to their binding to mononucleosomes isolated from the WT strain containing H3K4 methylation (Fig. 23B). This finding confirms the need for an intact PHD finger to interact with chromatin and importantly, suggests that the *in vitro* interaction between the Jhd2 PHD finger and mononucleosomes is not dependent on H3K4 methylation. Moreover, the pull-down assay showed that the Jhd2 PHD finger interacted with the purified recombinant, unmodified H3 *in vitro* (Fig. 26C). In the presence of ethidium bromide (EtBr), which can disrupt protein-DNA interaction (143), the Jhd2 PHD finger still binds to H3 (Fig. 26C, lanes 3-4), indicating that their association is not mediated by DNA and thus, the Jhd2 PHD finger may physically and directly interact with unmodified H3.

Consistent with the *in vitro* interaction between the Jhd2 PHD finger and unmodified H3, several PHD fingers, including the N-terminal PHD finger of human JARID1A H3K4 demethylase, have recently been shown to bind to nonmethylated-K4 containing H3 peptides comprised of amino acids 1-20 (103, 144-146). Interestingly, chromatin fractionation analysis in this study showed that Jhd2 associated with chromatin *in vivo* even in the absence of the H3 N-terminal tail region lacking amino acids 1-28

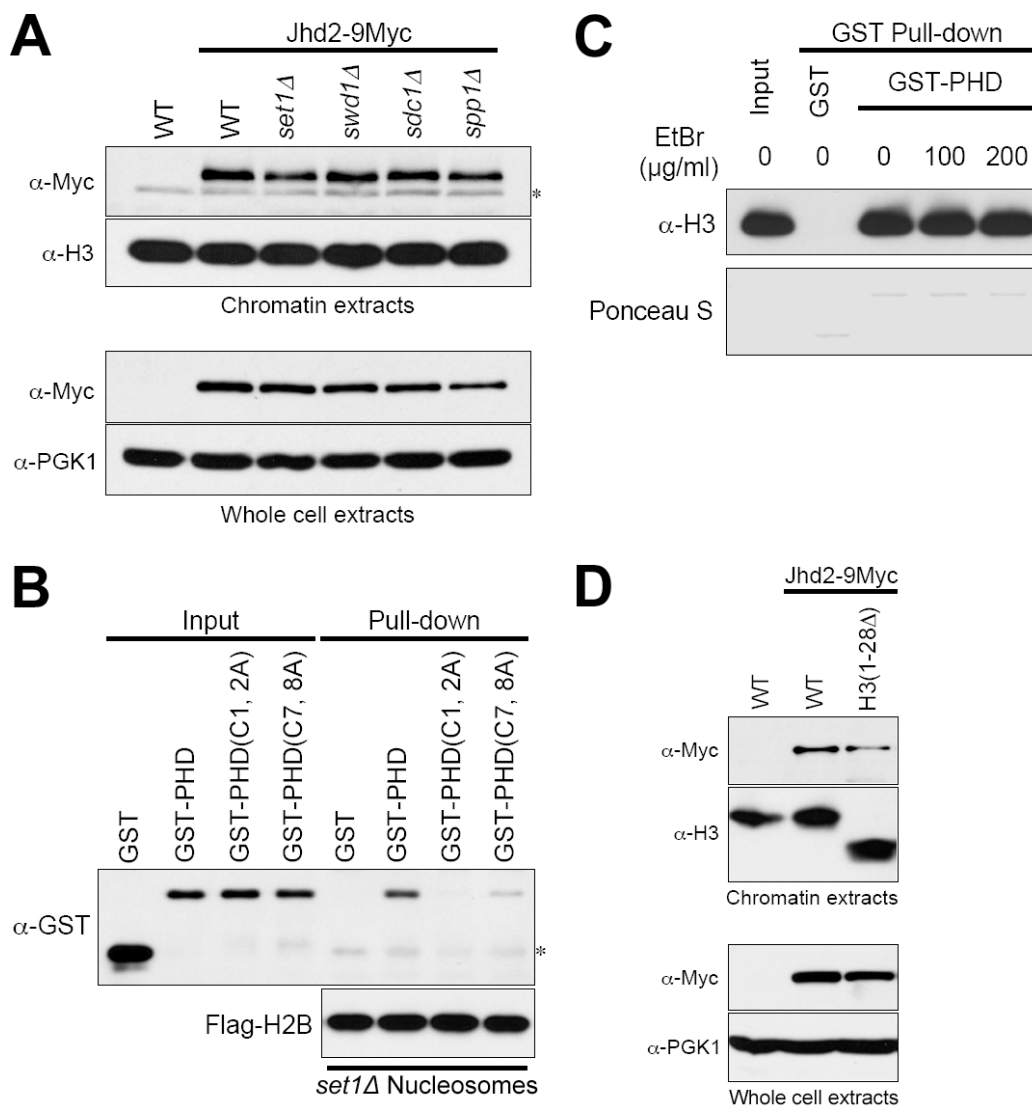


Figure 26. The Jhd2-chromatin association is independent of H3K4 methylation. (A) Western blot analysis of the Jhd2 levels in chromatin extracts (top panel) and WCEs (bottom panel) obtained from WT or strains lacking Set1-COMPASS complex components, Set1, Swd1, Sdc1 or Spp1. *Asterisk*, denotes a α -Myc cross-reacting protein. (B) *In vitro* mononucleosome binding assay was performed as described in Figure 23B using the immobilized mononucleosomes isolated from *set1* Δ . *Asterisk*, denotes the light chain of mouse IgG. (C) *In vitro* GST pull-down assay. The recombinant GST-tagged Jhd2 PHD finger (5 μ g) was incubated with recombinant H3 (0.25 μ g) in the absence or presence of ethidium bromide (EtBr) as indicated and pull-downed by the glutathione-conjugated beads. After extensive washing, the Jhd2 PHD finger-bound H3 were eluted in sample buffer. Recombinant H3 (12.5 ng, Input) and eluates (40%) were subjected to Western blot analysis using α -H3. The top part of the blot was stained with Ponceau S to show the equal loading of GST and GST-tagged Jhd2 PHD finger. (D) Western blot analysis of the Jhd2 levels in chromatin extracts (top panels) and WCEs (bottom panels) prepared from WT or H3(1-28 Δ) strains.

[H3(1-28 Δ)] (Fig. 26D). Therefore, my finding suggests that Jhd2 might be binding to some other region(s) of unmodified H3.

The N-terminal Region of Histone H2A is Important for its Interaction with the Jhd2 PHD Finger in vitro

To date, the known recognition targets for PHD fingers are restricted to H3 and H4 (37, 39, 41, 43, 91, 103, 139). However, it is possible that the Jhd2 PHD finger can also interact with other histones. To test this possibility, the *in vitro* pull-down assay was performed using purified recombinant GST-tagged PHD fingers and *E. coli* lysates containing either recombinant H2A or H2B. Interestingly, the GST-tagged Jhd2 PHD finger can pull-down H2A, but not H2B (Figs. 27A-B, lane 3). In contrast, the BHC80 PHD finger, which binds to unmodified H3K4 (103), did not show any detectable interaction with H2A or H2B (Figs. 27A-B, lane 4), while the ING2 PHD finger, which binds to trimethylated H3K4 (39), interacts with both H2A and H2B (Figs 27A-B, lane 5). These results suggest that only a subset of PHD fingers has the ability to recognize H2A and/or H2B, and the PHD finger in Jhd2 selectively binds to H2A. To identify which regions in H2A are important for its interaction with the Jhd2 PHD finger, mutant derivatives of H2A were generated (Fig. 28A), and the association of Jhd2 PHD finger with these H2A mutants was examined by *in vitro* pull-down assay. As shown in Fig. 28B, deletion of amino acids 2-38 or 25-38 from H2A resulted in the partial disruption of the H2A-JHD2 PHD finger interaction, suggesting that the α 1 helix in H2A (Fig. 28A) is important for this protein-protein interaction. However, less than 50% of the residues in the α 1 helix of H2A are accessible when H2A is incorporated in a nucleosome (Fig. 29A). Therefore, the residues (L24 to P27, R36 and R37) that are exposed to outside of the nucleosome may

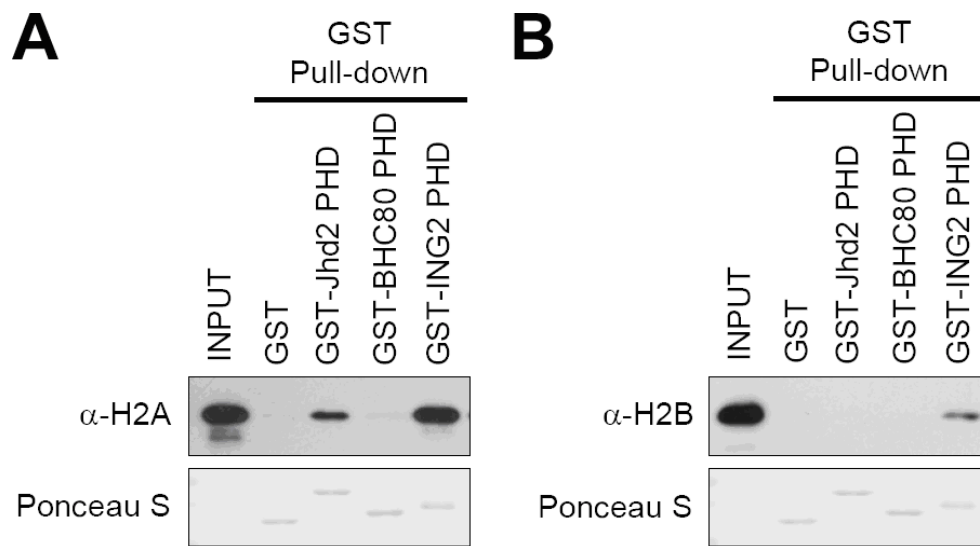


Figure 27. The Jhd2 PHD finger interacts with H2A *in vitro*. The recombinant GST-tagged PHD fingers (5 μ g) were incubated with the *E.coli* lysates containing recombinant H2A (A) or H2B (B), and were pull-down by the glutathione-conjugated beads. After extensive washing, the PHD finger-bound H2A (A) or H2B (B) were eluted in sample buffer. *E.coli* lysates (1%, Input) and eluates (40%) were subjected to Western blot analysis using α -H2A (A) or α -H2B (B). The top part of the blots was stained with Ponceau S to show the equal loading of GST and GST-tagged PHD fingers.

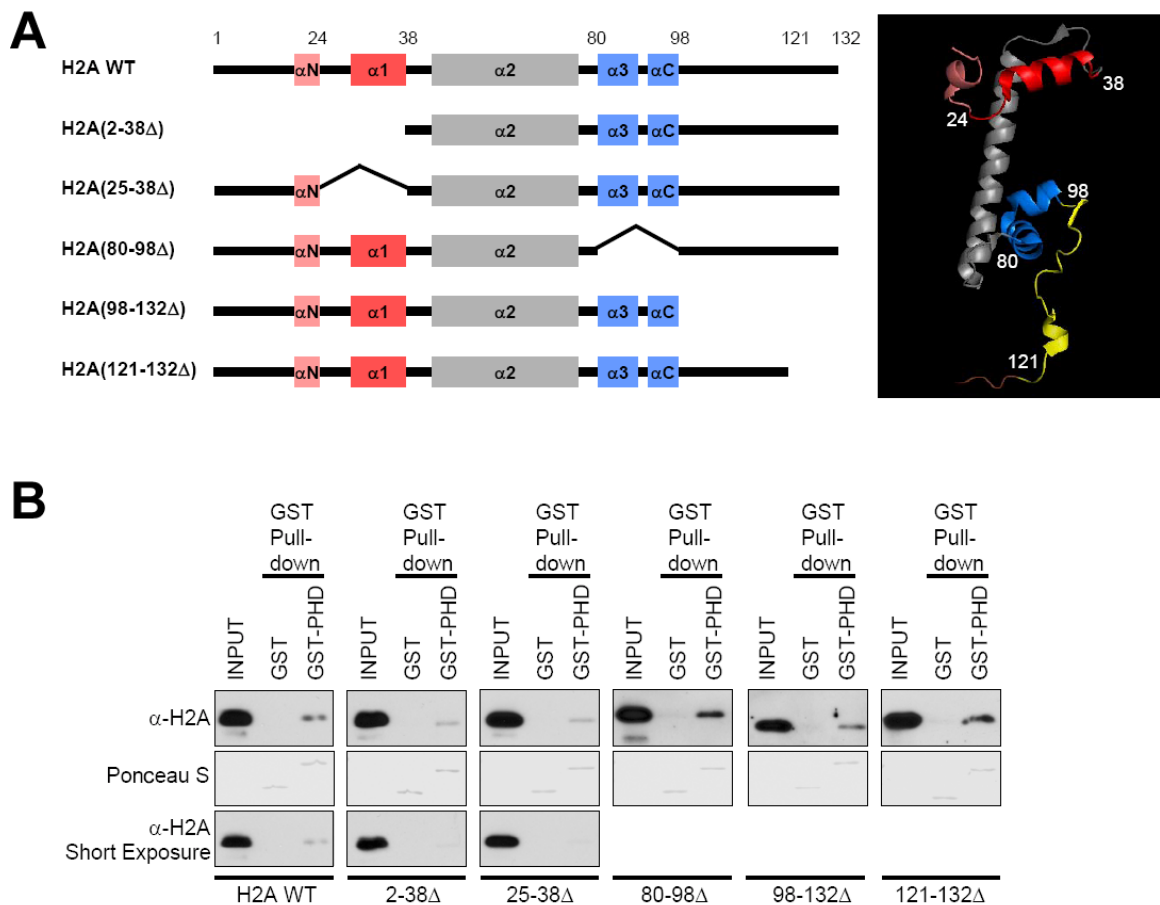


Figure 28. The $\alpha 1$ helix in H2A is important for the Jhd2 PHD finger-H2A interaction. (A) Left panel: Schematic representation of the H2A and its truncation mutants. The αN , $\alpha 1$, $\alpha 2$, $\alpha 3$ and αC helices are shown. Right panel: Crystal structure of H2A (PDB # 1ID3) with the αN , $\alpha 1$, $\alpha 2$, $\alpha 3$ and αC helices represented in the same color as shown in the left panel. The amino acids 99-120 and 121-132 are shown in yellow and brown, respectively. **(B)** *In vitro* GST pull-down assay was performed as described in Figure 27 using the *E.coli* lysates containing H2A or its truncation mutants.

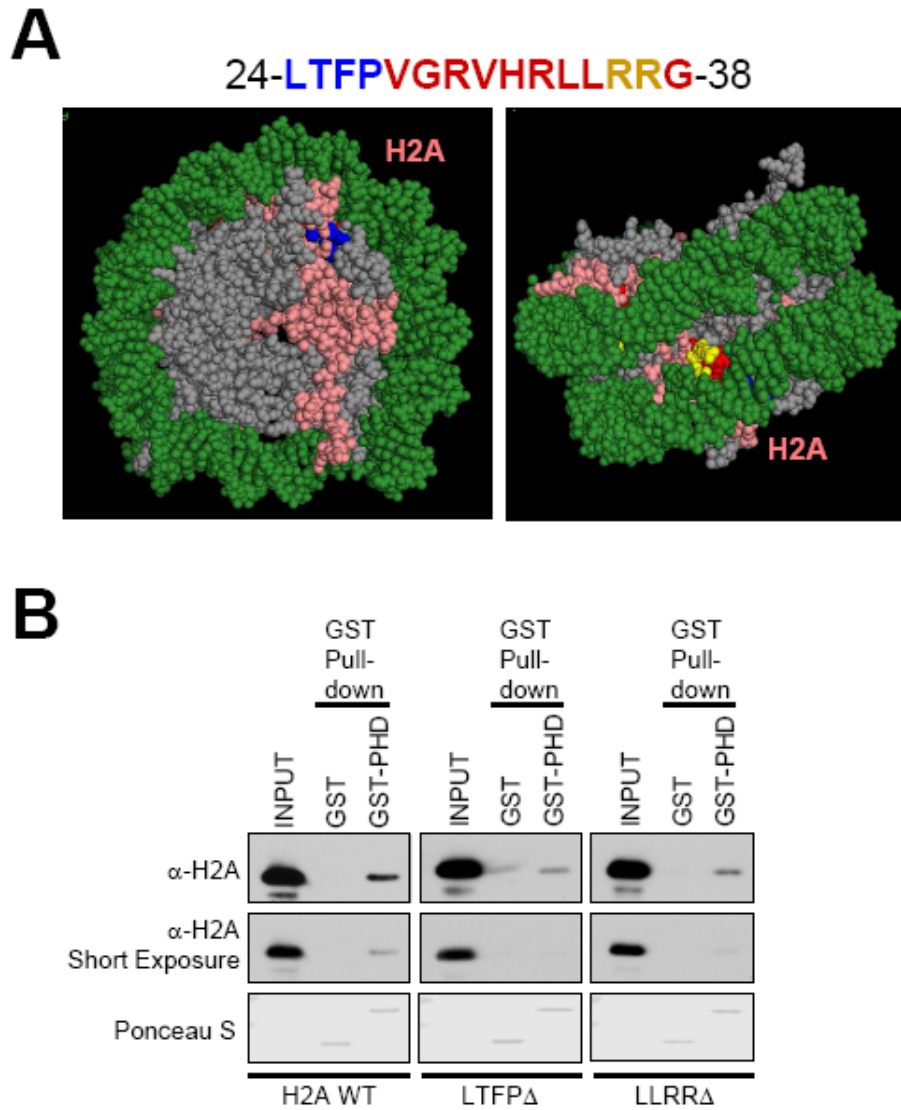


Figure 29. The amino acids 24-27 and 34-37 in H2A are important for the Jhd2 PHD finger-H2A interaction. (A) Crystal structure of yeast nucleosome (PDB # 1ID3). The two patches in the H2A α 1 helix that are exposed to the outside of nucleosome are shown in blue (amino acids 24-27; LTPF) and yellow (amino acids 36-37; RR), and other residues in this helix are shown in red. H2A, DNA and other histones are shown in pink, green and grey, respectively. (B) *In vitro* GST pull-down assay was performed as described in Figure 27 using the *E.coli* lysates containing H2A or its truncation mutants.

play a role in mediating the interaction between H2A and the Jhd2 PHD finger. To test this hypothesis, the H2A mutants lacking amino acids 24-27 (LTFPΔ) or 34-37 (LLRRΔ) were generated and subjected to the *in vitro* pull-down assay as described above. Indeed, both the H2A(LTFPΔ) and H2A(LLRRΔ) mutants showed reduced binding to the Jhd2 PHD finger as compared to the WT H2A (Fig 29B). Thus, my data suggest that the amino acids 24-27 and 34-37 in H2A are important for the Jhd2 PHD finger to interact with H2A *in vitro*.

The F26 Residue in H2A is Critical for the Chromatin Association of Jhd2 Mediated by its PHD Finger

Next, I tested whether those H2A residues are also critical for the demethylase function of Jhd2 *in vivo*. As shown in Fig. 30, overexpression of *JHD2* in the *H2A(L24A)* or *H2A(F26A)* mutant had no apparent effect on the H3K4me3 levels, indicating that these two residues, L24 and F26, in H2A are required for the demethylation of H3K4 by Jhd2. In addition, the protein levels of Jhd2 in the *H2A(L24A)* mutant were lower than those in the WT H2A cells (Fig. 30), suggesting that mutation of the L24 residue in H2A may compromise the expression or protein stability of Jhd2. Interestingly, the Jhd2 levels were not affected in *H2A(F26A)* (Fig. 30). Given that an intact PHD finger is critical for the normal chromatin association of Jhd2 (Fig. 24), I hypothesized that the F26A mutation in H2A may disrupt the chromatin association of Jhd2 mediated by its PHD finger. To test this hypothesis, ChIP assays were performed to assess the occupancy of Jhd2-9Myc on the *HSP104* and *PMA1* genes in cells containing WT H2A or the *H2A(F26A)* mutant. Indeed, the occupancy of Jhd2 was reduced in the promoter and 5'ORF regions of *HSP104* in the *H2A(F26A)* mutant as compared to that in the WT cells

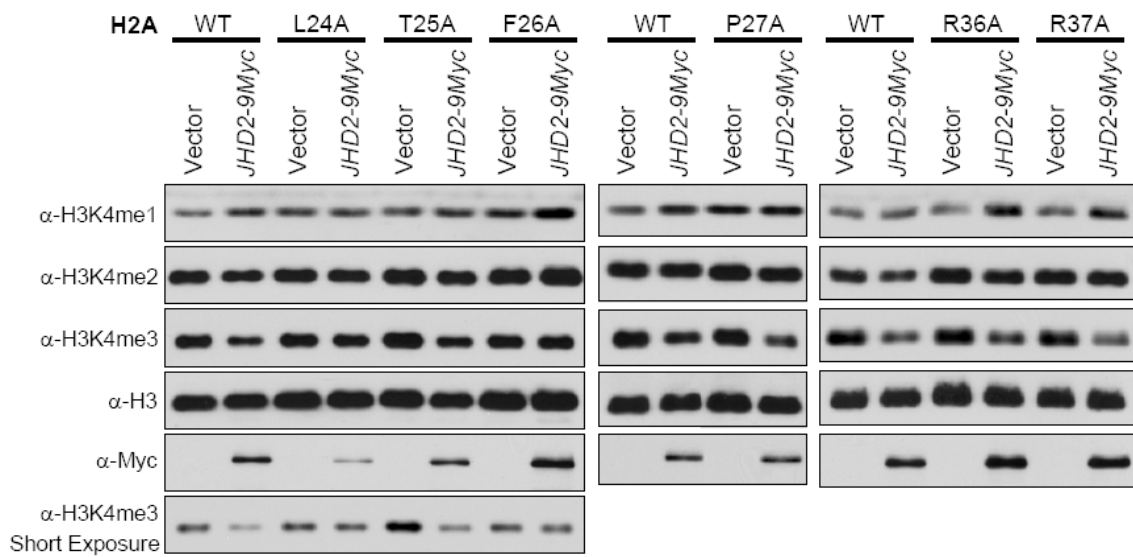
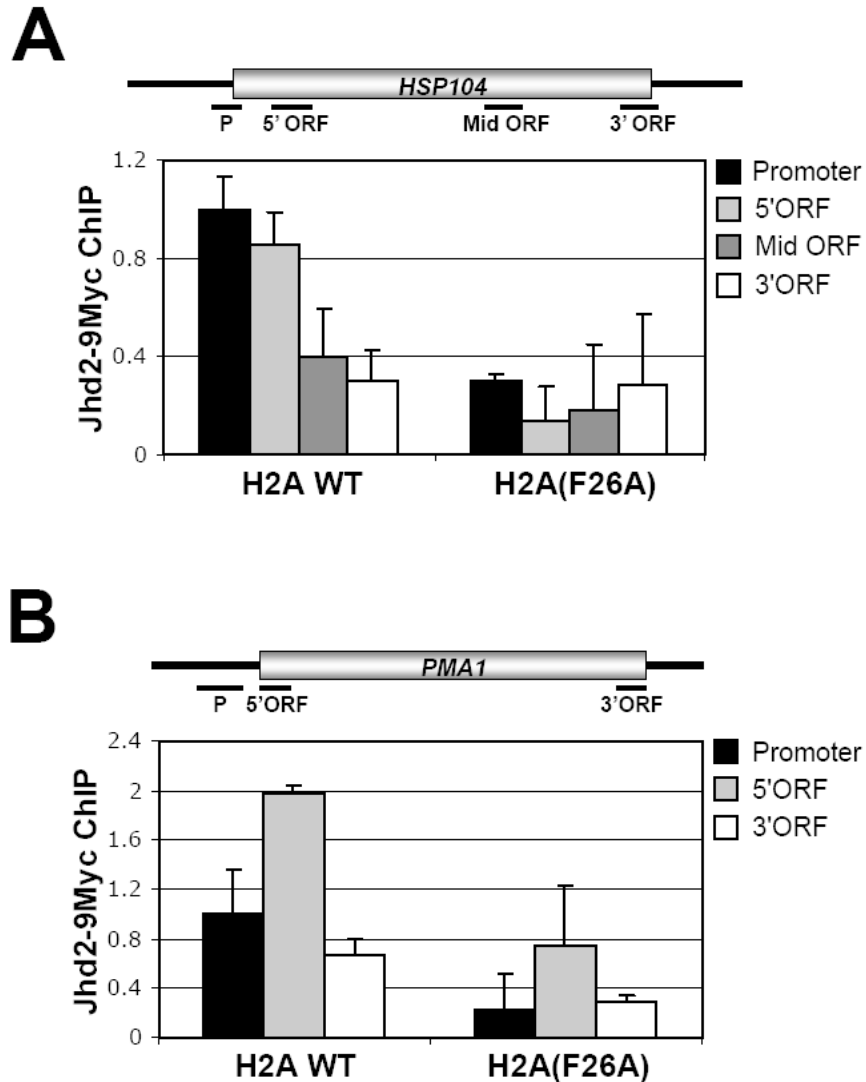


Figure 30. The L24 and F26 residues in H2A are important for Jhd2 function. Western blot analysis of H3K4 methylation levels in the crude nuclear extracts prepared from WT or H2A mutants overexpressing *JHD2*.



(Fig. 31A). Moreover, the occupancies of Jhd2 in the promoter and ORF regions of *PMA1* were also decreased in the *H2A(F26A)* mutant (Fig. 31B). Therefore, the results showed that the F26 residue in H2A is critical for Jhd2 binding to chromatin, probably through its PHD finger, and my findings reveal a novel docking-site on the nucleosome for Jhd2 to function as the H3K4 demethylase.

Discussion

Controlling the Chromatin Association of Jhd2

Exactly how the H3K4 demethylases belonging to the JARID1 family interact with chromatin is not fully understood. Although not present in Jhd2, all the JARID1 H3K4 demethylases from higher eukaryotes harbor an ARID/BRIGHT DNA-binding domain, which is required for their demethylation activities (93, 124-125, 147). However, it is not known whether the ARID/BRIGHT domain is essential for their association with chromatin. In this study, I showed that the PHD finger is important for Jhd2 to associate with chromatin and for its *in vivo* activity (Figs. 22-24). The PHD finger in most JmjC-domain-containing demethylases and transcription factors binds to either H3 containing methylated lysine (K4, K9, K27, K36) or unmodified H3 N-terminal tail region (140-141). However, while the PHD finger is important for Jhd2 chromatin association *in vivo* (Fig. 24), it binds to mononucleosomes independent of H3K4 methylation, and to unmodified recombinant H3 *in vitro* (Figs. 23B and 26B-C). Moreover, the *in vivo* association of Jhd2 with chromatin is not dependent on H3K4 methylation (Figs. 26A and D) and is independent of the first twenty-eight amino acids of

H3 (Fig. 26C). Collectively, this study put forth a novel possibility that through its PHD finger, Jhd2 might associate with chromatin via binding to H3 outside of its N-terminal tail region.

Other than H3, I demonstrated that the Jhd2 PHD finger also binds to H2A *in vitro* (Fig. 28A). Furthermore, the F26 residue in H2A is critical for Jhd2 to associate with chromatin and function as a H3K4 demethylase (Figs. 31-32). These results suggest that this H2A residue is critical for the chromatin association of Jhd2 mediated by its PHD finger. Interestingly, the N-terminus of H2A (amino acids 4-20) is important for high levels of H2B K123 mono-ubiquitination and the establishment of H3K4me3 (148). Given the close proximity of F26 residue to the N-terminus of H2A, it is possible that the N-terminal region of H2A may have a dual-property role in regulating the establishment and removal of H3K4 methylation through H2B-H3 *trans*-histone crosstalk and Jhd2, respectively. In summary, this study identifies a novel recognition target, H2A, for the PHD finger family, and my findings also suggest the N-terminal region of H2A as a novel docking-site for Jhd2 to associate with chromatin.

Linking the Chromatin Association and Demethylase Function of Jhd2

Jhd2 is 85 kD in size, which is comparable to the size of a histone octamer (110 kD). Therefore, when bound to H2A, Jhd2 may essentially cover the whole histone octamer. The amino acids 1-37 in H3 did not show a fixed conformation in the crystal structure of a yeast nucleosome (PDB # 1ID3), suggesting that the H3 N-terminal tail is highly flexible. This structural flexibility of the H3 N-terminal tail might enable the efficient presentation of methylated H3K4 to the JmjC domain of histone-bound Jhd2. Therefore,

it is conceivable that Jhd2 may bind to H2A via its PHD finger and remove the H3K4 methylation mark in the same nucleosome using its JmjC domain. Alternatively, Jhd2 may associate with one nucleosome and demethylate other nucleosomes that are in close proximity.

CHAPTER VI

SUMMARY AND FUTURE DIRECTIONS

Summary

As a recently identified and highly conserved JmjC-containing protein, Jhd2 was poorly understood regarding its function and regulation before this study. Prior studies have shown that Jhd2 actively removes the H3K4me2 and -me3 marks *in vivo*, and it is polyubiquitinated by the E3 ligase Not4 and degraded by the proteasome (Fig. 32, left panel) (88-90, 100). In this dissertation study, three major findings on the function and regulation of Jhd2 were made: First, I have demonstrated that Jhd2 has *in vivo* demethylase activity toward all three forms of H3K4 methylation (Fig. 32, right panel, 1). Furthermore, I found that Jhd2 binds to and regulates H3K4 methylation on both active and repressed genes, and in the sub-telomeric regions. Second, I demonstrated that the inter-domain interaction between JmjN and JmjC in Jhd2 is critical for its subcellular localization and for the protein stability modulated by the E3 ligase Not4 (Fig. 32, right panel, 2). Perturbation of this JmjN-JmjC interaction in Jhd2 led to its polyubiquitination by Not4 and subsequently, degradation by proteasome. Third, I have shown that the PHD finger of Jhd2 is important for its chromatin association by binding to H2A (Fig. 32, right panel, 3). I have also identified H2A F26 as an important residue for Jhd2-chromatin association. In summary, this dissertation study has revealed novel insights into the function and regulation of Jhd2 as an H3K4 demethylase.

Model for the regulation of Jhd2

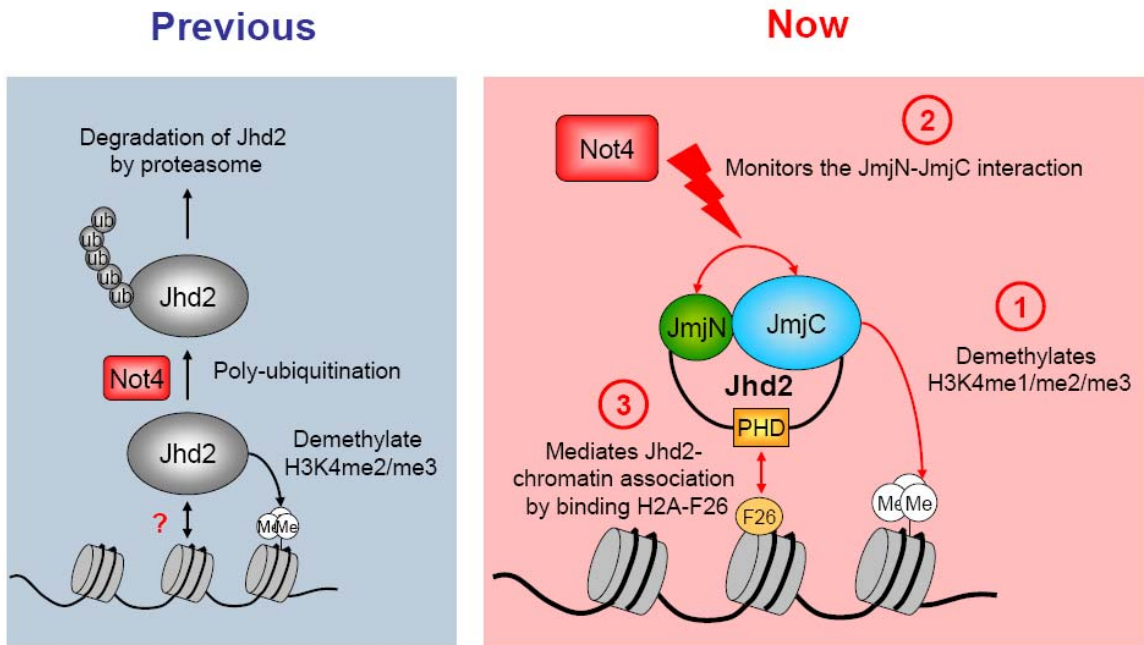


Figure 32. Model for the regulation of Jhd2. Left panel, Jhd2 has been shown to demethylate H3K4me2 and -me3 *in vivo*, and to be polyubiquitinated by the E3 ligase Not4 and degraded by proteasome in the previous studies (88-90, 99-100). Right panel, the three major findings in this dissertation study are shown: (1) Jhd2 demethylates H3K4me1, -me2 and -me3 *in vivo*. (2) The E3 ligase Not4 plays a role in monitoring the JmjN-JmjC interaction in Jhd2. (3) The PHD finger in Jhd2 mediates its chromatin association by binding to H2A, and the H2A F26 residue is important for this Jhd2-chromatin association.

Future Directions

What is the Role of Jhd2 in Transcriptional Regulation?

Jhd2 plays a role in removing H3K4me₃, the histone mark for active transcription, during gene repression at both *GALI* and *INO1* (Figs. 12A-B) (99, 149). However, in the absence of Jhd2, the dissociation of Pol II from the *INO1* gene upon transcriptional repression following induction is not affected (Fig. 12D). In addition, the *GALI* transcript levels remain unaffected in the cells lacking either Jhd2 or Jhd1 (an H3K36 demethylase) alone, but are up-regulated in the absence of both Jhd2 and Jhd1 (99). These results suggest that Jhd2 and Jhd1 may play redundant repressive roles in regulating gene expression. Intriguingly, expressing LexA DNA-binding domain-tagged Jhd2 in cells harboring the *(lexAop)₈-LacZ* reporter leads to the activation of *LacZ* expression (Fig. 33), suggesting that Jhd2 can also positively regulate transcription when recruited to DNA. Taken together, it is possible that Jhd2 can play either a positive or a negative role in the transcriptional regulation in a context-dependent manner. Therefore, genome-wide analysis of genes up- or down-regulated in the absence of Jhd2 by RNA microarray may provide important clues for the role of Jhd2 in regulating transcription. Also, although Jhd2 does not form a stable protein complex *in vivo* (88), it is possible that Jhd2 may transiently associate with other proteins to exert its transcriptional regulatory function. Thus, purification of Jhd2-containing protein complex from cells crosslinked with formaldehyde followed by MudPIT (Multidimensional Protein Identification Technology) (150) will be an important step to identify the Jhd2-interacting proteins and to further delineate the function of Jhd2.

What is the Mechanism that Regulates the Subcellular Localization of Jhd2?

The JmjN-JmjC interaction in Jhd2 is important for its normal subcellular localization (Fig. 19). Both the Jhd2(JmjN Δ) and Jhd2(K37E) mutants showed lower global and higher nuclear protein levels as compared to the WT Jhd2 (Figs. 15C and 19C). The higher nuclear levels of mutant Jhd2 might be due to an increased nuclear import rate, a reduced nuclear export rate, higher nuclear retention, a lower nuclear protein degradation rate, or a combination of these possible causes. Interestingly, Jhd2 contains two putative bipartite and one putative monopartite NLSs (Nuclear Localization Signals), and it also contains one putative leucine-rich NES (Nuclear Export Signal) (Fig. 34). It is possible that the interaction between the JmjN and JmjC domains in Jhd2 can modulate the presentation of its NLS/NES to the karyopherins to mediate the nuclear import/export of Jhd2. Therefore, to delineate the mechanism governing the subcellular localization of Jhd2 through its JmjN-JmjC interaction, it would be important to examine whether the putative NLSs/NES in Jhd2 indeed contribute to the regulation of its nuclear localization.

As shown in the bottom panel of Fig. 34, the putative NES of Jhd2 overlaps with one of its putative NLSs. Intriguingly, an NES of the yeast actin-binding protein, Pan1, also overlaps with its third NLS (NLS3), and the nuclear export effect of this NES overwhelmed the nuclear import effect of NLS3 when they were fused to the NLS of histone H2B (151). However, inactivation of the Pan1 NES allowed the NLS3 to direct the fusion protein into the nucleus (151). Therefore, the overlapped NLS/NES in Jhd2 might function as a “switch” in controlling its nuclear import/export. Therefore, testing these possibilities should provide important insights into the regulation of subcellular localization of Jhd2.

Bipartite NLS

142-FRRKLKFRDISQLRGDISLWRTISKKFNP-171 *

313-RLLPARKLSIDELEEMFWSLVTKNRRS-340

Monopartite NLS

654-YKRHKNHLSIRQW-667

Leucine-rich NES

151-ISQLRGDISL-160 *

Overlapping NLS/NES

142-FRRKLKFRDISQLRGDISLWRTISKKFNP-171

Figure 34. The putative NLSs and NES in Jhd2. Putative NLSs of Jhd2 are predicted by cNLS Mapper, an NLS-predicting algorithm based on the knowledge obtained from nuclear import assays in budding yeast (<http://nls-mapper.iab.keio.ac.jp/>) (152-153). A putative NES of Jhd2 is predicted by NetNES, an NES-predicting algorithm based on the sequences of 67 identified NESs (<http://www.cbs.dtu.dk/services/NetNES/>) (154). *Asterisks*, denote the putative NLS and NES that overlap with each other as shown in the bottom panel.

How is the JmjN-JmjC Inter-domain Interaction in Jhd2 Regulated?

The K37 residue in the JmjN domain of Jhd2 is critical for its JmjN-JmjC interaction (Figs. 19 and 21). I have tested the possibility that acetylation may occur on the Jhd2 K37 residue and disrupt the inter-domain interaction in Jhd2. However, I was unable to detect any Jhd2 K37 acetylation by mass-spectrometry or Western blotting. It is possible that the Jhd2 K37 residue is modified only under certain cellular condition(s). Interestingly, MMS (methyl methanesulfonate) treatment decreased the global protein levels of Jhd2, but increased its nuclear protein levels in a concentration-dependent manner (Fig. 35A), which is very similar to the effects caused by disrupting the JmjN-JmjC interaction in Jhd2. Since MMS is an alkylating agent that causes oxidative stress, this result suggests that the K37 residue in Jhd2 may be modified to disrupt this inter-domain interaction in response to the alkylation-induced stress. Consistent with this hypothesis, overexpression of *JHD2* led to slightly increased sensitivity to MMS (Fig. 35B, top panel), and the cells lacking Jhd2 exhibited a subtle enhancement in the resistance to MMS (Fig. 35B, bottom panel), implying that reducing the global levels of Jhd2 may promote cell survival under MMS-induced stress. Therefore, the identification of the modification(s) occurring on Jhd2 in response to MMS treatment may be beneficial to understand the physiological role and regulation of the JmjN-JmjC interaction in Jhd2.

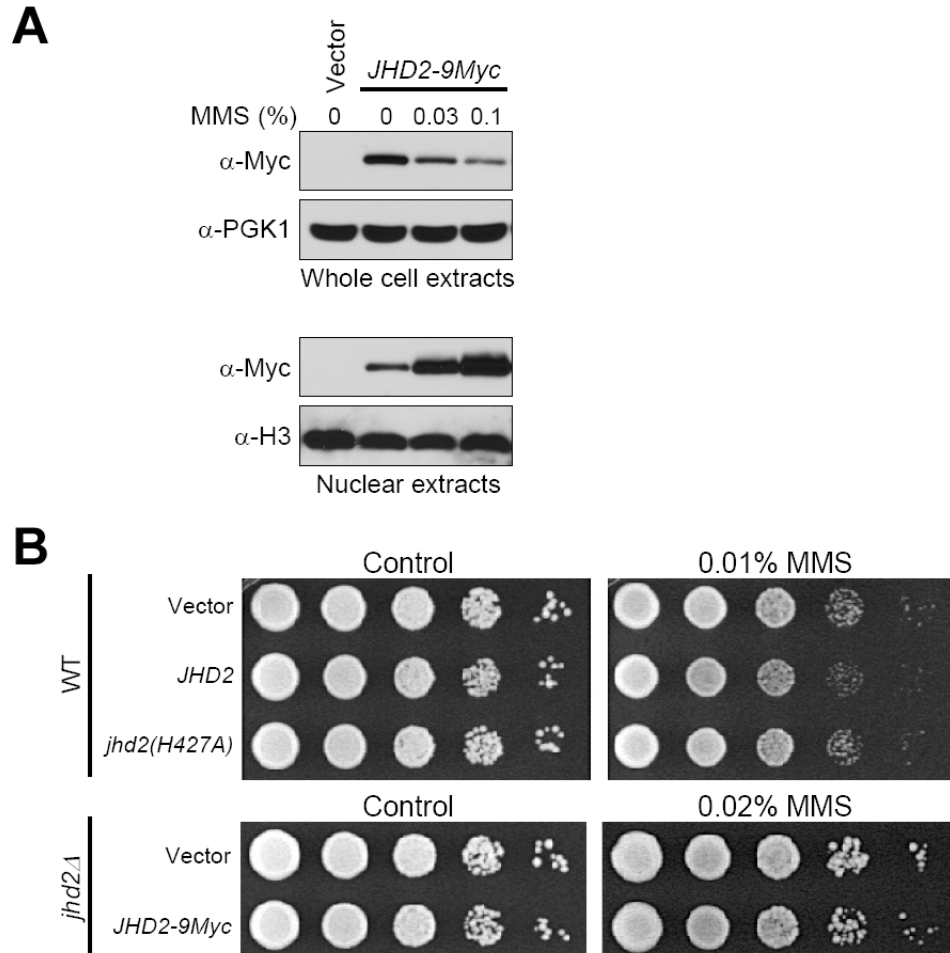


Figure 35. MMS treatment affects the global protein levels and subcellular localization of Jhd2. (A) Western blot analysis of the Jhd2 levels in the WCEs and nuclear extracts obtained from cells treated with the indicated concentrations of MMS. (B) Analysis of the *JHD2*-overexpressed or -deleted cells for MMS sensitivity. Top panel, ten-fold serial dilutions of cells overexpressing *JHD2* or *jhd2(H427A)* were plated onto medium with or without 0.01% MMS. Bottom panel, ten-fold serial dilutions of *jhd2 Δ* cells with or without *JHD2-9Myc* expressing from a low-copy plasmid were plated onto medium with or without 0.02% MMS.

What is the Role of H2A in the Trans-histone Regulation of H3K4 Methylation?

In addition to H2B, H2A also plays a role in the *trans*-histone regulation of H3K4 methylation. An N-terminal patch (amino acids 16-20) in H2A is critical for high levels of H3K4me3 by modulating the levels of H2B K123 mono-ubiquitination (H2Bub1) (148). H2Bub1 is catalyzed by the E2 conjugating enzyme Rad6 and the E3 ligase Bre1 (155-156), and this histone mark is removed by the ubiquitin proteases Ubp8 and Ubp10 (157-158). Given the close proximity in the nucleosome between the H2A N-terminal patch and the H2B K123 residue (Fig. 36), it was proposed that this H2A patch may promote H2Bub1 by Rad6/Bre1 and thereby, contribute to the establishment of H3K4me3 (148). In addition, my study has demonstrated that the H2A F26 residue is important for the Jhd2-chromatin association (Fig. 31). Interestingly, the F26 residue of H2A is also located close to the H2B K123 residue in the nucleosome (Fig. 36). Since ubiquitination is a bulky modification (7 kD), it is conceivable that H2Bub1 may hinder the binding of Jhd2 to its docking site (including F26) on H2A. Therefore, these findings raise a possibility that H2Bub1 together with the N-terminal region of H2A may play roles in regulating both the establishment and the removal of H3K4 methylation. Future examination of this hypothesis by ChIP analysis of the chromatin occupancy of Jhd2 in *rad6Δ* cells (lacking H2Bub1) and *ubp8Δ/ubp10Δ* cells (containing high levels of H2Bub1) will provide important mechanistic information for the *trans*-histone regulation of H3K4 methylation.

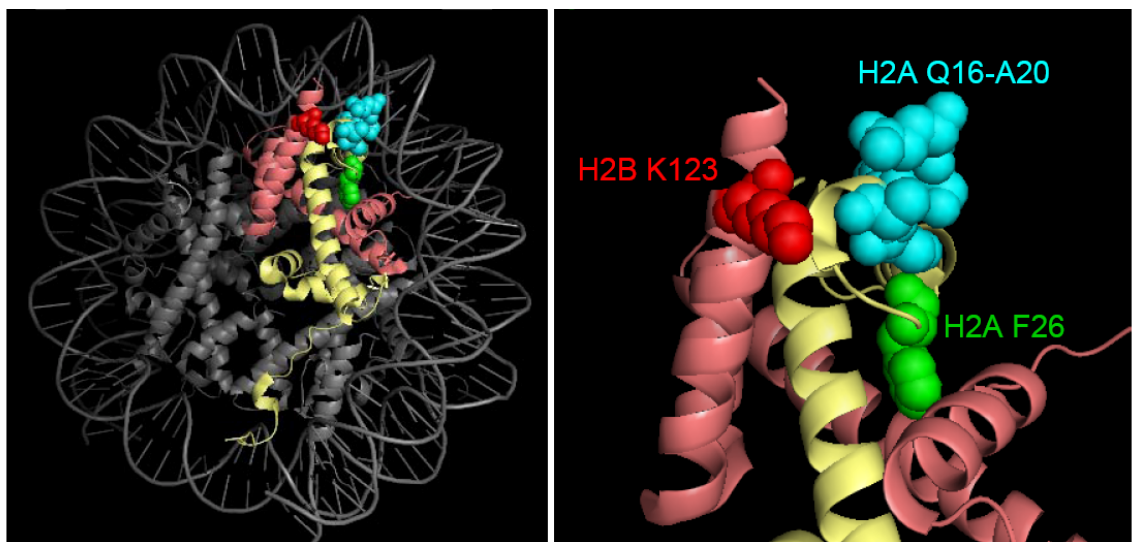


Figure 36. The H2A F26 residue is in close proximity to the H2B K123 residue. Crystal structure of the H2A (yellow)-H2B (pink) dimer in a yeast nucleosome is shown (PDB # 1ID3). The H2B K123 residue (red) is in close proximity to both the N-terminal patch (amino acids 16-20, blue) and the F26 residue (green) of H2A.

REFERENCES

1. Luger, K., Mader, A. W., Richmond, R. K., Sargent, D. F., and Richmond, T. J. (1997) Crystal structure of the nucleosome core particle at 2.8 Å resolution, *Nature* 389, 251-260.
2. White, C. L., Suto, R. K., and Luger, K. (2001) Structure of the yeast nucleosome core particle reveals fundamental changes in internucleosome interactions, *EMBO J* 20, 5207-5218.
3. Davey, C. A., Sargent, D. F., Luger, K., Maeder, A. W., and Richmond, T. J. (2002) Solvent mediated interactions in the structure of the nucleosome core particle at 1.9 Å resolution, *J Mol Biol* 319, 1097-1113.
4. Luger, K., and Richmond, T. J. (1998) The histone tails of the nucleosome, *Curr Opin Genet Dev* 8, 140-146.
5. Huang, R. C., and Bonner, J. (1962) Histone, a suppressor of chromosomal RNA synthesis, *Proc Natl Acad Sci U S A* 48, 1216-1222.
6. Han, M., and Grunstein, M. (1988) Nucleosome loss activates yeast downstream promoters in vivo, *Cell* 55, 1137-1145.
7. Kriaucionis, S., and Heintz, N. (2009) The nuclear DNA base 5-hydroxymethylcytosine is present in Purkinje neurons and the brain, *Science* 324, 929-930.
8. Holliday, R., and Pugh, J. E. (1975) DNA modification mechanisms and gene activity during development, *Science* 187, 226-232.
9. Srinivasan, P. R., and Borek, E. (1964) Enzymatic Alteration of Nucleic Acid Structure, *Science* 145, 548-553.
10. Tahiliani, M., Koh, K. P., Shen, Y., Pastor, W. A., Bandukwala, H., Brudno, Y., Agarwal, S., Iyer, L. M., Liu, D. R., Aravind, L., and Rao, A. (2009) Conversion of 5-methylcytosine to 5-hydroxymethylcytosine in mammalian DNA by MLL partner TET1, *Science* 324, 930-935.
11. Racki, L. R., and Narlikar, G. J. (2008) ATP-dependent chromatin remodeling enzymes: two heads are not better, just different, *Curr Opin Genet Dev* 18, 137-144.
12. Ransom, M., Dennehey, B. K., and Tyler, J. K. (2010) Chaperoning histones during DNA replication and repair, *Cell* 140, 183-195.

13. Campos, E. I., and Reinberg, D. (2009) Histones: annotating chromatin, *Annu Rev Genet* 43, 559-599.
14. Allfrey, V. G., Faulkner, R., and Mirsky, A. E. (1964) Acetylation and Methylation of Histones and Their Possible Role in the Regulation of Rna Synthesis, *Proc Natl Acad Sci U S A* 51, 786-794.
15. Spivakov, M., and Fisher, A. G. (2007) Epigenetic signatures of stem-cell identity, *Nat Rev Genet* 8, 263-271.
16. Turner, B. M. (2002) Cellular memory and the histone code, *Cell* 111, 285-291.
17. Berger, S. L. (2007) The complex language of chromatin regulation during transcription, *Nature* 447, 407-412.
18. Lee, J. S., Smith, E., and Shilatifard, A. (2010) The language of histone crosstalk, *Cell* 142, 682-685.
19. Honda, B. M., Dixon, G. H., and Candido, E. P. (1975) Sites of in vivo histone methylation in developing trout testis, *J Biol Chem* 250, 8681-8685.
20. Ng, H. H., Robert, F., Young, R. A., and Struhl, K. (2003) Targeted recruitment of Set1 histone methylase by elongating Pol II provides a localized mark and memory of recent transcriptional activity, *Mol Cell* 11, 709-719.
21. Pokholok, D. K., Harbison, C. T., Levine, S., Cole, M., Hannett, N. M., Lee, T. I., Bell, G. W., Walker, K., Rolfe, P. A., Herbolsheimer, E., Zeitlinger, J., Lewitter, F., Gifford, D. K., and Young, R. A. (2005) Genome-wide map of nucleosome acetylation and methylation in yeast, *Cell* 122, 517-527.
22. Bernstein, B. E., Kamal, M., Lindblad-Toh, K., Bekiranov, S., Bailey, D. K., Huebert, D. J., McMahon, S., Karlsson, E. K., Kulbokas, E. J., 3rd, Gingeras, T. R., Schreiber, S. L., and Lander, E. S. (2005) Genomic maps and comparative analysis of histone modifications in human and mouse, *Cell* 120, 169-181.
23. Schneider, R., Bannister, A. J., Myers, F. A., Thorne, A. W., Crane-Robinson, C., and Kouzarides, T. (2004) Histone H3 lysine 4 methylation patterns in higher eukaryotic genes, *Nat Cell Biol* 6, 73-77.
24. Schubeler, D., MacAlpine, D. M., Scalzo, D., Wirbelauer, C., Kooperberg, C., van Leeuwen, F., Gottschling, D. E., O'Neill, L. P., Turner, B. M., Delrow, J., Bell, S. P., and Groudine, M. (2004) The histone modification pattern of active genes revealed through genome-wide chromatin analysis of a higher eukaryote, *Genes Dev* 18, 1263-1271.
25. van Dijk, K., Ding, Y., Malkaram, S., Riethoven, J. J., Liu, R., Yang, J., Laczko, P.,

- Chen, H., Xia, Y., Ladunga, I., Avramova, Z., and Fromm, M. (2010) Dynamic changes in genome-wide histone H3 lysine 4 methylation patterns in response to dehydration stress in *Arabidopsis thaliana*, *BMC Plant Biol* 10, 238.
26. Millar, C. B., and Grunstein, M. (2006) Genome-wide patterns of histone modifications in yeast, *Nat Rev Mol Cell Biol* 7, 657-666.
 27. Kirmizis, A., Santos-Rosa, H., Penkett, C. J., Singer, M. A., Vermeulen, M., Mann, M., Bahler, J., Green, R. D., and Kouzarides, T. (2007) Arginine methylation at histone H3R2 controls deposition of H3K4 trimethylation, *Nature* 449, 928-932.
 28. van Dijk, K., Marley, K. E., Jeong, B. R., Xu, J., Hesson, J., Cerny, R. L., Waterborg, J. H., and Cerutti, H. (2005) Monomethyl histone H3 lysine 4 as an epigenetic mark for silenced euchromatin in *Chlamydomonas*, *Plant Cell* 17, 2439-2453.
 29. Heintzman, N. D., Hon, G. C., Hawkins, R. D., Kheradpour, P., Stark, A., Harp, L. F., Ye, Z., Lee, L. K., Stuart, R. K., Ching, C. W., Ching, K. A., Antosiewicz-Bourget, J. E., Liu, H., Zhang, X., Green, R. D., Lobanenkov, V. V., Stewart, R., Thomson, J. A., Crawford, G. E., Kellis, M., and Ren, B. (2009) Histone modifications at human enhancers reflect global cell-type-specific gene expression, *Nature* 459, 108-112.
 30. Heintzman, N. D., Stuart, R. K., Hon, G., Fu, Y., Ching, C. W., Hawkins, R. D., Barrera, L. O., Van Calcar, S., Qu, C., Ching, K. A., Wang, W., Weng, Z., Green, R. D., Crawford, G. E., and Ren, B. (2007) Distinct and predictive chromatin signatures of transcriptional promoters and enhancers in the human genome, *Nat Genet* 39, 311-318.
 31. Kim, T., and Buratowski, S. (2009) Dimethylation of H3K4 by Set1 recruits the Set3 histone deacetylase complex to 5' transcribed regions, *Cell* 137, 259-272.
 32. Govind, C. K., Qiu, H., Ginsburg, D. S., Ruan, C., Hofmeyer, K., Hu, C., Swaminathan, V., Workman, J. L., Li, B., and Hinnebusch, A. G. (2010) Phosphorylated Pol II CTD recruits multiple HDACs, including Rpd3C(S), for methylation-dependent deacetylation of ORF nucleosomes, *Mol Cell* 39, 234-246.
 33. Pinskaya, M., Gourvenec, S., and Morillon, A. (2009) H3 lysine 4 di- and tri-methylation deposited by cryptic transcription attenuates promoter activation, *EMBO J* 28, 1697-1707.
 34. Santos-Rosa, H., Bannister, A. J., Dehe, P. M., Geli, V., and Kouzarides, T. (2004) Methylation of H3 lysine 4 at euchromatin promotes Sir3p association with heterochromatin, *J Biol Chem* 279, 47506-47512.
 35. Mueller, J. E., Canze, M., and Bryk, M. (2006) The requirements for COMPASS

- and Paf1 in transcriptional silencing and methylation of histone H3 in *Saccharomyces cerevisiae*, *Genetics* 173, 557-567.
36. Flanagan, J. F., Mi, L. Z., Chruszcz, M., Cymborowski, M., Clines, K. L., Kim, Y., Minor, W., Rastinejad, F., and Khorasanizadeh, S. (2005) Double chromodomains cooperate to recognize the methylated histone H3 tail, *Nature* 438, 1181-1185.
 37. Li, H., Ilin, S., Wang, W., Duncan, E. M., Wysocka, J., Allis, C. D., and Patel, D. J. (2006) Molecular basis for site-specific read-out of histone H3K4me3 by the BPTF PHD finger of NURF, *Nature* 442, 91-95.
 38. Martin, D. G., Baetz, K., Shi, X., Walter, K. L., MacDonald, V. E., Wlodarski, M. J., Gozani, O., Hieter, P., and Howe, L. (2006) The Yng1p plant homeodomain finger is a methyl-histone binding module that recognizes lysine 4-methylated histone H3, *Mol Cell Biol* 26, 7871-7879.
 39. Shi, X., Hong, T., Walter, K. L., Ewalt, M., Michishita, E., Hung, T., Carney, D., Pena, P., Lan, F., Kaadige, M. R., Lacoste, N., Cayrou, C., Davrazou, F., Saha, A., Cairns, B. R., Ayer, D. E., Kutateladze, T. G., Shi, Y., Cote, J., Chua, K. F., and Gozani, O. (2006) ING2 PHD domain links histone H3 lysine 4 methylation to active gene repression, *Nature* 442, 96-99.
 40. Taverna, S. D., Ilin, S., Rogers, R. S., Tanny, J. C., Lavender, H., Li, H., Baker, L., Boyle, J., Blair, L. P., Chait, B. T., Patel, D. J., Aitchison, J. D., Tackett, A. J., and Allis, C. D. (2006) Yng1 PHD finger binding to H3 trimethylated at K4 promotes NuA3 HAT activity at K14 of H3 and transcription at a subset of targeted ORFs, *Mol Cell* 24, 785-796.
 41. Wysocka, J., Swigut, T., Xiao, H., Milne, T. A., Kwon, S. Y., Landry, J., Kauer, M., Tackett, A. J., Chait, B. T., Badenhorst, P., Wu, C., and Allis, C. D. (2006) A PHD finger of NURF couples histone H3 lysine 4 trimethylation with chromatin remodelling, *Nature* 442, 86-90.
 42. Oettinger, M. A., Schatz, D. G., Gorka, C., and Baltimore, D. (1990) RAG-1 and RAG-2, adjacent genes that synergistically activate V(D)J recombination, *Science* 248, 1517-1523.
 43. Matthews, A. G., Kuo, A. J., Ramon-Maiques, S., Han, S., Champagne, K. S., Ivanov, D., Gallardo, M., Carney, D., Cheung, P., Ciccone, D. N., Walter, K. L., Utz, P. J., Shi, Y., Kutateladze, T. G., Yang, W., Gozani, O., and Oettinger, M. A. (2007) RAG2 PHD finger couples histone H3 lysine 4 trimethylation with V(D)J recombination, *Nature* 450, 1106-1110.
 44. Nislow, C., Ray, E., and Pillus, L. (1997) SET1, a yeast member of the trithorax family, functions in transcriptional silencing and diverse cellular processes, *Mol Biol Cell* 8, 2421-2436.

45. Briggs, S. D., Bryk, M., Strahl, B. D., Cheung, W. L., Davie, J. K., Dent, S. Y., Winston, F., and Allis, C. D. (2001) Histone H3 lysine 4 methylation is mediated by Set1 and required for cell growth and rDNA silencing in *Saccharomyces cerevisiae*, *Genes Dev* 15, 3286-3295.
46. Miller, T., Krogan, N. J., Dover, J., Erdjument-Bromage, H., Tempst, P., Johnston, M., Greenblatt, J. F., and Shilatifard, A. (2001) COMPASS: a complex of proteins associated with a trithorax-related SET domain protein, *Proc Natl Acad Sci U S A* 98, 12902-12907.
47. Roguev, A., Schaft, D., Shevchenko, A., Pijnappel, W. W., Wilm, M., Aasland, R., and Stewart, A. F. (2001) The *Saccharomyces cerevisiae* Set1 complex includes an Ash2 homologue and methylates histone 3 lysine 4, *EMBO J* 20, 7137-7148.
48. Nagy, P. L., Griesenbeck, J., Kornberg, R. D., and Cleary, M. L. (2002) A trithorax-group complex purified from *Saccharomyces cerevisiae* is required for methylation of histone H3, *Proc Natl Acad Sci U S A* 99, 90-94.
49. Dehe, P. M., Dichtl, B., Schaft, D., Roguev, A., Pamblanco, M., Lebrun, R., Rodriguez-Gil, A., Mkandawire, M., Landsberg, K., Shevchenko, A., Rosaleny, L. E., Tordera, V., Chavez, S., Stewart, A. F., and Geli, V. (2006) Protein interactions within the Set1 complex and their roles in the regulation of histone 3 lysine 4 methylation, *J Biol Chem* 281, 35404-35412.
50. Goo, Y. H., Sohn, Y. C., Kim, D. H., Kim, S. W., Kang, M. J., Jung, D. J., Kwak, E., Barlev, N. A., Berger, S. L., Chow, V. T., Roeder, R. G., Azorsa, D. O., Meltzer, P. S., Suh, P. G., Song, E. J., Lee, K. J., Lee, Y. C., and Lee, J. W. (2003) Activating signal cointegrator 2 belongs to a novel steady-state complex that contains a subset of trithorax group proteins, *Mol Cell Biol* 23, 140-149.
51. Hughes, C. M., Rozenblatt-Rosen, O., Milne, T. A., Copeland, T. D., Levine, S. S., Lee, J. C., Hayes, D. N., Shanmugam, K. S., Bhattacharjee, A., Biondi, C. A., Kay, G. F., Hayward, N. K., Hess, J. L., and Meyerson, M. (2004) Menin associates with a trithorax family histone methyltransferase complex and with the *hoxc8* locus, *Mol Cell* 13, 587-597.
52. Lee, J. H., and Skalnik, D. G. (2005) CpG-binding protein (CXXC finger protein 1) is a component of the mammalian Set1 histone H3-Lys4 methyltransferase complex, the analogue of the yeast Set1/COMPASS complex, *J Biol Chem* 280, 41725-41731.
53. Milne, T. A., Briggs, S. D., Brock, H. W., Martin, M. E., Gibbs, D., Allis, C. D., and Hess, J. L. (2002) MLL targets SET domain methyltransferase activity to Hox gene promoters, *Mol Cell* 10, 1107-1117.
54. Wysocka, J., Myers, M. P., Laherty, C. D., Eisenman, R. N., and Herr, W. (2003)

- Human Sin3 deacetylase and trithorax-related Set1/Ash2 histone H3-K4 methyltransferase are tethered together selectively by the cell-proliferation factor HCF-1, *Genes Dev* 17, 896-911.
55. Yokoyama, A., Wang, Z., Wysocka, J., Sanyal, M., Aufiero, D. J., Kitabayashi, I., Herr, W., and Cleary, M. L. (2004) Leukemia proto-oncoprotein MLL forms a SET1-like histone methyltransferase complex with menin to regulate Hox gene expression, *Mol Cell Biol* 24, 5639-5649.
 56. Beisel, C., Imhof, A., Greene, J., Kremmer, E., and Sauer, F. (2002) Histone methylation by the Drosophila epigenetic transcriptional regulator Ash1, *Nature* 419, 857-862.
 57. Hamamoto, R., Furukawa, Y., Morita, M., Iimura, Y., Silva, F. P., Li, M., Yagyu, R., and Nakamura, Y. (2004) SMYD3 encodes a histone methyltransferase involved in the proliferation of cancer cells, *Nat Cell Biol* 6, 731-740.
 58. Hayashi, K., Yoshida, K., and Matsui, Y. (2005) A histone H3 methyltransferase controls epigenetic events required for meiotic prophase, *Nature* 438, 374-378.
 59. Nishioka, K., Chuikov, S., Sarma, K., Erdjument-Bromage, H., Allis, C. D., Tempst, P., and Reinberg, D. (2002) Set9, a novel histone H3 methyltransferase that facilitates transcription by precluding histone tail modifications required for heterochromatin formation, *Genes Dev* 16, 479-489.
 60. Wang, H., Cao, R., Xia, L., Erdjument-Bromage, H., Borchers, C., Tempst, P., and Zhang, Y. (2001) Purification and functional characterization of a histone H3-lysine 4-specific methyltransferase, *Mol Cell* 8, 1207-1217.
 61. Glaser, S., Schaft, J., Lubitz, S., Vintersten, K., van der Hoeven, F., Tufteland, K. R., Aasland, R., Anastassiadis, K., Ang, S. L., and Stewart, A. F. (2006) Multiple epigenetic maintenance factors implicated by the loss of Mll2 in mouse development, *Development* 133, 1423-1432.
 62. Lee, S., Lee, D. K., Dou, Y., Lee, J., Lee, B., Kwak, E., Kong, Y. Y., Lee, S. K., Roeder, R. G., and Lee, J. W. (2006) Coactivator as a target gene specificity determinant for histone H3 lysine 4 methyltransferases, *Proc Natl Acad Sci U S A* 103, 15392-15397.
 63. Yu, B. D., Hess, J. L., Horning, S. E., Brown, G. A., and Korsmeyer, S. J. (1995) Altered Hox expression and segmental identity in Mll-mutant mice, *Nature* 378, 505-508.
 64. Ruthenburg, A. J., Allis, C. D., and Wysocka, J. (2007) Methylation of lysine 4 on histone H3: intricacy of writing and reading a single epigenetic mark, *Mol Cell* 25, 15-30.

65. Shilatifard, A. (2008) Molecular implementation and physiological roles for histone H3 lysine 4 (H3K4) methylation, *Curr Opin Cell Biol* 20, 341-348.
66. Krogan, N. J., Dover, J., Wood, A., Schneider, J., Heidt, J., Boateng, M. A., Dean, K., Ryan, O. W., Golshani, A., Johnston, M., Greenblatt, J. F., and Shilatifard, A. (2003) The Paf1 complex is required for histone H3 methylation by COMPASS and Dot1p: linking transcriptional elongation to histone methylation, *Mol Cell* 11, 721-729.
67. Milne, T. A., Kim, J., Wang, G. G., Stadler, S. C., Basrur, V., Whitcomb, S. J., Wang, Z., Ruthenburg, A. J., Elenitoba-Johnson, K. S., Roeder, R. G., and Allis, C. D. (2010) Multiple interactions recruit MLL1 and MLL1 fusion proteins to the HOXA9 locus in leukemogenesis, *Mol Cell* 38, 853-863.
68. Muntean, A. G., Tan, J., Sitwala, K., Huang, Y., Bronstein, J., Connelly, J. A., Basrur, V., Elenitoba-Johnson, K. S., and Hess, J. L. (2010) The PAF complex synergizes with MLL fusion proteins at HOX loci to promote leukemogenesis, *Cancer Cell* 17, 609-621.
69. Wang, Z., Song, J., Milne, T. A., Wang, G. G., Li, H., Allis, C. D., and Patel, D. J. (2010) Pro isomerization in MLL1 PHD3-bromo cassette connects H3K4me readout to Cyp33 and HDAC-mediated repression, *Cell* 141, 1183-1194.
70. Govind, C. K., Zhang, F., Qiu, H., Hofmeyer, K., and Hinnebusch, A. G. (2007) Gcn5 promotes acetylation, eviction, and methylation of nucleosomes in transcribed coding regions, *Mol Cell* 25, 31-42.
71. Nakanishi, S., Sanderson, B. W., Delventhal, K. M., Bradford, W. D., Staehling-Hampton, K., and Shilatifard, A. (2008) A comprehensive library of histone mutants identifies nucleosomal residues required for H3K4 methylation, *Nat Struct Mol Biol* 15, 881-888.
72. Shahbazian, M. D., Zhang, K., and Grunstein, M. (2005) Histone H2B ubiquitylation controls processive methylation but not monomethylation by Dot1 and Set1, *Mol Cell* 19, 271-277.
73. Sun, Z. W., and Allis, C. D. (2002) Ubiquitination of histone H2B regulates H3 methylation and gene silencing in yeast, *Nature* 418, 104-108.
74. Chandrasekharan, M. B., Huang, F., and Sun, Z. W. (2009) Ubiquitination of histone H2B regulates chromatin dynamics by enhancing nucleosome stability, *Proc Natl Acad Sci U S A* 106, 16686-16691.
75. Lee, J. S., Shukla, A., Schneider, J., Swanson, S. K., Washburn, M. P., Florens, L., Bhaumik, S. R., and Shilatifard, A. (2007) Histone crosstalk between H2B monoubiquitination and H3 methylation mediated by COMPASS, *Cell* 131,

1084-1096.

76. Vitaliano-Prunier, A., Menant, A., Hobeika, M., Geli, V., Gwizdek, C., and Dargemont, C. (2008) Ubiquitylation of the COMPASS component Swd2 links H2B ubiquitylation to H3K4 trimethylation, *Nat Cell Biol* 10, 1365-1371.
77. Chandrasekharan, M. B., Huang, F., Chen, Y. C., and Sun, Z. W. (2010) Histone H2B C-terminal helix mediates trans-histone H3K4 methylation independent of H2B ubiquitination, *Mol Cell Biol* 30, 3216-3232.
78. Chandrasekharan, M. B., Huang, F., and Sun, Z. W. (2010) Histone H2B ubiquitination and beyond: Regulation of nucleosome stability, chromatin dynamics and the trans-histone H3 methylation, *Epigenetics* 5.
79. Byvoet, P., Shepherd, G. R., Hardin, J. M., and Noland, B. J. (1972) The distribution and turnover of labeled methyl groups in histone fractions of cultured mammalian cells, *Arch Biochem Biophys* 148, 558-567.
80. Thomas, G., Lange, H. W., and Hempel, K. (1972) [Relative stability of lysine-bound methyl groups in arginine-rich histones and their subfractions in Ehrlich ascites tumor cells in vitro], *Hoppe Seylers Z Physiol Chem* 353, 1423-1428.
81. Shi, Y., Lan, F., Matson, C., Mulligan, P., Whetstine, J. R., Cole, P. A., and Casero, R. A. (2004) Histone demethylation mediated by the nuclear amine oxidase homolog LSD1, *Cell* 119, 941-953.
82. Tsukada, Y., Fang, J., Erdjument-Bromage, H., Warren, M. E., Borchers, C. H., Tempst, P., and Zhang, Y. (2006) Histone demethylation by a family of JmjC domain-containing proteins, *Nature* 439, 811-816.
83. Cloos, P. A., Christensen, J., Agger, K., Maiolica, A., Rappsilber, J., Antal, T., Hansen, K. H., and Helin, K. (2006) The putative oncogene GASC1 demethylates tri- and dimethylated lysine 9 on histone H3, *Nature* 442, 307-311.
84. Fodor, B. D., Kubicek, S., Yonezawa, M., O'Sullivan, R. J., Sengupta, R., Perez-Burgos, L., Opravil, S., Mechtler, K., Schotta, G., and Jenuwein, T. (2006) Jmjd2b antagonizes H3K9 trimethylation at pericentric heterochromatin in mammalian cells, *Genes Dev* 20, 1557-1562.
85. Whetstine, J. R., Nottke, A., Lan, F., Huarte, M., Smolikov, S., Chen, Z., Spooner, E., Li, E., Zhang, G., Colaiacovo, M., and Shi, Y. (2006) Reversal of histone lysine trimethylation by the JMJD2 family of histone demethylases, *Cell* 125, 467-481.
86. Mosammamarast, N., and Shi, Y. (2010) Reversal of histone methylation:

biochemical and molecular mechanisms of histone demethylases, *Annu Rev Biochem* 79, 155-179.

87. Secombe, J., and Eisenman, R. N. (2007) The function and regulation of the JARID1 family of histone H3 lysine 4 demethylases: the Myc connection, *Cell Cycle* 6, 1324-1328.
88. Liang, G., Klose, R. J., Gardner, K. E., and Zhang, Y. (2007) Yeast Jhd2p is a histone H3 Lys4 trimethyl demethylase, *Nat Struct Mol Biol* 14, 243-245.
89. Seward, D. J., Cubberley, G., Kim, S., Schonewald, M., Zhang, L., Tripet, B., and Bentley, D. L. (2007) Demethylation of trimethylated histone H3 Lys4 in vivo by JARID1 JmjC proteins, *Nat Struct Mol Biol* 14, 240-242.
90. Tu, S., Bulloch, E. M., Yang, L., Ren, C., Huang, W. C., Hsu, P. H., Chen, C. H., Liao, C. L., Yu, H. M., Lo, W. S., Freitas, M. A., and Tsai, M. D. (2007) Identification of histone demethylases in *Saccharomyces cerevisiae*, *J Biol Chem* 282, 14262-14271.
91. Iwase, S., Lan, F., Bayliss, P., de la Torre-Ubieta, L., Huarte, M., Qi, H. H., Whetstine, J. R., Bonni, A., Roberts, T. M., and Shi, Y. (2007) The X-linked mental retardation gene SMCX/JARID1C defines a family of histone H3 lysine 4 demethylases, *Cell* 128, 1077-1088.
92. Klose, R. J., Yan, Q., Tothova, Z., Yamane, K., Erdjument-Bromage, H., Tempst, P., Gilliland, D. G., Zhang, Y., and Kaelin, W. G., Jr. (2007) The retinoblastoma binding protein RBP2 is an H3K4 demethylase, *Cell* 128, 889-900.
93. Lee, M. G., Norman, J., Shilatifard, A., and Shiekhatter, R. (2007) Physical and functional association of a trimethyl H3K4 demethylase and Ring6a/MBLR, a polycomb-like protein, *Cell* 128, 877-887.
94. Secombe, J., Li, L., Carlos, L., and Eisenman, R. N. (2007) The Trithorax group protein Lid is a trimethyl histone H3K4 demethylase required for dMyc-induced cell growth, *Genes Dev* 21, 537-551.
95. Benevolenskaya, E. V., Murray, H. L., Branton, P., Young, R. A., and Kaelin, W. G., Jr. (2005) Binding of pRB to the PHD protein RBP2 promotes cellular differentiation, *Mol Cell* 18, 623-635.
96. Jensen, L. R., Amende, M., Gurok, U., Moser, B., Gimmel, V., Tzschach, A., Janecke, A. R., Tariverdian, G., Chelly, J., Fryns, J. P., Van Esch, H., Kleefstra, T., Hamel, B., Moraine, C., Gecz, J., Turner, G., Reinhardt, R., Kalscheuer, V. M., Ropers, H. H., and Lenzner, S. (2005) Mutations in the JARID1C gene, which is involved in transcriptional regulation and chromatin remodeling, cause X-linked mental retardation, *Am J Hum Genet* 76, 227-236.

97. Tahiliani, M., Mei, P., Fang, R., Leonor, T., Rutenberg, M., Shimizu, F., Li, J., Rao, A., and Shi, Y. (2007) The histone H3K4 demethylase SMCX links REST target genes to X-linked mental retardation, *Nature* 447, 601-605.
98. Roesch, A., Fukunaga-Kalabis, M., Schmidt, E. C., Zabierowski, S. E., Brafford, P. A., Vultur, A., Basu, D., Gimotty, P., Vogt, T., and Herlyn, M. (2010) A temporarily distinct subpopulation of slow-cycling melanoma cells is required for continuous tumor growth, *Cell* 141, 583-594.
99. Ingvarsdottir, K., Edwards, C., Lee, M. G., Lee, J. S., Schultz, D. C., Shilatifard, A., Shiekhattar, R., and Berger, S. L. (2007) Histone H3 K4 demethylation during activation and attenuation of GAL1 transcription in *Saccharomyces cerevisiae*, *Mol Cell Biol* 27, 7856-7864.
100. Mersman, D. P., Du, H. N., Fingerman, I. M., South, P. F., and Briggs, S. D. (2009) Polyubiquitination of the demethylase Jhd2 controls histone methylation and gene expression, *Genes Dev* 23, 951-962.
101. Osborne, E. A., Dudoit, S., and Rine, J. (2009) The establishment of gene silencing at single-cell resolution, *Nat Genet* 41, 800-806.
102. Chen, Z., Zang, J., Whetstone, J., Hong, X., Davrazou, F., Kutateladze, T. G., Simpson, M., Mao, Q., Pan, C. H., Dai, S., Hagman, J., Hansen, K., Shi, Y., and Zhang, G. (2006) Structural insights into histone demethylation by JMJD2 family members, *Cell* 125, 691-702.
103. Lan, F., Collins, R. E., De Cegli, R., Alpatov, R., Horton, J. R., Shi, X., Gozani, O., Cheng, X., and Shi, Y. (2007) Recognition of unmethylated histone H3 lysine 4 links BHC80 to LSD1-mediated gene repression, *Nature* 448, 718-722.
104. Mellor, J. (2006) It takes a PHD to read the histone code, *Cell* 126, 22-24.
105. Knop, M., Siegers, K., Pereira, G., Zachariae, W., Winsor, B., Nasmyth, K., and Schiebel, E. (1999) Epitope tagging of yeast genes using a PCR-based strategy: more tags and improved practical routines, *Yeast* 15, 963-972.
106. Gietz, R. D., and Sugino, A. (1988) New yeast-*Escherichia coli* shuttle vectors constructed with in vitro mutagenized yeast genes lacking six-base pair restriction sites, *Gene* 74, 527-534.
107. Beranger, F., Aresta, S., de Gunzburg, J., and Camonis, J. (1997) Getting more from the two-hybrid system: N-terminal fusions to LexA are efficient and sensitive baits for two-hybrid studies, *Nucleic Acids Res* 25, 2035-2036.
108. Zhang, Y., Sun, Z. W., Iratni, R., Erdjument-Bromage, H., Tempst, P., Hampsey, M., and Reinberg, D. (1998) SAP30, a novel protein conserved between human

- and yeast, is a component of a histone deacetylase complex, *Mol Cell* *1*, 1021-1031.
109. Matsubara, K., Sano, N., Umehara, T., and Horikoshi, M. (2007) Global analysis of functional surfaces of core histones with comprehensive point mutants, *Genes Cells* *12*, 13-33.
 110. Hollenberg, S. M., Sternglanz, R., Cheng, P. F., and Weintraub, H. (1995) Identification of a new family of tissue-specific basic helix-loop-helix proteins with a two-hybrid system, *Mol Cell Biol* *15*, 3813-3822.
 111. Kim, T. D., Shin, S., and Janknecht, R. (2008) Repression of Smad3 activity by histone demethylase SMCX/JARID1C, *Biochem Biophys Res Commun* *366*, 563-567.
 112. Wittmeyer, J., Saha, A., and Cairns, B. (2004) DNA translocation and nucleosome remodeling assays by the RSC chromatin remodeling complex, *Methods Enzymol* *377*, 322-343.
 113. Mumberg, D., Muller, R., and Funk, M. (1995) Yeast vectors for the controlled expression of heterologous proteins in different genetic backgrounds, *Gene* *156*, 119-122.
 114. Sikorski, R. S., and Hieter, P. (1989) A system of shuttle vectors and yeast host strains designed for efficient manipulation of DNA in *Saccharomyces cerevisiae*, *Genetics* *122*, 19-27.
 115. Schuller, H. J., Schorr, R., Hoffmann, B., and Schweizer, E. (1992) Regulatory gene INO4 of yeast phospholipid biosynthesis is positively autoregulated and functions as a transactivator of fatty acid synthase genes FAS1 and FAS2 from *Saccharomyces cerevisiae*, *Nucleic Acids Res* *20*, 5955-5961.
 116. Gardner, R. G., Nelson, Z. W., and Gottschling, D. E. (2005) Ubp10/Dot4p regulates the persistence of ubiquitinated histone H2B: distinct roles in telomeric silencing and general chromatin, *Mol Cell Biol* *25*, 6123-6139.
 117. Kao, C. F., Hillyer, C., Tsukuda, T., Henry, K., Berger, S., and Osley, M. A. (2004) Rad6 plays a role in transcriptional activation through ubiquitylation of histone H2B, *Genes Dev* *18*, 184-195.
 118. Belle, A., Tanay, A., Bitincka, L., Shamir, R., and O'Shea, E. K. (2006) Quantification of protein half-lives in the budding yeast proteome, *Proc Natl Acad Sci U S A* *103*, 13004-13009.
 119. Klose, R. J., Kallin, E. M., and Zhang, Y. (2006) JmjC-domain-containing proteins and histone demethylation, *Nat Rev Genet* *7*, 715-727.

120. Yamane, K., Toumazou, C., Tsukada, Y., Erdjument-Bromage, H., Tempst, P., Wong, J., and Zhang, Y. (2006) JHDM2A, a JmjC-containing H3K9 demethylase, facilitates transcription activation by androgen receptor, *Cell* 125, 483-495.
121. Kouzarides, T. (2007) Chromatin modifications and their function, *Cell* 128, 693-705.
122. Sanchez, Y., and Lindquist, S. L. (1990) HSP104 required for induced thermotolerance, *Science* 248, 1112-1115.
123. Chen, M., Hancock, L. C., and Lopes, J. M. (2007) Transcriptional regulation of yeast phospholipid biosynthetic genes, *Biochim Biophys Acta* 1771, 310-321.
124. Xiang, Y., Zhu, Z., Han, G., Ye, X., Xu, B., Peng, Z., Ma, Y., Yu, Y., Lin, H., Chen, A. P., and Chen, C. D. (2007) JARID1B is a histone H3 lysine 4 demethylase up-regulated in prostate cancer, *Proc Natl Acad Sci U S A* 104, 19226-19231.
125. Yamane, K., Tateishi, K., Klose, R. J., Fang, J., Fabrizio, L. A., Erdjument-Bromage, H., Taylor-Papadimitriou, J., Tempst, P., and Zhang, Y. (2007) PLU-1 is an H3K4 demethylase involved in transcriptional repression and breast cancer cell proliferation, *Mol Cell* 25, 801-812.
126. Bernstein, B. E., Humphrey, E. L., Erlich, R. L., Schneider, R., Bouman, P., Liu, J. S., Kouzarides, T., and Schreiber, S. L. (2002) Methylation of histone H3 Lys 4 in coding regions of active genes, *Proc Natl Acad Sci U S A* 99, 8695-8700.
127. Balciunas, D., and Ronne, H. (2000) Evidence of domain swapping within the jumonji family of transcription factors, *Trends Biochem Sci* 25, 274-276.
128. Klose, R. J., and Zhang, Y. (2007) Regulation of histone methylation by demethylimination and demethylation, *Nat Rev Mol Cell Biol* 8, 307-318.
129. Chang, Y., Wu, J., Tong, X. J., Zhou, J. Q., and Ding, J. (2010) Crystal structure of the catalytic core of *Saccharomyces cerevesiae* histone demethylase Rph1: insights into the substrate specificity and catalytic mechanism, *Biochem J* 433, 295-302.
130. Klose, R. J., Yamane, K., Bae, Y., Zhang, D., Erdjument-Bromage, H., Tempst, P., Wong, J., and Zhang, Y. (2006) The transcriptional repressor JHDM3A demethylates trimethyl histone H3 lysine 9 and lysine 36, *Nature* 442, 312-316.
131. Santos, C., Rodriguez-Revenga, L., Madrigal, I., Badenas, C., Pineda, M., and Mila, M. (2006) A novel mutation in JARID1C gene associated with mental retardation, *Eur J Hum Genet* 14, 583-586.
132. Tzschach, A., Lenzner, S., Moser, B., Reinhardt, R., Chelly, J., Fryns, J. P.,

- Kleefstra, T., Raynaud, M., Turner, G., Ropers, H. H., Kuss, A., and Jensen, L. R. (2006) Novel JARID1C/SMCX mutations in patients with X-linked mental retardation, *Hum Mutat* 27, 389.
133. Christensen, J., Agger, K., Cloos, P. A., Pasini, D., Rose, S., Sennels, L., Rappsilber, J., Hansen, K. H., Salcini, A. E., and Helin, K. (2007) RBP2 belongs to a family of demethylases, specific for tri- and dimethylated lysine 4 on histone 3, *Cell* 128, 1063-1076.
 134. Dehe, P. M., and Geli, V. (2006) The multiple faces of Set1, *Biochem Cell Biol* 84, 536-548.
 135. Huh, W. K., Falvo, J. V., Gerke, L. C., Carroll, A. S., Howson, R. W., Weissman, J. S., and O'Shea, E. K. (2003) Global analysis of protein localization in budding yeast, *Nature* 425, 686-691.
 136. Durchschlag, E., Reiter, W., Ammerer, G., and Schuller, C. (2004) Nuclear localization destabilizes the stress-regulated transcription factor Msn2, *J Biol Chem* 279, 55425-55432.
 137. Shin, S., and Janknecht, R. (2007) Diversity within the JMJD2 histone demethylase family, *Biochem Biophys Res Commun* 353, 973-977.
 138. Schindler, U., Beckmann, H., and Cashmore, A. R. (1993) HAT3.1, a novel Arabidopsis homeodomain protein containing a conserved cysteine-rich region, *Plant J* 4, 137-150.
 139. Lange, M., Kaynak, B., Forster, U. B., Tonjes, M., Fischer, J. J., Grimm, C., Schlesinger, J., Just, S., Dunkel, I., Krueger, T., Mebus, S., Lehrach, H., Lurz, R., Gobom, J., Rottbauer, W., Abdelilah-Seyfried, S., and Sperling, S. (2008) Regulation of muscle development by DPF3, a novel histone acetylation and methylation reader of the BAF chromatin remodeling complex, *Genes Dev* 22, 2370-2384.
 140. Baker, L. A., Allis, C. D., and Wang, G. G. (2008) PHD fingers in human diseases: disorders arising from misinterpreting epigenetic marks, *Mutat Res* 647, 3-12.
 141. Bienz, M. (2006) The PHD finger, a nuclear protein-interaction domain, *Trends Biochem Sci* 31, 35-40.
 142. Taverna, S. D., Li, H., Ruthenburg, A. J., Allis, C. D., and Patel, D. J. (2007) How chromatin-binding modules interpret histone modifications: lessons from professional pocket pickers, *Nat Struct Mol Biol* 14, 1025-1040.
 143. Gell, D., and Jackson, S. P. (1999) Mapping of protein-protein interactions within the DNA-dependent protein kinase complex, *Nucleic Acids Res* 27, 3494-3502.

144. Ooi, S. K., Qiu, C., Bernstein, E., Li, K., Jia, D., Yang, Z., Erdjument-Bromage, H., Tempst, P., Lin, S. P., Allis, C. D., Cheng, X., and Bestor, T. H. (2007) DNMT3L connects unmethylated lysine 4 of histone H3 to de novo methylation of DNA, *Nature* 448, 714-717.
145. Org, T., Chignola, F., Hetenyi, C., Gaetani, M., Rebane, A., Liiv, I., Maran, U., Mollica, L., Bottomley, M. J., Musco, G., and Peterson, P. (2008) The autoimmune regulator PHD finger binds to non-methylated histone H3K4 to activate gene expression, *EMBO Rep* 9, 370-376.
146. Wang, G. G., Song, J., Wang, Z., Dormann, H. L., Casadio, F., Li, H., Luo, J. L., Patel, D. J., and Allis, C. D. (2009) Haematopoietic malignancies caused by dysregulation of a chromatin-binding PHD finger, *Nature* 459, 847-851.
147. Tu, S., Teng, Y. C., Yuan, C., Wu, Y. T., Chan, M. Y., Cheng, A. N., Lin, P. H., Juan, L. J., and Tsai, M. D. (2008) The ARID domain of the H3K4 demethylase RBP2 binds to a DNA CCGCC motif, *Nat Struct Mol Biol* 15, 419-421.
148. Zheng, S., Wyrick, J. J., and Reese, J. C. (2010) Novel trans-tail regulation of H2B ubiquitylation and H3K4 methylation by the N terminus of histone H2A, *Mol Cell Biol* 30, 3635-3645.
149. Huang, F., Chandrasekharan, M. B., Chen, Y. C., Bhaskara, S., Hiebert, S. W., and Sun, Z. W. (2010) The JmjN domain of Jhd2 is important for its protein stability, and the plant homeodomain (PHD) finger mediates its chromatin association independent of H3K4 methylation, *J Biol Chem* 285, 24548-24561.
150. Washburn, M. P., Wolters, D., and Yates, J. R., 3rd. (2001) Large-scale analysis of the yeast proteome by multidimensional protein identification technology, *Nat Biotechnol* 19, 242-247.
151. Kaminska, J., Sedek, M., Wysocka-Kapcinska, M., and Zoladek, T. (2007) Characterization of nuclear localization and nuclear export signals of yeast actin-binding protein Pan1, *FEBS Lett* 581, 5371-5376.
152. Kosugi, S., Hasebe, M., Tomita, M., and Yanagawa, H. (2009) Systematic identification of cell cycle-dependent yeast nucleocytoplasmic shuttling proteins by prediction of composite motifs, *Proc Natl Acad Sci U S A* 106, 10171-10176.
153. Kosugi, S., Hasebe, M., Entani, T., Takayama, S., Tomita, M., and Yanagawa, H. (2008) Design of peptide inhibitors for the importin alpha/beta nuclear import pathway by activity-based profiling, *Chem Biol* 15, 940-949.
154. la Cour, T., Kierner, L., Molgaard, A., Gupta, R., Skriver, K., and Brunak, S. (2004) Analysis and prediction of leucine-rich nuclear export signals, *Protein Eng Des Sel* 17, 527-536.

155. Robzyk, K., Recht, J., and Osley, M. A. (2000) Rad6-dependent ubiquitination of histone H2B in yeast, *Science* 287, 501-504.
156. Wood, A., Krogan, N. J., Dover, J., Schneider, J., Heidt, J., Boateng, M. A., Dean, K., Golshani, A., Zhang, Y., Greenblatt, J. F., Johnston, M., and Shilatifard, A. (2003) Bre1, an E3 ubiquitin ligase required for recruitment and substrate selection of Rad6 at a promoter, *Mol Cell* 11, 267-274.
157. Henry, K. W., Wyce, A., Lo, W. S., Duggan, L. J., Emre, N. C., Kao, C. F., Pillus, L., Shilatifard, A., Osley, M. A., and Berger, S. L. (2003) Transcriptional activation via sequential histone H2B ubiquitylation and deubiquitylation, mediated by SAGA-associated Ubp8, *Genes Dev* 17, 2648-2663.
158. Emre, N. C., Ingvarsdottir, K., Wyce, A., Wood, A., Krogan, N. J., Henry, K. W., Li, K., Marmorstein, R., Greenblatt, J. F., Shilatifard, A., and Berger, S. L. (2005) Maintenance of low histone ubiquitylation by Ubp10 correlates with telomere-proximal Sir2 association and gene silencing, *Mol Cell* 17, 585-594.